

AD 730513

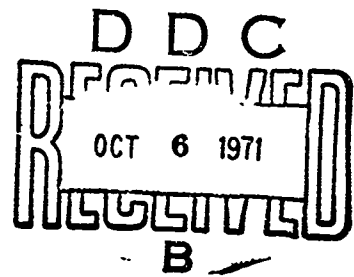
# CHEMICAL AND PHYSICAL STUDY OF FUELS GELLED WITH CARBOHYDRATE RESINS

James Teng and James M. Lucas  
Anheuser-Busch, Inc.  
St. Louis, Missouri 63118

Details of illustrations in this document may be better studied on microfiche



SEPTEMBER 1971



FINAL REPORT

Availability is unlimited. Document may be released to the National Technical Information Service, Springfield, Virginia 22151, for sale to the public.

Reproduced by  
NATIONAL TECHNICAL  
INFORMATION SERVICE  
Springfield, Va. 22151

Prepared for

DEPARTMENT OF TRANSPORTATION  
FEDERAL AVIATION ADMINISTRATION  
Systems Research & Development Service  
Washington D. C., 20590

TECHNICAL REPORT STANDARD TITLE PAGE

1. Report No. FAA-RD-71-43		2. Government Accession No.		3. Recipient's Catalog No.	
4. Title and Subtitle CHEMICAL AND PHYSICAL STUDY OF FUELS GELLED WITH CARBOHYDRATE RESINS				5. Report Date September 1971	
				6. Performing Organization Code	
7. Author(s) James Teng, James M. Lucas				8. Performing Organization Report No. FAA-NA-71-18	
9. Performing Organization Name and Address Anheuser-Busch, Inc. St. Louis, Missouri 63118				10. Work Unit No.	
				11. Contract or Grant No. DOT-FA70NA-497	
12. Sponsoring Agency Name and Address Federal Aviation Administration Systems Research & Development Service Washington, D. C. 20590				13. Type of Report and Period Covered Final Report 6-22-70 to 2-2-71	
				14. Sponsoring Agency Code	
15. Supplementary Notes					
16. Abstract  <p>→ A carbohydrate derivative was designed as a gelling agent for turbine fuel. The gelling agent is effective in reducing the fire hazard of the fuel. The free flowing gelled fuel could be adapted readily to existing fuel systems. The rheological profile of this gelled fuel was established over a range of conditions, by means of a rotating viscometer, Rotovisco Viscometer, equipped with special measuring heads. Among the rheological parameters which were measured, the viscoelasticity of the gelled fuel appears likely to be a major factor in contributing to the crash-safe character of the fuel.</p> <p>Pertinent physical properties and microbiological data were also compiled to demonstrate that the fuel gelled with the carbohydrate based gelling agent is compatible with present aircraft fuel systems. ( ) ←</p>					
17. Key Words Gelled Fuels Fuel Thickeners Aircraft Fires Fire Safety			18. Distribution Statement Availability is unlimited. Document may be released to the National Technical Information Service, Springfield, Virginia, 22151, for sale to the public.		
19. Security Classif. (of this report) Unclassified		20. Security Classif. (of this page) Unclassified		21. No. of Pages 95	22. Price

## PREFACE

This report was prepared by Anheuser-Busch, Inc., St. Louis, Missouri for the Federal Aviation Administration. The work was administered under the direction of Mr. Ralph A. Russell, Project Manager, Propulsion Section, Aircraft Branch, National Aviation Facilities Experimental Center, (NAFEC) Atlantic City, New Jersey.

The authors appreciate the overall direction and advice given them by Dr. B. L. Scallet, Associate Director of Research of Anheuser-Busch, Inc., in the course of this investigation. They are also grateful to Professor J. D. Ferry of the University of Wisconsin for his critical review of the experimental data, to Professor J. J. Cooney of the University of Dayton for the supply of micro-organisms, and to Dr. K. Shieh of Anheuser-Busch, Inc., for his microbiological examination.

## TABLE OF CONTENTS

	Page
INTRODUCTION	1
Purpose	1
Background	1
RHEOLOGICAL CHARACTERIZATION - PART A	2
Results and Discussions	2
Program	2
Plasticity and Yield Stress	2
Shear Rate and Shear Stress Relationship	2
Thixotropy	15
Viscoelasticity	23
Experimental Procedures	32
RHEOLOGICAL CHARACTERIZATION - PART B	38
Results and Discussions	38
Program	38
Plasticity and Yield Stress	38
Shear Rate and Shear Stress Relationship	38
Thixotropy	42
Viscoelasticity	42
SYSTEM COMPATIBILITY STUDY	47
Results and Discussion	47
Vibrational Stability	47
Thermal Stability	47
Filterability	47
Residual Gel Measurement	47
Material Compatibility	52
Physical Properties	52
Microbial Activity	55
Electron Microscopy	61
Experimental Procedures	70
SUMMARY	74
CONCLUSIONS	76
APPENDIX A	1-1
Calculation of Constants for Power Law Equations	
APPENDIX B	2-1
Derivation of Equations for Linear Flow	
APPENDIX C	3-1
Glossary of Symbols	
APPENDIX D	4-1
Bibliography	

## LIST OF ILLUSTRATIONS

Figure		Page
1	Yield Stresses of Gels at Various Temperatures	4
2	Shear Rate vs. Shear Stress at Various Temperatures - Gel A	5
3	Shear Rate vs. Shear Stress at Various Temperatures - Gel B	6
4	Shear Rate vs. Shear Stress at Various Temperatures - Gel C	7
5	Shear Rate vs. Shear Stress at Various Temperatures - Gel D	8
6	Shear Rate vs. (Shear Stress Less Yield Stress) at Various Temperatures - Gel A	9
7	Shear Rate vs. (Shear Stress Less Yield Stress) at Various Temperatures - Gel B	10
8	Shear Rate vs. (Shear Stress Less Yield Stress) at Various Temperatures - Gel C	11
9	Shear Rate vs. (Shear Stress Less Yield Stress) at Various Temperatures - Gel D	12
10	Calculated Flow Rate of Gel Through 10-Foot Long Straight Pipe	16
11	Thixotropy of Gels A, B, C and D at 25°C. Temperature	17
12	Stress Recovery of Gels	18
13	Hysteresis Loop of Gel A	19
14	Hysteresis Loop of Gel B	20
15	Hysteresis Loop of Gel C	21
16	Hysteresis Loop of Gel D	22
17	Viscoelasticity Measurements of Gel A - 20 sec. <sup>-1</sup> Shear Rate at 10°C. Temperature	24
18	Viscoelasticity Measurements of Gel A - 264 sec. <sup>-1</sup> Shear Rate at 10°C. Temperature	24
19	Viscoelasticity Measurements of Gel A - 20 sec. <sup>-1</sup> Shear Rate at 40°C. Temperature	25

LIST OF ILLUSTRATIONS (continued)

Figure		Page
20	Viscoelasticity Measurements of Gel A - 264 sec. <sup>-1</sup> Shear Rate at 40°C. Temperature	25
21	Viscoelasticity Measurements of Gel B - 20 sec. <sup>-1</sup> Shear Rate at 10°C. Temperature	26
22	Viscoelasticity Measurements of Gel C - 20 sec. <sup>-1</sup> Shear Rate at 10°C. Temperature	26
23	Viscoelasticity Measurements of Gel D - 20 sec. <sup>-1</sup> Shear Rate at 10°C. Temperature	27
24	Correlation of Viscoelasticity With Crash-Fire Safety	31
25	Rotovisco Viscometer With Cone and Plate Attachments	33
26	Rotovisco Viscometer With Yield Stress Attachment	34
27	Rotovisco Viscometer With Viscoelastic Attachment	35
28	Viscoelastic Measuring Head - Rotovisco Viscometer	36
29	Yield Stress of Gel E at Various Temperatures	39
30	Shear Rate vs. Shear Stress at Various Temperatures - Gel E	40
31	Shear Rate vs. (Shear Stress Less Yield Stress) at Various Temperatures - Gel E	41
32	Hysteresis Loop of Gel E at Various Temperatures	43
33	Thixotropy of Gel E at 25°C. Temperature	44
34	Viscosity Measurements of Gel E at Various Temperatures	45
35	Viscoelastic Measurement of Gel E - 4000 sec. <sup>-1</sup> Shear Rate at -20°C. and 58°C. Temperatures	46
36	Flow Rate of Gel C in Relation to Pressure Drop	48
37	Influence of Concentration on Amount of Residual Gels	50
38	Influence of Temperature on Amount of Residual Gels	51
39	Temperature and Gelled Fuel Density Relationship	53
40	Net Heat of Combustion for Gels	58

LIST OF ILLUSTRATIONS (continued)

Figure		Page
41	Growth Curve of <u>Pseudomonas Aeruginosa</u> in the Aqueous Phase of Jet A and Gelled Jet A	59
42	Growth Curves of <u>Bacillus sp.</u> in the Aqueous Phase of Jet A and Gelled Jet A	60
43	Structure of Hydroxysterate Grease - Magnification: 15000X	64
44	Structure of Silica Base Grease - Magnification: 15000X	65
45	Structure of Indanthrene Blue-Base Grease - Magnification: 15000X	66
46	Structure of AB Gelling Agent in Jet A Fuel - Magnification: 39000X	67
47	Structure of AB Gelling Agent in Jet A Fuel - Magnification: 56000X	68
48	Structure of AB Gelling Agent in Jet A Fuel - Magnification: 77000X	69
1-1	Dependence of (k) on the Inverse of Temperature	1-2

## LIST OF TABLES

Table		Page
1	Yield Stresses at Various Temperature and Gelling Agent Concentration Levels	3
2	Temperature and Concentration Effects on the Values of Slope (n)	14
3	Temperature and Concentration Effects on the Values of Intercept (k)	14
4	Equilibrium Stress at Various Temperature and Concentration Levels	28
5	Relaxation Time at Various Temperature and Concentration Levels	29
6	Yield Stresses at Various Temperatures	38
7	Effect of Temperature on Values of Intercept (k)	42
8	Residual Gel on Aluminum Coupons	49
9	Comparison of the Variation of Density With Temperature for Gelled and Jet A Fuels	54
10	Ash Content of Gelled Fuel	54
11	Components of Ash in Gelled Fuel	56
12	Thermal Conductivity of Gelled Fuel	57
13	Net Heat of Combustion of Gelled Fuel	57
14	Effect of Gelled Fuel on Growth of <u>Hormodendrum SP.</u>	62
15	Growth of <u>Hormodendrum SP.</u> in Solid Test Systems	63
16	Summary of Gel Properties (Gel E)	75



## INTRODUCTION

### Purpose

The purpose of this study was to use the fuel thickened with the Anheuser-Busch (AB) gelling agent as a model; perform on it rheological characterization, describe the pertinent parameters and set forth a preliminary profile specification to guide future development.

### Background

Since 1964, the Federal Aviation Administration has actively carried out a research program designed to reduce the fire hazard associated with the crash of aircraft. As a result of this continuous study, thickened fuels were shown<sup>1</sup> to be both effective and safe. Of all the methods of thickening, gellation with suitable agents appears to be particularly promising.

Recent FAA sponsored research<sup>2</sup> indicated that gelled fuels, in addition to possessing the prerequisite crash-safe properties, must be fluid enough to drain from fuel cells without extensive modification of the aircraft fuel system. Therefore, it is imperative that a gelled fuel be developed that meets this criterion. The rheological properties of the fuel must be quantitatively defined so that the fuels can be screened and only the best candidate be subjected to further testing.

A few of the numerous gelling agents examined by the FAA approach the qualifications required for safety and system compatibility. The Corn Products Research Section of the Central Research Department of Anheuser-Busch, Inc. has specifically developed a carbohydrate-based polymeric gelling agent for jet fuels. Fuel containing this gelling agent has met the preliminary NAFEC safety and rheological requirements. It has been demonstrated to be a versatile and promising gelling agent.

The main text of the report is divided into five major sections. The first two sections describe rheological characterizations; the third covers the physical properties, compatibility and structure of the gelled fuels. The measured properties are discussed and the detailed experimental procedures are described in separate parts entitled, "Experimental Procedures." The summary section integrates the individual findings and presents an overall discussion of the gelled fuel. Findings of this investigation are itemized and listed in the concluding section.

## RHEOLOGICAL CHARACTERIZATION - PART A

### Results and Discussions

Program - A broad range of gel consistency is represented by four selected gel samples prepared with the AB gelling agent. The broad range is designed to permit ready interpolation of the data to the gel which is ultimately chosen. The four gel samples are identified in this section as A, B, C and D with the gelling agent concentrations of 2.73%, 2.03%, 1.67% and 1.11%, respectively. Concentrations are expressed as weight per cent throughout this report. Wherever possible, the gel properties are measured at five temperature levels (-52°C. to 52.8°C.).

Plasticity and Yield Stress - The gelled fuels exhibit non-Newtonian (i.e., variable shear-stress/shear-rate ratio) and plastic behavior with a small but definite amount of associated yield stress. The yield stresses ( $\psi$ ) for each of the gels at various temperatures, are given in Table 1 and illustrated in Figure 1. The data indicate that in the higher temperature range (0-52°C.), the yield stress value of  $230 \pm 50$  dynes/cm<sup>2</sup> is relatively independent of temperature and concentration. However, as the temperature drops below 0°C., the yield stress increases rapidly to approximately 2000 dynes/cm<sup>2</sup>. The reduced temperature also magnifies the influence of concentrations on yield stress.

Shear Rate and Shear Stress Relationship - The non-Newtonian flow properties of the gelled fuel are demonstrated by the measurements of the shear rate and shear stress ( $\sigma$ ) relationships. The shear rate was varied in 10 steps, covering a range of 74 sec.<sup>-1</sup> to 12,000 sec.<sup>-1</sup>. Figures 2, 3, 4 and 5 illustrate the relationship for each gel at several temperature levels. Within these limits the corresponding stresses developed in the gel ranges from 200 to 10,000 dynes/cm<sup>2</sup>. From these graphs, one may obtain the "apparent viscosity" ( $\eta$ ), which is the ratio of shear stress to shear rate. The ratio is not a constant value; it is dependent on the shear rate. As expected of non-Newtonian and thixotropic fluids, the shear stress of these gels does not increase as rapidly at higher shear rate as at lower shear rate.

The data given above may be presented conveniently and usefully as a family of straight lines which permits easy interpolation and some degree of extrapolation. When the difference between shear stress and yield stress ( $\sigma - \psi$ ) is plotted against the shear rate on a logarithmic scale (Figures 6, 7, 8, 9), the lines are represented by the following linear equation:<sup>3</sup>

$$\log (\sigma - \psi) = \log k + n \log \dot{\gamma} \quad (1)$$

where:  $\sigma$  = shear stress

$\psi$  = yield stress

$\dot{\gamma}$  = shear rate

$k, n$  are constants

TABLE 1

YIELD STRESSES AT VARIOUS TEMPERATURE AND GELLING AGENT CONCENTRATION LEVELS

<u>T</u> °C.	YIELD STRESSES, dynes/cm <sup>2</sup>			
	<u>Concentration, Weight %</u>			
	<u>2.73(A)</u>	<u>2.03(B)</u>	<u>1.67(C)</u>	<u>1.11(D)</u>
52.8	290	240	190	170
25.0	250	210	190	180
0.0	260	240	210	170
-20.7	800	600	500	380
-52.0	2200	2100	1700	1300

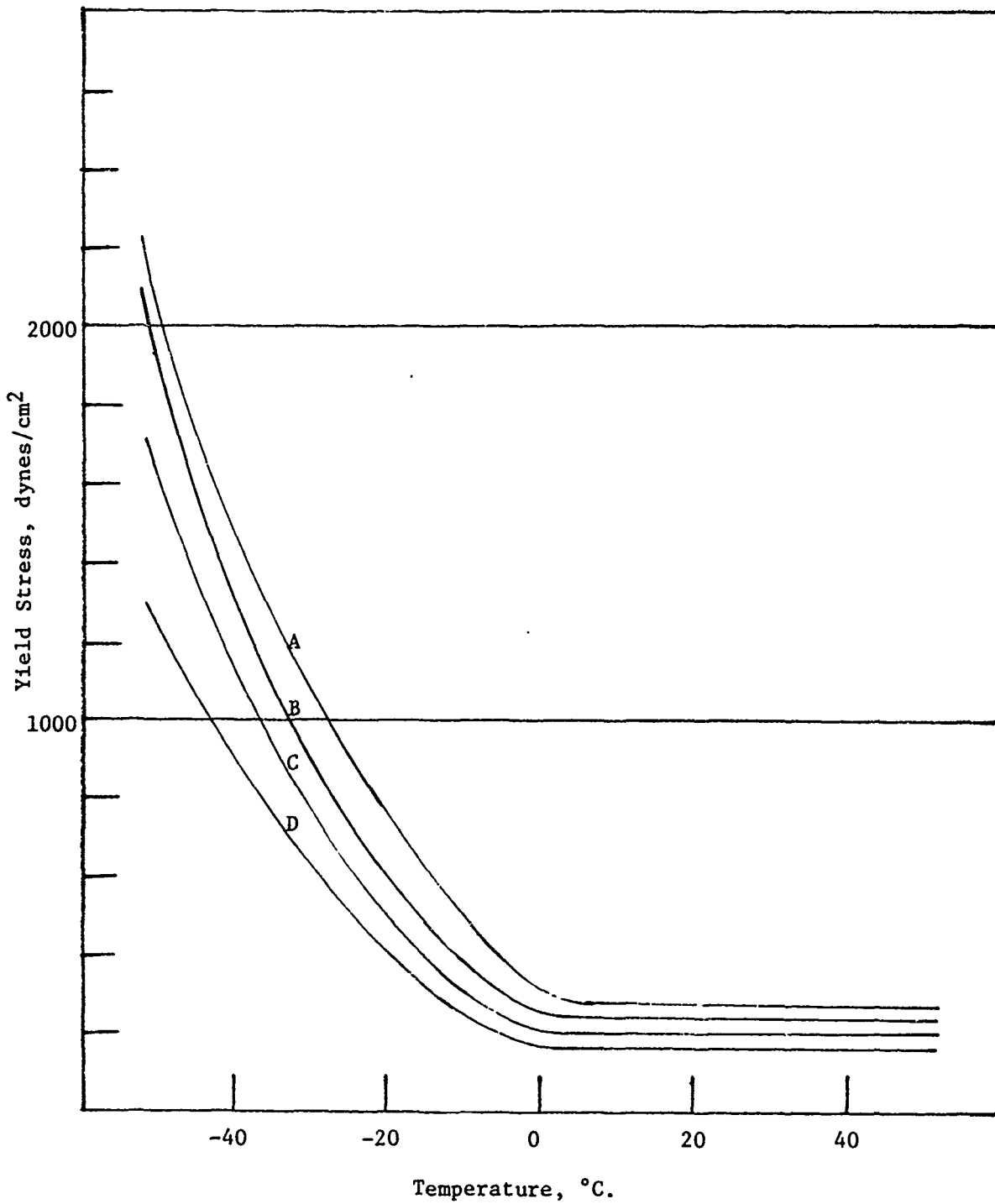


Fig. 1 - Yield Stresses of Gels at Various Temperatures

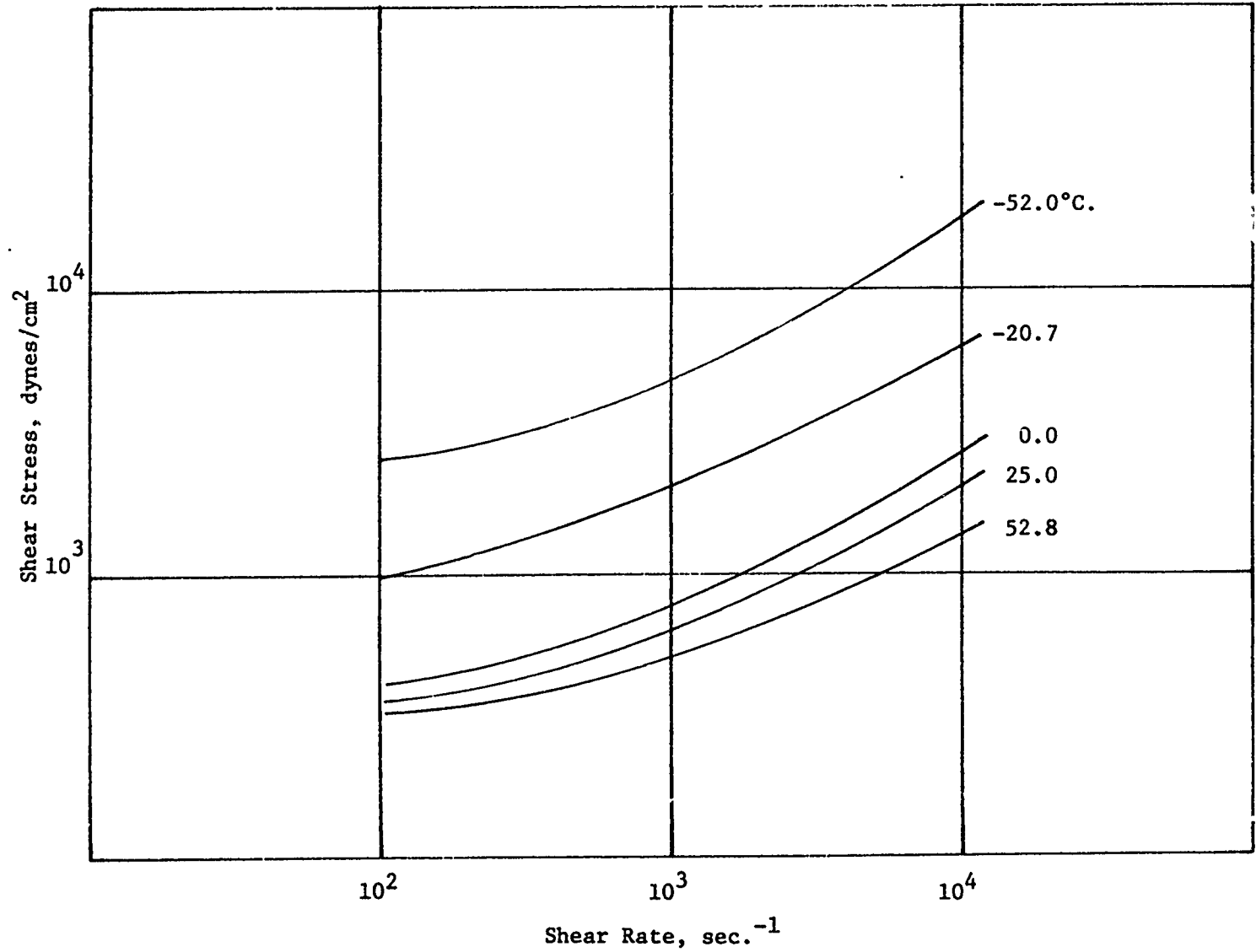


Fig. 2 - Shear Rate vs. Shear Stress at Various Temperatures - Gel A

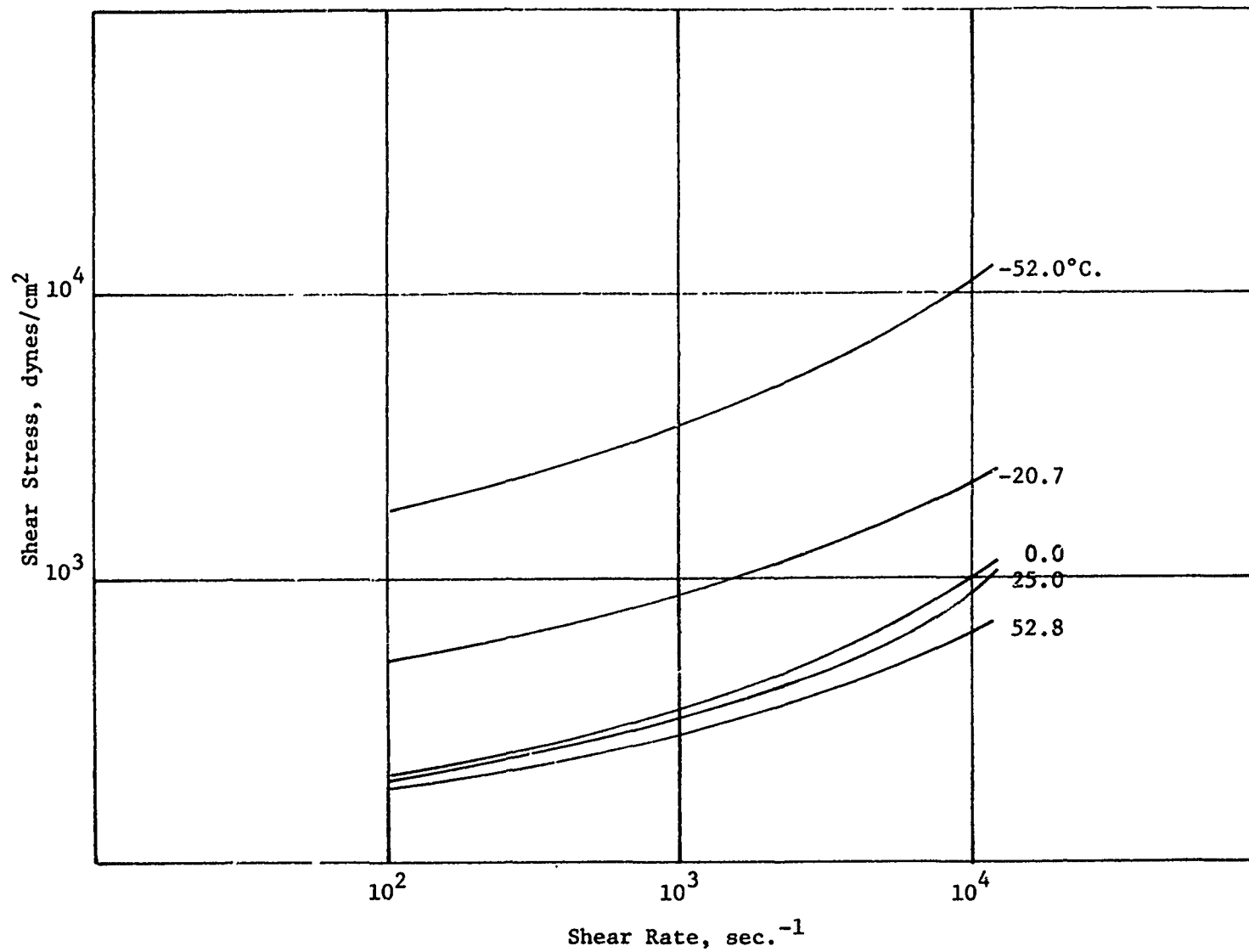


Fig. 3 - Shear Rate vs. Shear Stress at Various Temperatures, Gel B

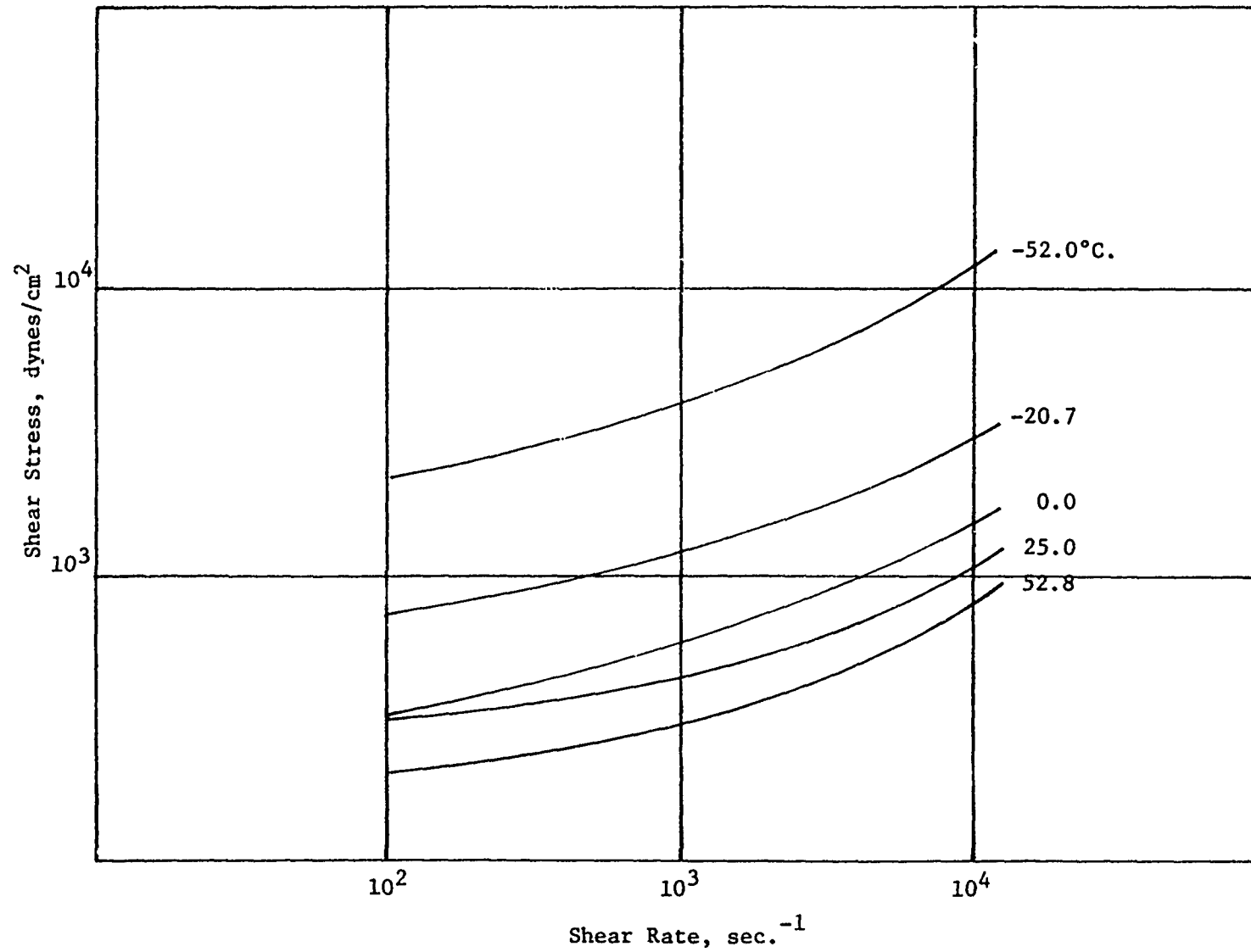


Fig. 4 - Shear Rate vs. Shear Stress at Various Temperatures - Gel C

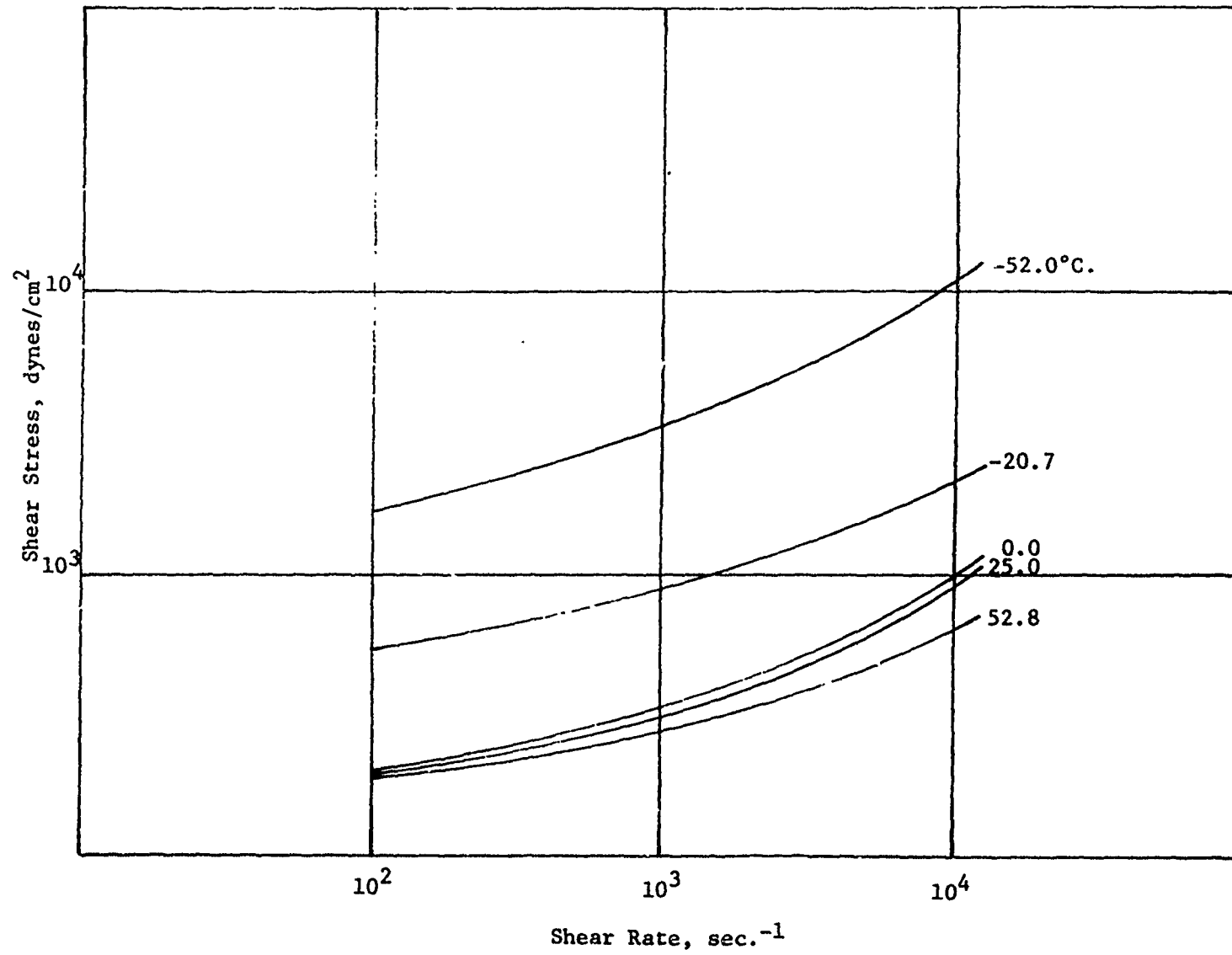


Fig. 5 - Shear Rate vs. Shear Stress at Various Temperatures - Gel D



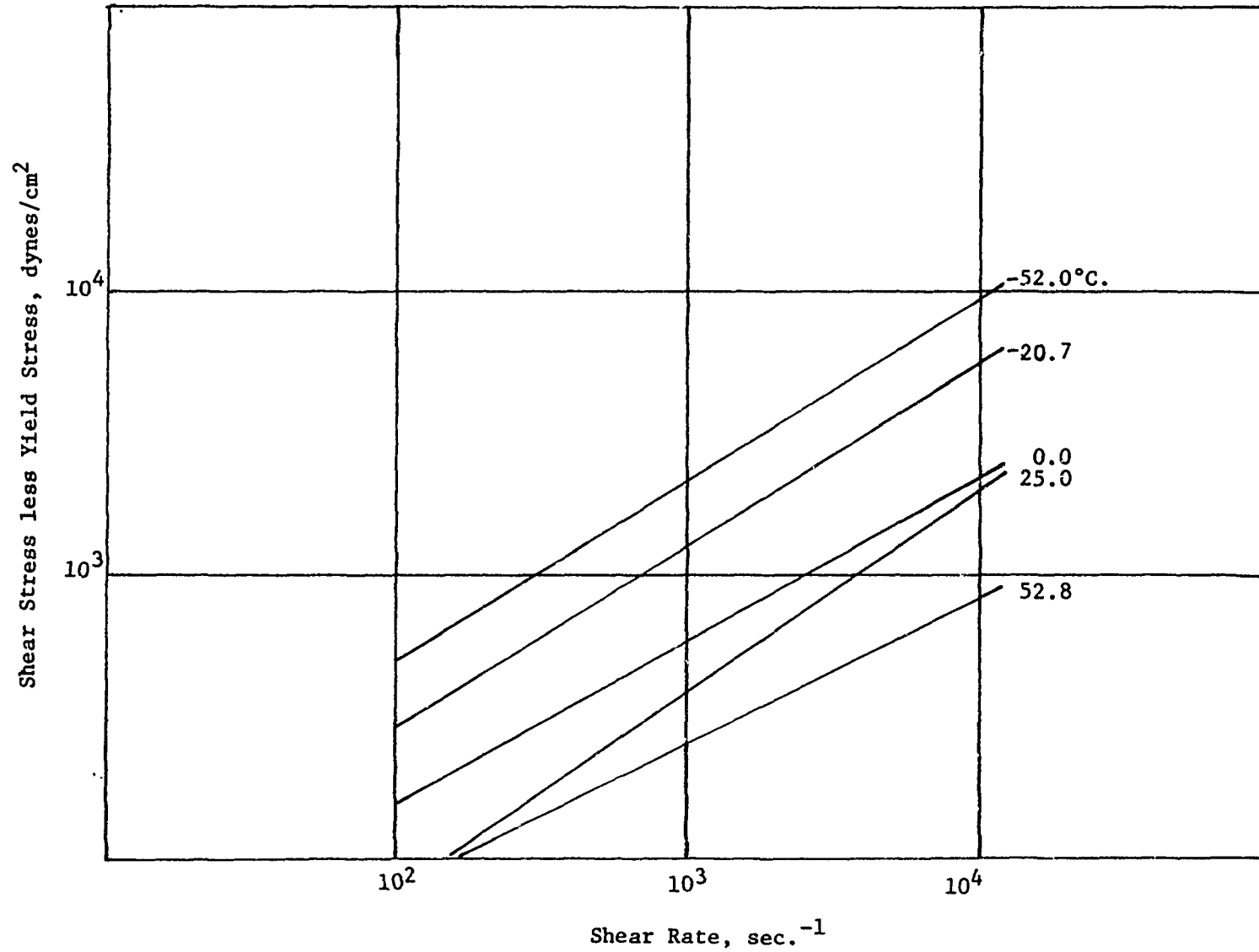


Fig. 6 - Shear Rate vs. (Shear Stress less Yield Stress) at Various Temperatures - Gel A

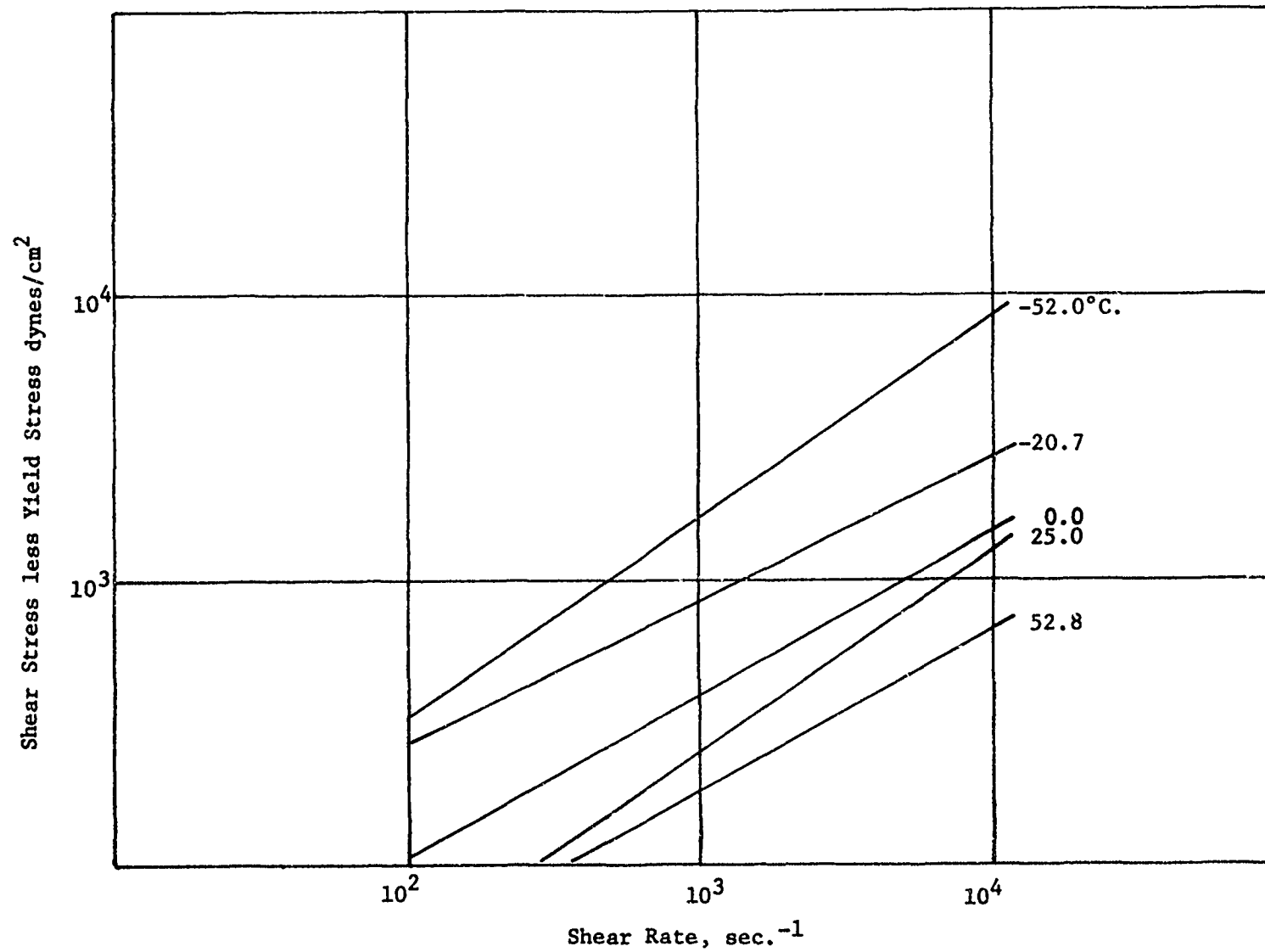


Fig. 7 - Shear Rate vs. (Shear Stress less Yield Stress) at Various Temperatures - Gel. B

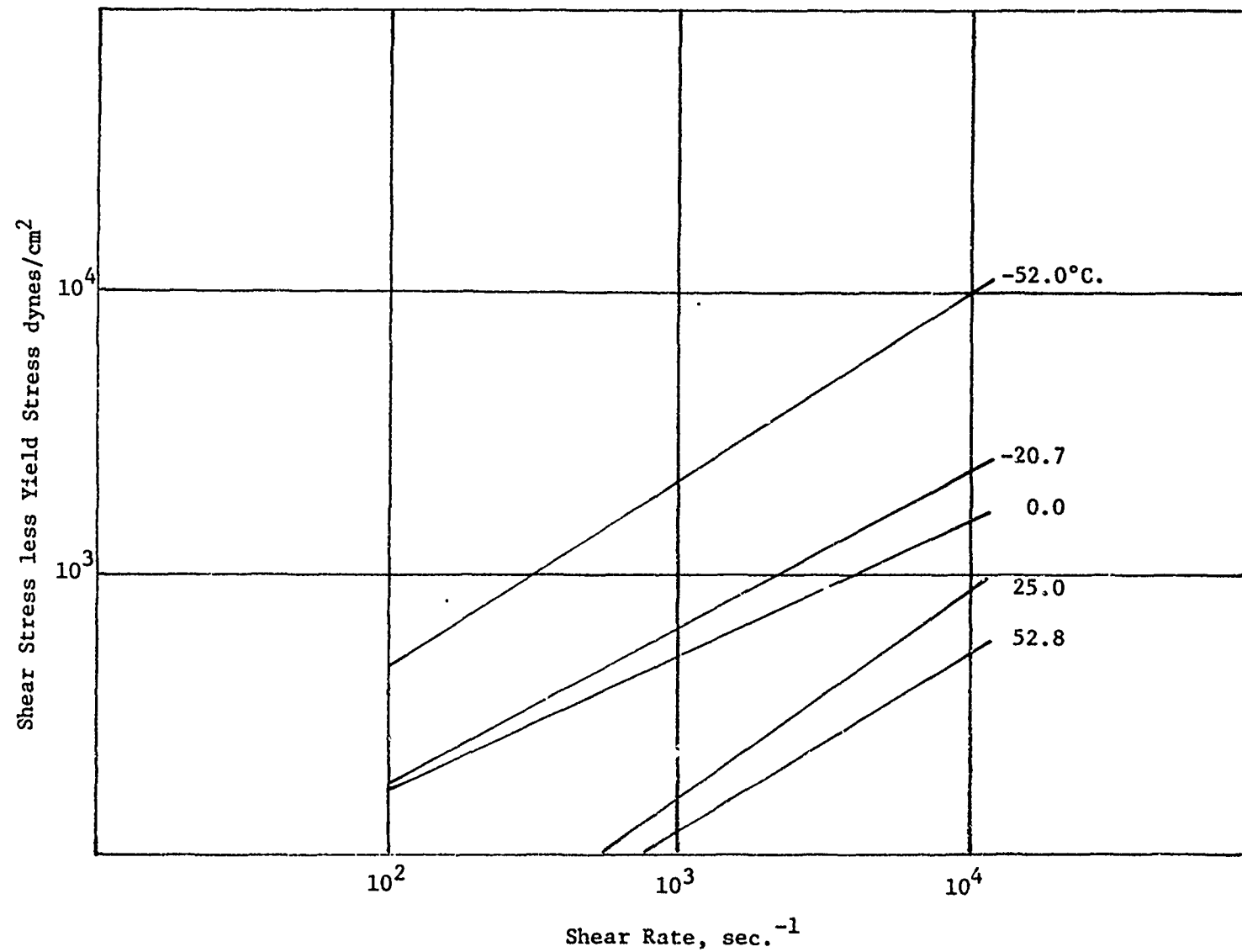


Fig. 8 - Shear Rate vs. (Shear Stress less Yield Stress) at Various Temperatures - Gel C

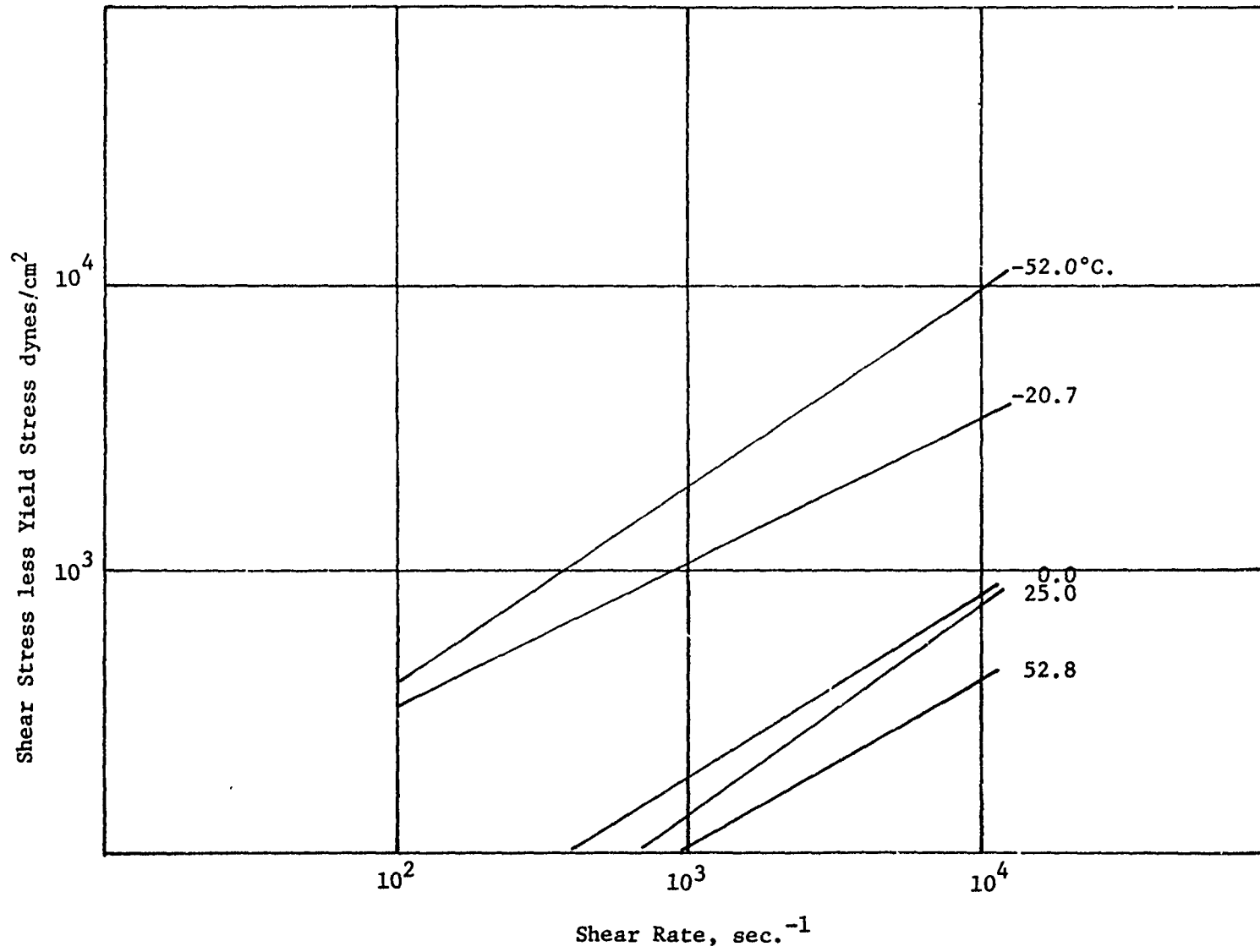


Fig. 9 - Shear Rate vs. (Shear Stress less Yield Stress) at Various Temperatures - Gel D

Equation (1) may also be written as:

$$(\sigma - \psi) = k\dot{\gamma}^n \quad (2)$$

which is its more familiar form, commonly referred to in rheology as the power law.<sup>4</sup>

The data in Figures 6, 7, 8 and 9 were analyzed by the method of least squares. The constants in Equation (1) are given in Tables 2 and 3. They hold true for the gelled fuel within the concentration range of 1.11 to 2.73%, the temperature range of -52°C. to 53°C., and shear rates from 75 sec.<sup>-1</sup> to 12,000 sec.<sup>-1</sup>. A more detailed mathematical analysis of the data is given in Appendix A.

While the logarithmic plots represented by Equation (1) conveniently relate the shear stress to shear rate under various conditions, one finds it difficult not to speculate on the usefulness or the significance of the slope (n) and intercept (k) of the plot (Appendix A). We believe that these functions may aid the estimation of the flow rate of gels in pipes.

Wohl<sup>5</sup> had proposed an equation characterizing the flow of non-Newtonian fluid as:

$$Q/\pi R^3 = 1/\sigma_w \int_0^{\sigma_w} \sigma_a^2 F(\sigma_a) d\sigma_a \quad (3)$$

where: Q = volumetric flow rate

R = radius of pipe

$\sigma_w$  = shear stress at wall of pipe

$\sigma_a$  = shear, stress in axial direction

at radius r.

TABLE 2

THE TEMPERATURE AND CONCENTRATION EFFECT ON THE VALUES OF SLOPE (n)

SLOPE (n)  $\times 10^{-2}$

<u>TEMP.</u>	<u>Concentration, Weight %</u>			
<u>°C.</u>	<u>2.73</u>	<u>2.63</u>	<u>1.67</u>	<u>1.11</u>
52.8	62.0 $\pm$ 2.6	57.7 $\pm$ 0.7	61.9 $\pm$ 4.9	49.4 $\pm$ 5.3
25.0	72.1 $\pm$ 2.3	68.6 $\pm$ 3.9	73.3 $\pm$ 3.1	70.4 $\pm$ 3.3
0.0	56.5 $\pm$ 0.6	55.7 $\pm$ 1.5	63.7 $\pm$ 2.7	57.1 $\pm$ 2.3
-20.7	65.0 $\pm$ 1.1	50.5 $\pm$ 2.1	58.0 $\pm$ 4.9	49.0 $\pm$ 5.8
-52.0	64.7 $\pm$ 2.1	65.0 $\pm$ 2.2	66.7 $\pm$ 2.4	73.9 $\pm$ 3.8

TABLE 3

THE TEMPERATURE AND CONCENTRATION EFFECT ON THE VALUES OF INTERCEPT (k)

<u>TEMP.</u>	<u>INTERCEPT, k <math>\times 10^2</math></u>			
<u>°C.</u>	<u>Concentration, Weight %</u>			
	<u>2.73</u>	<u>2.03</u>	<u>1.67</u>	<u>1.11</u>
52.8	55.0 $\pm$ 8.5	54.5 $\pm$ 2.4	24.5 $\pm$ 12.8	63.7 $\pm$ 17.7
25.0	41.1 $\pm$ 7.3	35.3 $\pm$ 11.9	1.5 $\pm$ 9.2	2.5 $\pm$ 10.1
0.0	108.1 $\pm$ 5.8	95.4 $\pm$ 4.8	61.8 $\pm$ 7.3	55.4 $\pm$ 6.9
-20.7	115.3 $\pm$ 10.6	142.8 $\pm$ 71.0	105.7 $\pm$ 16.4	157.4 $\pm$ 19.1
-52.0	138.7 $\pm$ 6.5	138.6 $\pm$ 7.0	132.0 $\pm$ 7.5	103.6 $\pm$ 11.6

This equation (3) can be modified (Appendix B) to allow its application to AB gelled fuel systems.

The flow rates of Gel C at 25°C. were calculated for 1-in. and 2-in. diameter pipes and the results are shown in Figure 10. The mathematical exercise described herein and in Appendices A and B exemplifies the potential application of the logarithmic plot beyond its obvious value in stress-rate relationships.

Thixotropy - The AB gelled fuel responds quickly to shearing action as was demonstrated in terms of the resultant shear stress (Figure 11). The shear stress declines as the shearing action persists, even though the rate of shear is constant. This is the phenomenon of thixotropy, and it is a useful property because it facilitates the transfer of gelled fuel.

In Figure 11, Gel A exhibits the greatest thixotropy while Gel D shows the least at a temperature of 25°C. and a constant shear rate of 525 sec.<sup>-1</sup>. The more thixotropic the gel, the longer will be the shearing time required to reach an asymptotic shear stress value. The time required for Gel A to reach one-half of its asymptotic shear stress of 550 dynes was 29 seconds; the time for Gel C to reach its final shear stress of 210 dynes was 20 sec.

This shear thinning, however, is reversible. After a short period of rest the gels completely regain the original viscosity, as is illustrated in Figure 12. The gels at higher concentrations recover less rapidly than those at lesser concentrations. Gel A (2.73%) requires 8 minutes to reach its original stress value at the shear rate of 3.3 sec.<sup>-1</sup>; whereas Gel C requires 5 minutes. The time required to shear thin is relatively insensitive to the shear rate.

The shear stress-shear rate relationship of the gel is dependent not only upon time but also its previous shearing history. A thixotropic system can be studied under gradually increasing and then decreasing rate of shear without waiting for equilibrium to be reached. The so-called hysteresis loops obtained from such measurements are shown in Figures 13, 14, 15, 16. In Figure 13, as the shear rate is gradually increased, the initial shear stress is large. When the shear rate reaches beyond 2000 sec.<sup>-1</sup>, the change in shear stress is nearly constant. When the shear rate is reduced gradually, the corresponding shear stress is significantly less than the stresses developed along the upward path. The initial high stress reflects the structural resistance of the solution to the shearing action. As the structure is disrupted by the shearing, its resistance to shear becomes weaker and hence the reduced rate of increase in stresses. The difference in stresses between the upward and downward path indicates the extent of structural disruption. There is much less structural disruption in the gels of lower concentrations (Figures 15, 16) than in cases of higher concentrations (Figures 13, 14).

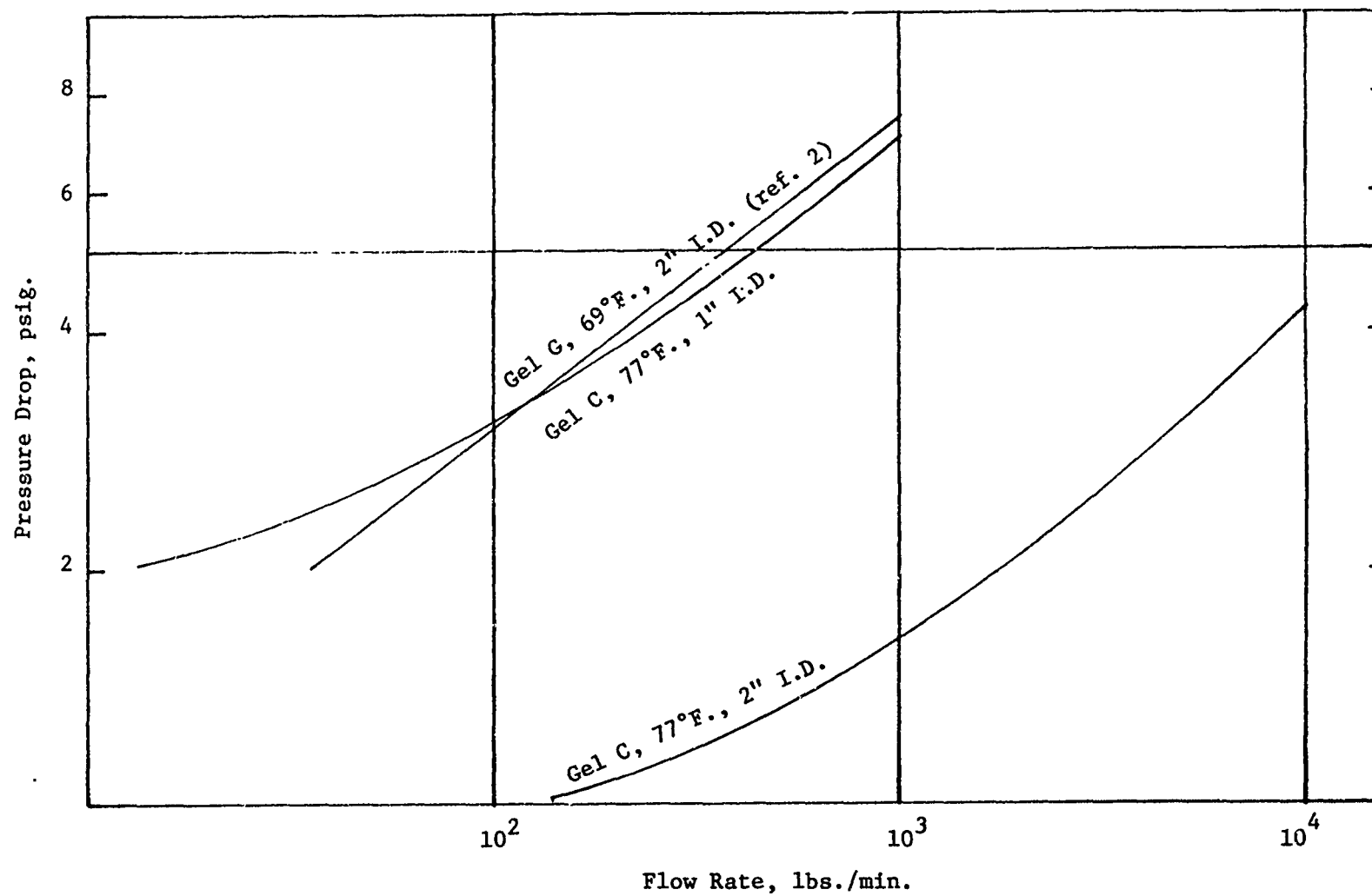


Fig. 10 - Calculated Flow Rate of Gel Through 10-Foot-Long Straight Pipe



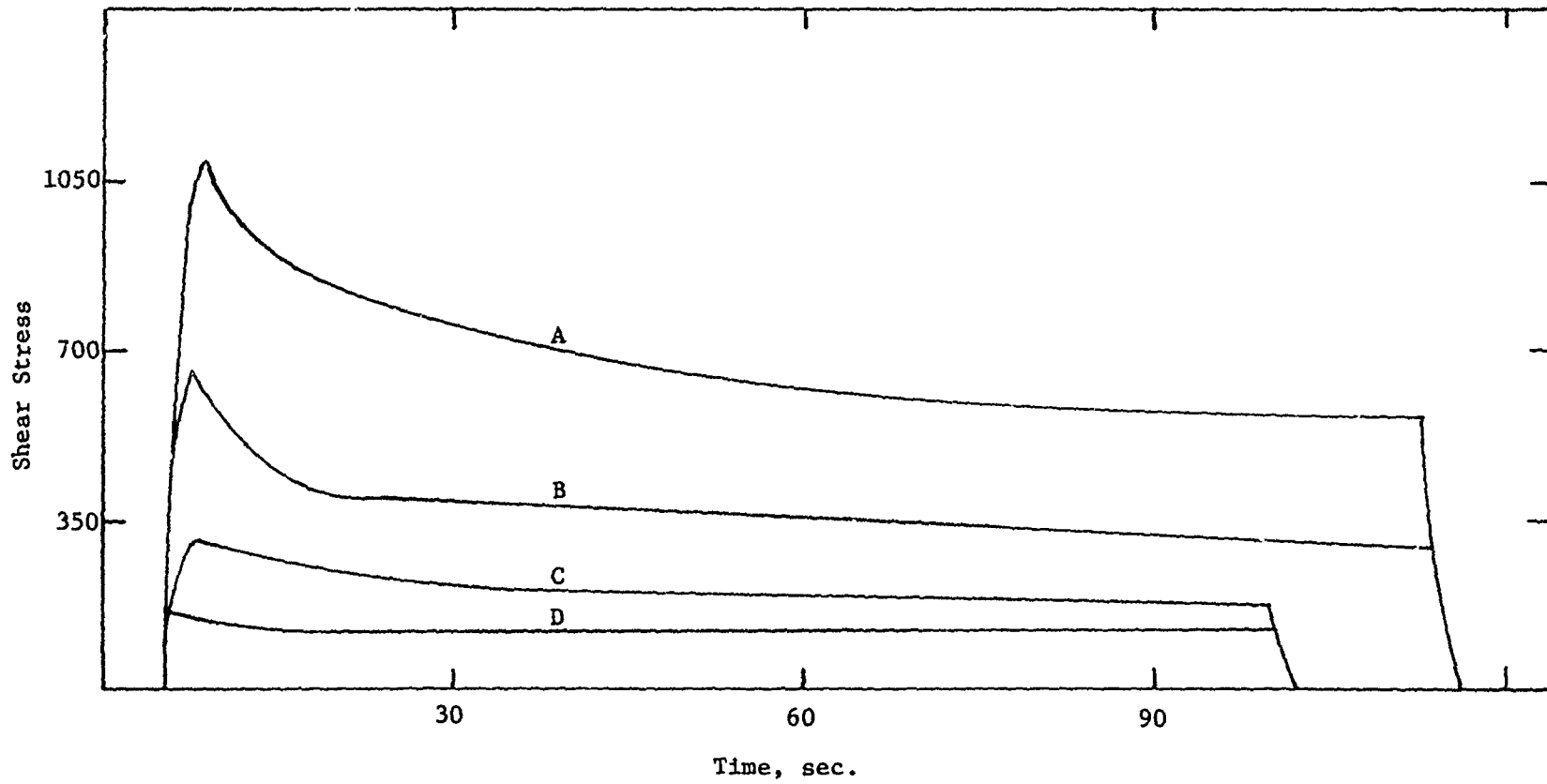


Fig. 11 - Thixotropy of Gels A, B, C and D at 25°C. Temperature

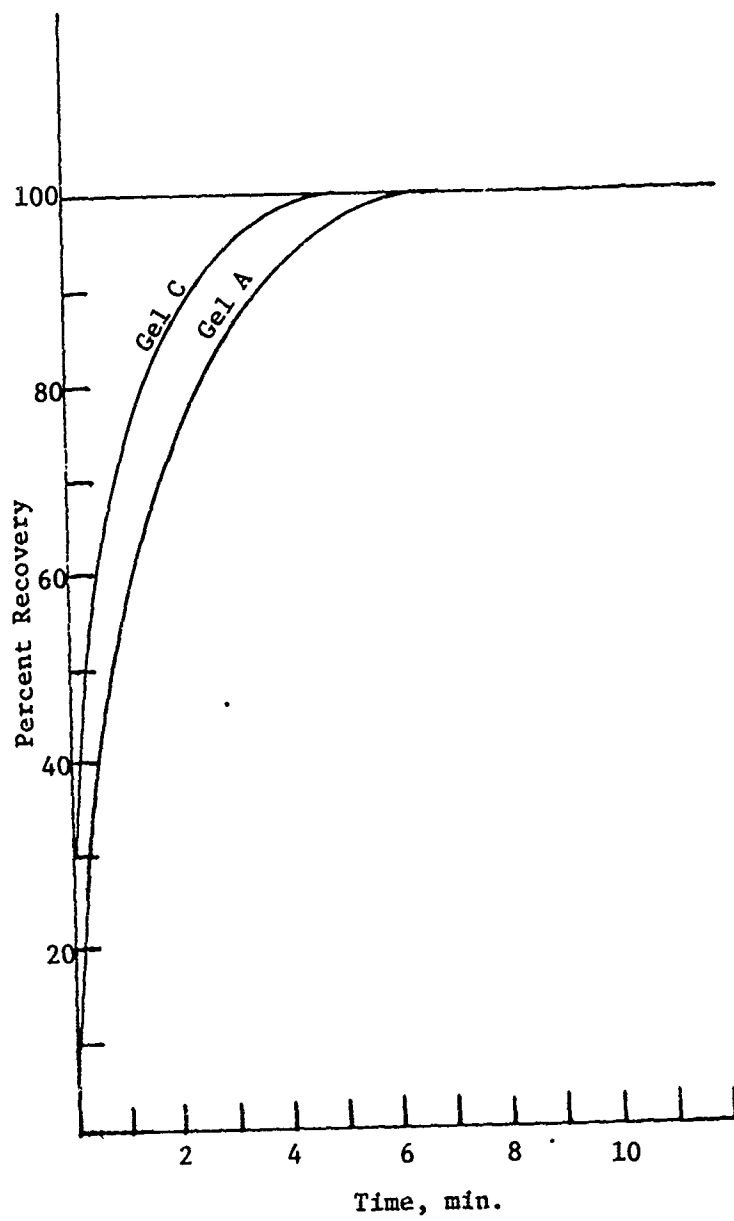


Fig. 12 - Stress Recovery of Gels

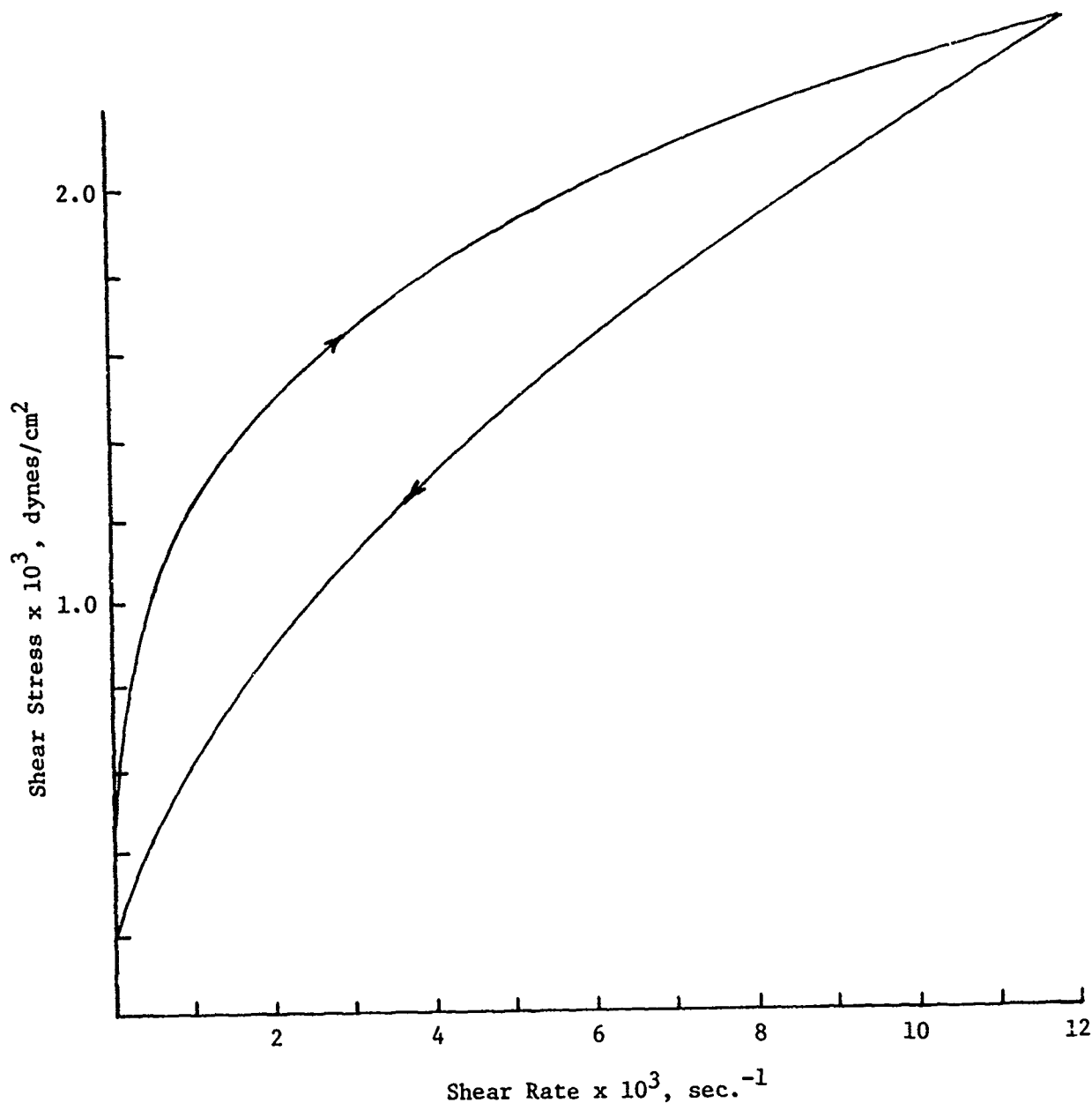


Fig. 13 - Hysteresis Loop of Gel A

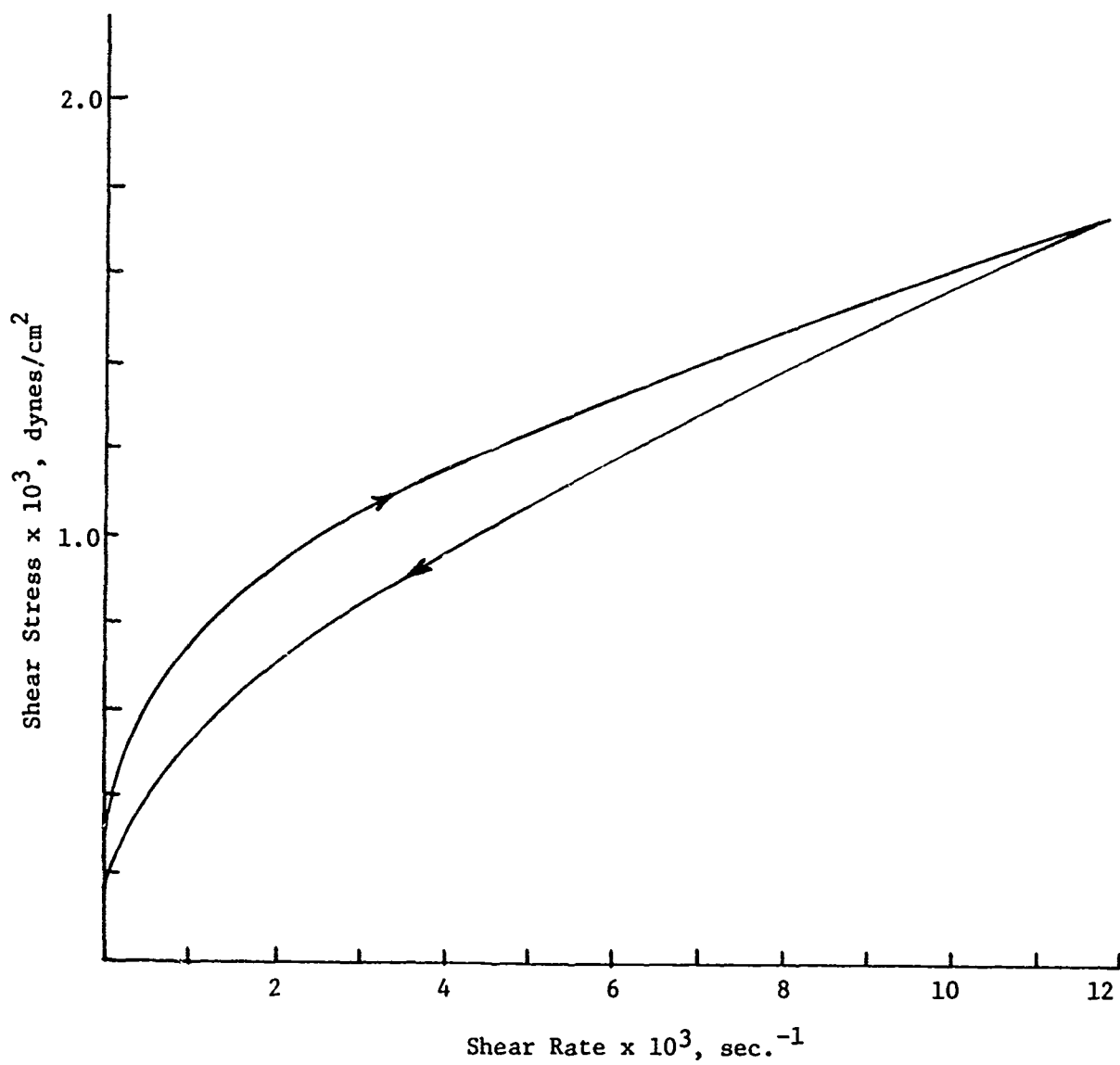


Fig. 14 - Hysteresis Loop of Gel B

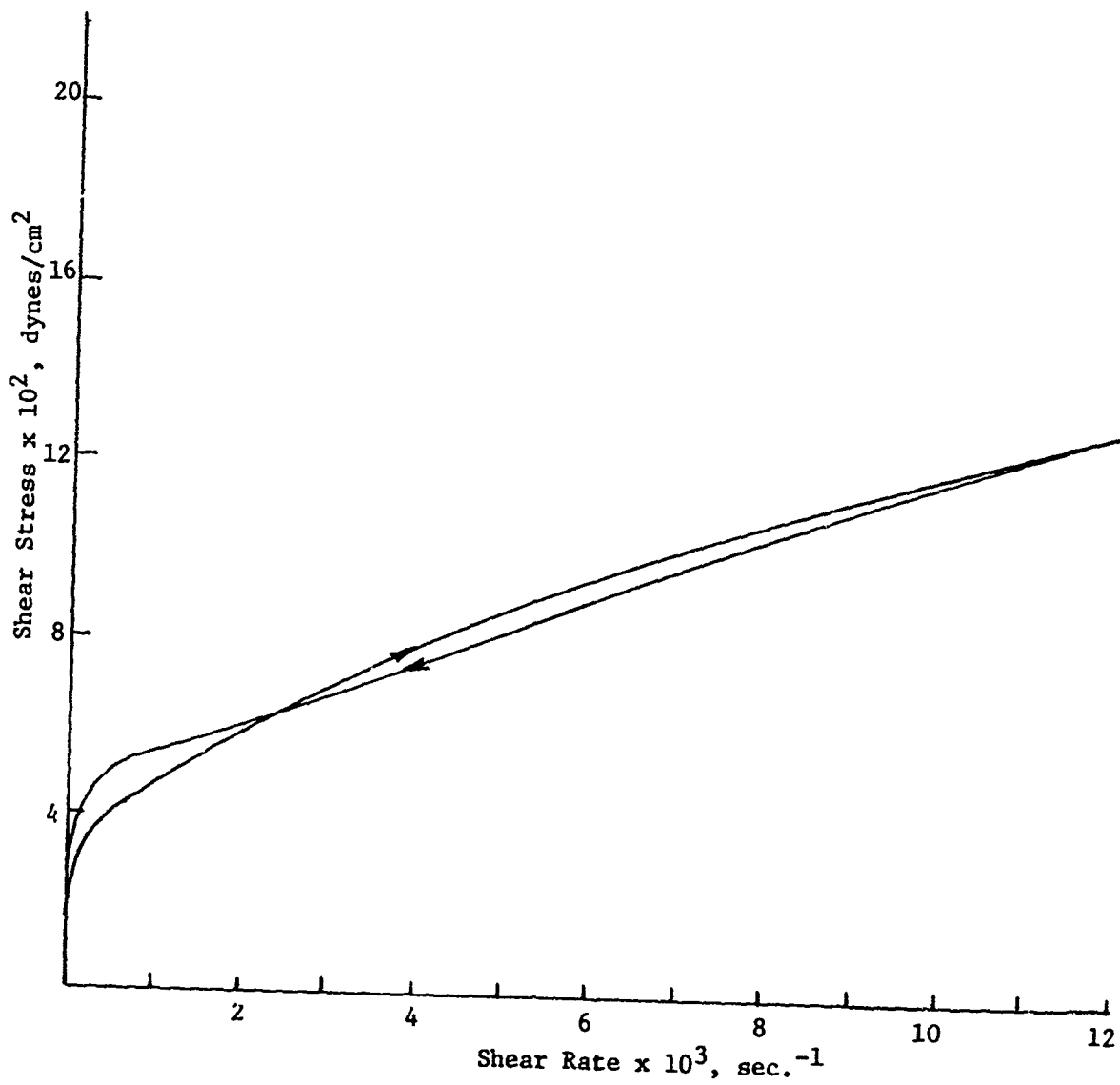


Fig. 15 - Hysteresis Loop of Gel C

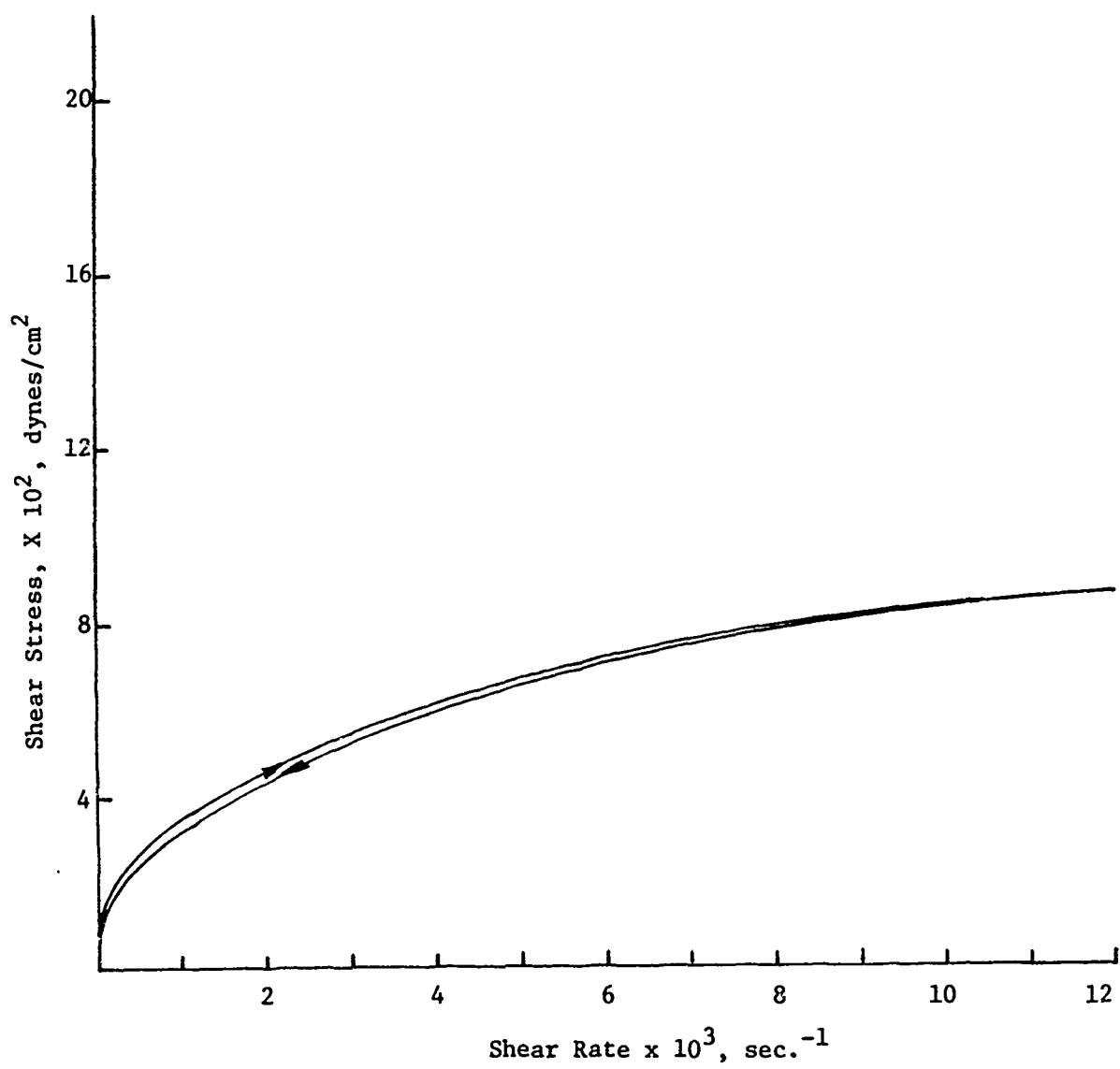


Fig. 16 - Hysteresis Loop fo Gel D

Viscoelasticity - The difficulty in relating rheological measurements to crash-fire safety tests has been quite apparent to investigators for some time. Gelled fuels of similar viscosity and yield stress do not produce similar safety scores. It is also evident that gels have various degrees of structural coherence that significantly affect their flow behavior, their tendency to adhere to the walls of containers, and their misting pattern under impact. So far this degree of structural coherence has eluded quantitative evaluation. We have attempted to deal with the evaluation of this structural coherence under the rather general term, "viscoelasticity."

A viscoelastic<sup>6</sup> substance exhibits both viscous and elastic properties. For example, when it is subjected to force, it deforms continuously (viscosity), but when the force is removed it tends to return spontaneously, though not completely to its original state (elasticity).

A number of sophisticated instruments<sup>7</sup> are available for the measurement of viscoelasticity. In order to meet the contract deadline, it was decided to carry out the preliminary study of viscoelasticity on the available Rotovisco-Viscometer with its viscoelastic attachment.

Viscoelasticity in this case is manifested by two parameters, the equilibrium stress ( $\sigma_{ec}$ ) and the relaxation time ( $\tau_{rx}$ ). They were arbitrarily chosen for the time being and there could be others added latter for consideration. When an applied shear at constant rate is suddenly terminated, the induced stress in the gel decays rapidly. The stress does not decay to zero but to a final finite level. This is not a commonly observed occurrence in fluids and the final stress at equilibrium is termed the "equilibrium stress." The time required for the stress to decay to a predetermined fraction ( $1/e$  or 36.9%) of the stress differential ( $\sigma_0 - \sigma_{ec}$ ) is defined as the relaxation time. The symbol  $\sigma_0$  stands for the steady state stress at constant shear rate just prior to the cessation of the shearing action. Figures 17, 18, 19 and 20 depict the viscoelastic behavior of Gel A at 10° and 40°C. Figures 21 to 23 show the influence of concentration on equilibrium stress. Equilibrium stress varies directly with gel concentration, and has no measurable value in gels more dilute than Gel C. The relationships of the two viscoelastic parameters with gel concentration and temperature are shown in Table 4 and Table 5. The equilibrium stress is dependent upon temperature and concentration but is independent of shear rate up to a critical value where it becomes zero.

The equilibrium stress of the gels above the critical shear rate and temperatures is zero. Gels above these temperatures (sheared above the critical rate) flow as viscous non-Newtonian liquids and exhibit no viscoelasticity.

The relaxation time is a function of concentration, temperature and shear rate. In all cases where the equilibrium stress is nil, a measurable relaxation time, e.g. 1.2 sec., was observed. This small measurement of 1.2 sec. can be considered as some limiting constant of the instrument.

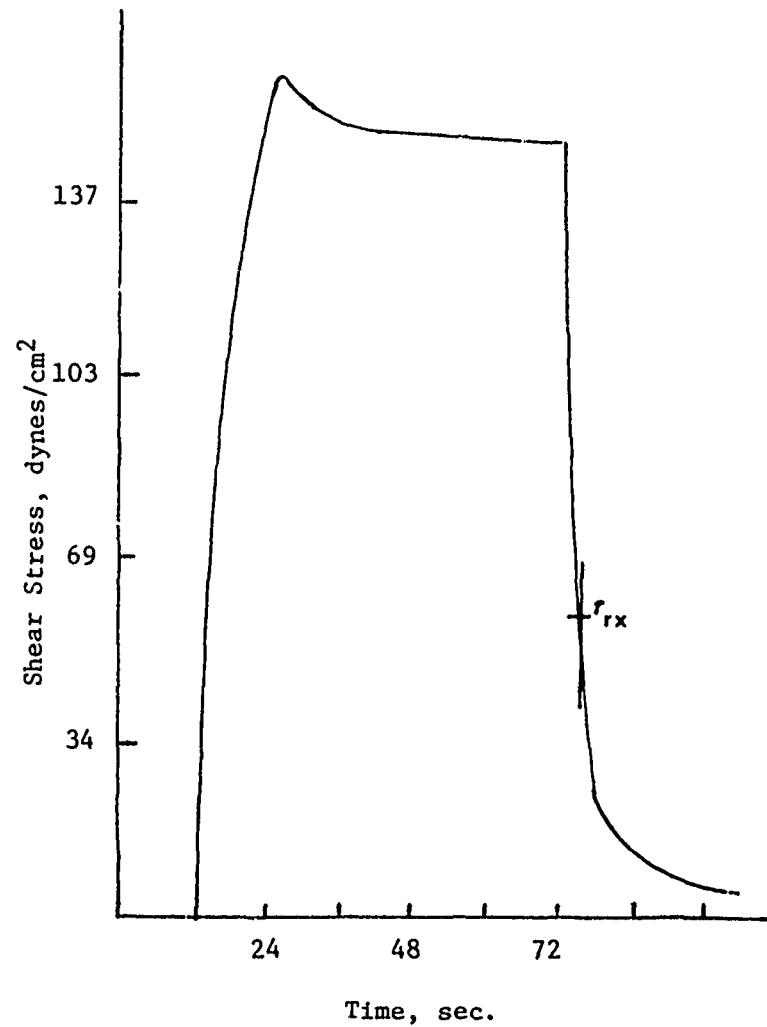


Fig. 17 - Viscoelasticity Measurements  
of Gel A - 20 sec.<sup>-1</sup> Shear  
Rate at 10°C. Temperature

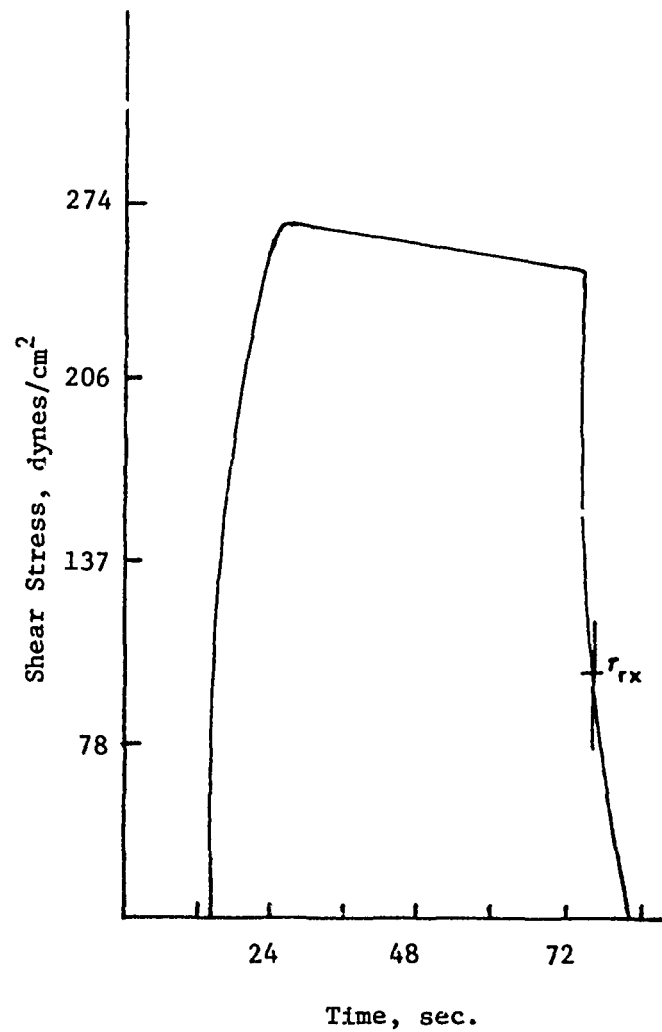


Fig. 18 - Viscoelasticity Measurements  
of Gel A - 264 sec.<sup>-1</sup> Shear  
Rate at 10°C. Temperature



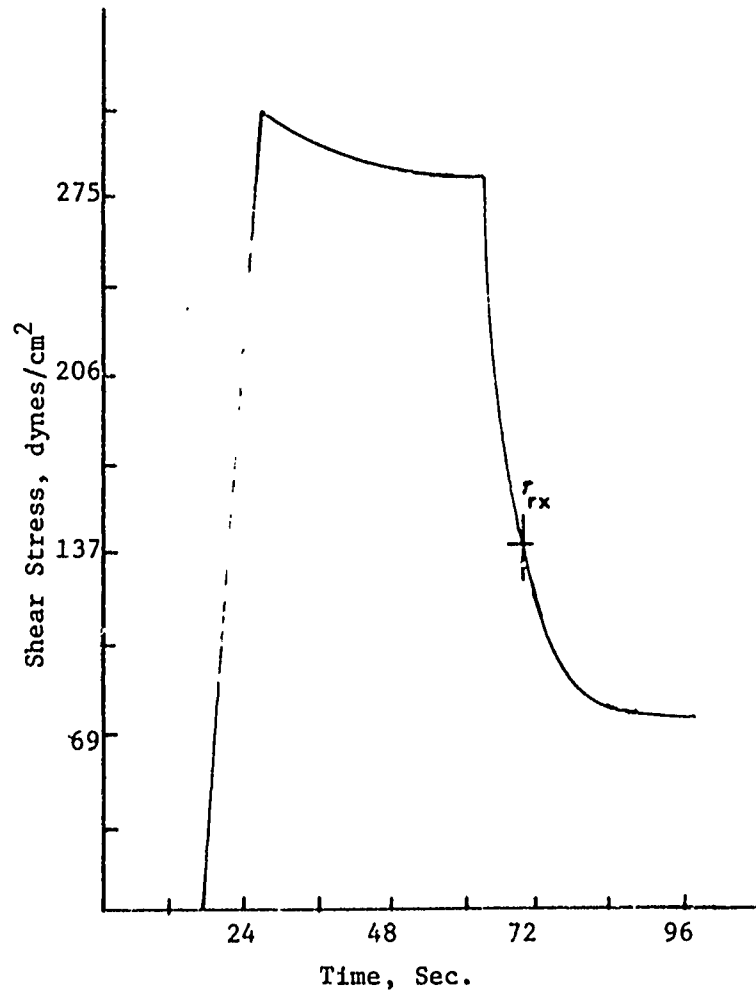


Fig. 19 - Viscoelasticity Measurements of Gel A - 20 sec.<sup>-1</sup> Shear Rate at 40°C. Temperature

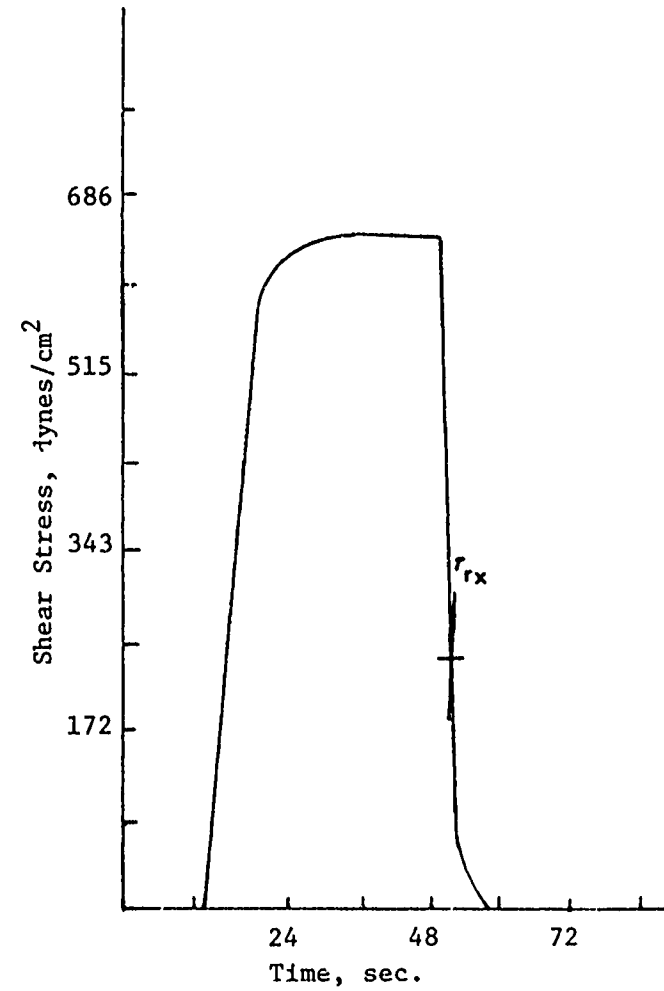


Fig. 20 - Viscoelasticity Measurements of Gel A - 264 sec.<sup>-1</sup> Shear Rate at 40°C. Temperature

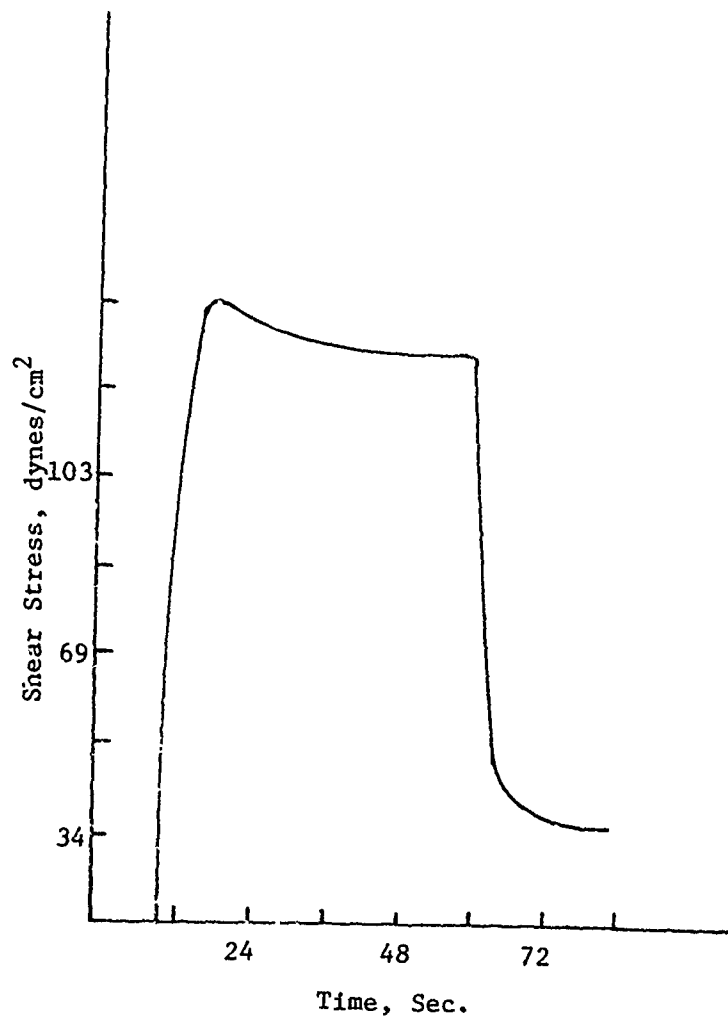


Fig. 21 - Viscoelasticity Measurements of Gel B - 20 sec.<sup>-1</sup> Shear Rate at 10°C. Temperature

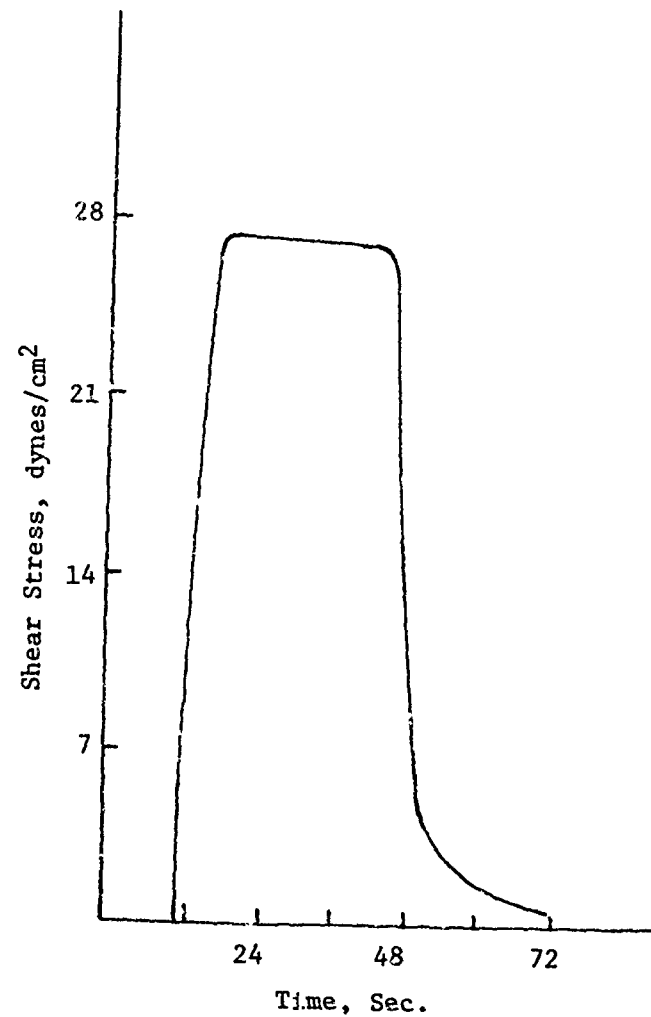


Fig. 22 - Viscoelasticity Measurements of Gel C - 20 sec.<sup>-1</sup> Shear Rate at 10°C. Temperature

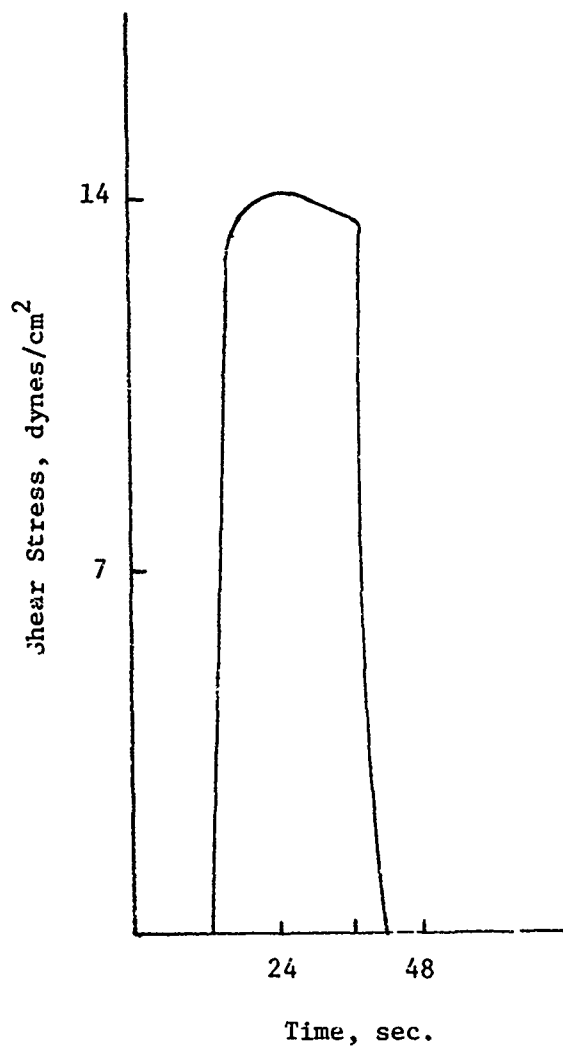


Fig. 23 - Viscoelasticity Measurements of Gel D - 20 sec.<sup>-1</sup> Shear  
Rate at 10°C. Temperature

TABLE 4

EQUILIBRIUM STRESS AT VARIOUS TEMPERATURES AND CONCENTRATION LEVELS

SHEAR RATE Sec. <sup>-1</sup>	C O N C E N T R A T I O N   O F   G E L L I N G   A G E N T , W E I G H T   P E R   C E N T											
	<u>2.73</u>			<u>2.03</u>			<u>1.67</u>			<u>1.11</u>		
	T E M P E R A T U R E ,   ° C .											
	40	25	10	40	25	10	40	25	10	40	25	10
E Q U I L I B R I U M   S T R E S S ,   D Y N E S / c m <sup>2</sup>												
3.3	3	19	69	0	16	17	0	0.8	4.5	0	0	0
6.6	3	19	69	0	16	17	0	0.8	4.5	0	0	0
9.8	3	19	69	0	16	17	0	0.8	4.5	0	0	0
19.6	3	19	69	0	16	17	0	0.8	4.5	0	0	0
29.4	3	19	69	0	16	17	0	0	0	0	0	0
58.8	3	19	69	0	0	0	0	0	0	0	0	0
88.2	0	0	69	0	0	0	0	0	0	0	0	0
176	0	0	0	0	0	0	0	0	0	0	0	0

TABLE 5

RELAXATION TIME AT VARIOUS TEMPERATURE AND CONCENTRATION LEVELS

Shear Rate sec. <sup>-1</sup>	Concentration of Gelling Agent						
	<u>2.73</u>	<u>2.03<sup>*</sup></u>			<u>1.67<sup>*</sup></u>		
	Temperature, °C.						
	<u>40</u>	<u>25</u>	<u>10</u>	<u>25</u>	<u>10</u>	<u>25</u>	<u>10</u>
	Relaxation Time $\tau_{rx}$ , sec.						
3.3	--	3.6	4.8	3.6	4.2	1.8	3.0
6.6	3.0	3.0	4.8	2.4	3.0	1.8	2.4
9.8	3.6	2.4	3.6	2.4	2.4	1.8	2.4
19.6	2.4	3.0	3.6	2.0	2.4	1.8	1.8
29.4	2.4	1.2	1.8	2.0	1.8	1.2	1.2
58.8	2.4	1.8	1.8	1.2	1.2	1.2	1.2
88.2	1.2	1.2	1.2	1.2	1.2	1.2	1.2
176	1.2	1.2	1.2	1.2	1.2	1.2	1.2

$\tau_{rx} = 1.2$  is equivalent to the rheogram illustrated in Figure 19 and 21.

\*Values of  $\tau_{rx}$  for gels containing 1.67 and 2.03% at 40°C. were 1.2 sec. and gel contain 1.11% at 10, 25 and 40°C. were 1.2 sec. or less.

It is generally agreed that the misting of the fuel during a crash is the primary fire hazard. The NAFEC impact test, which involves propelling a quantity of fuel under controlled conditions against a screen set in front of ignition sources, is one convenient and useful method for simulating and assessing such fire hazard. The extent of combustion is monitored by measurement of the radiant heat energy. The finer the fuel mist, the more intense is the radiant energy from the fire.

A plot (Figure 24) of viscoelasticity, represented by the relaxation time, versus the radiation heat flux suggests that gels having a relaxation time higher than 1.6 sec. do not ignite. Below this value the tendency to mist and form a fireball increases drastically. The relationship between the relaxation time and radiant heat flux is empirical but could be used as a convenient criterion of the safety property of a gel.

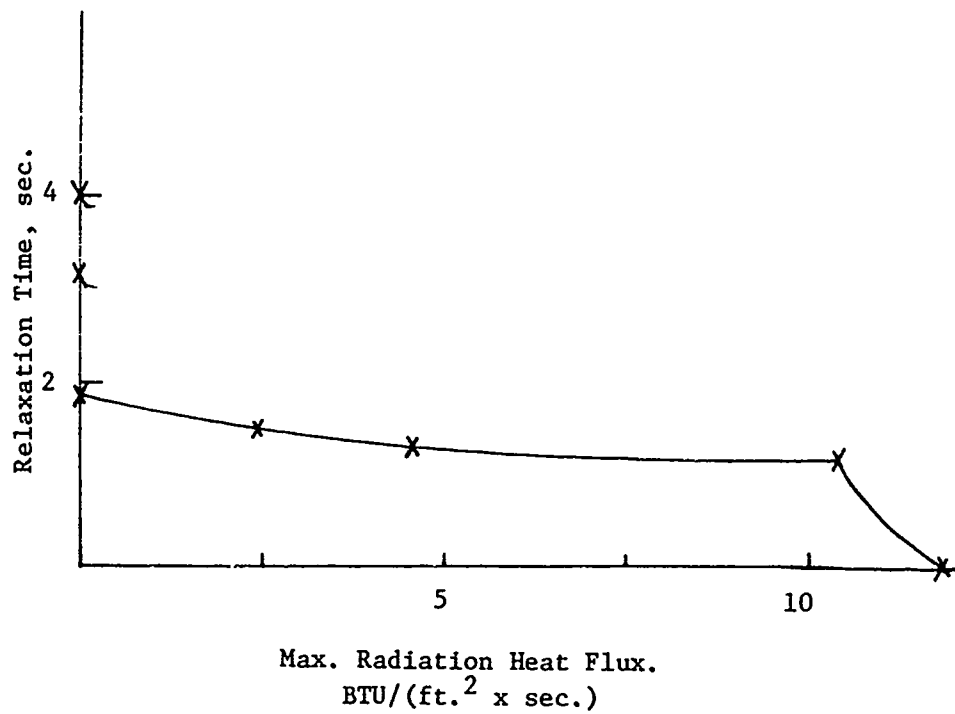


Fig. 24 - Correlation of Viscoelasticity with Crash-Fire Safety

## Experimental Procedures

Gelled Fuel Preparation - Gelled fuel samples were prepared by blending the Anheuser-Busch gelling agent (FAA-CL-10) with Jet A fuel at the designated concentration levels. Blending was continued until the dispersion of gelling agent was visibly uniform. The mixture was then clarified by centrifugation. The clear supernatant solution gelled within a short period.

Flow Curves Plasticity - The rheology of the gel was measured with the Haake Rotovisko viscometer. The shear stresses of the gel at shear rates from 77 to 12,000  $\text{sec.}^{-1}$  were measured with a cone (PK-I), and plate (Figure 25). The system was temperature controlled by a circulating thermostat; KT-41, Kryokool (-30 to +100°C.). For temperatures less than -25°C., it was necessary to use an auxiliary cooling coil immersed in a Dry Ice-methanol bath and in series with the thermostat. Rheological measurements at temperatures less than 0°C. were performed by enclosing the measuring systems in a plastic glove bag that was constantly flushed with dry air. The torques at various speeds were recorded as millivolts output by a Leeds and Northrup Speedomax XL 680 Recorder equipped with an AZAR range selector and five standard chart speeds. The torque was converted to shear stress and rotor speeds to shear rates by appropriate constants.

Yield Stresses - Yield stresses were measured by a star-shaped rotor (SV-II FL), and beaker (SV) (Figure 26), in a temperature-controlled assembly. The yield stress was confirmed by extrapolating the plot of  $\log \sigma$  versus  $\log \dot{\gamma}$  (Figures 2 to 5) to zero shear rate.

The shear stresses for shear rates from 3.3 to 529  $\text{sec.}^{-1}$  were measured with cylindrical rotor (MV-I or II) and beaker (MV) in a temperature-controlled assembly.

Viscoelasticity - The viscoelastic measurements were performed using rotors (MV-I or II) and beaker (MV) (Figures 27, 28). The rotor was abruptly stopped after the torque became constant at constant speed. The torque decayed with time to either zero or a finite equilibrium value. The decay of the torque with time was recorded. The time for the torque differential to decay 38% ( $100/e$ ) was measured; it was called the relaxation time.

Thixotropy - The recovery time was measured by the MV-I or II system. The gel was sheared for approximately 5 minutes or until the stress was constant at a constant speed. The rotor was stopped and the gel allowed to rest for a given time. The procedure was repeated for the different rest times. The difference between the initial shear stress after each rest period and the constant shear stress divided by the initial shear stress of the fresh sample was used to calculate the per cent recovery.



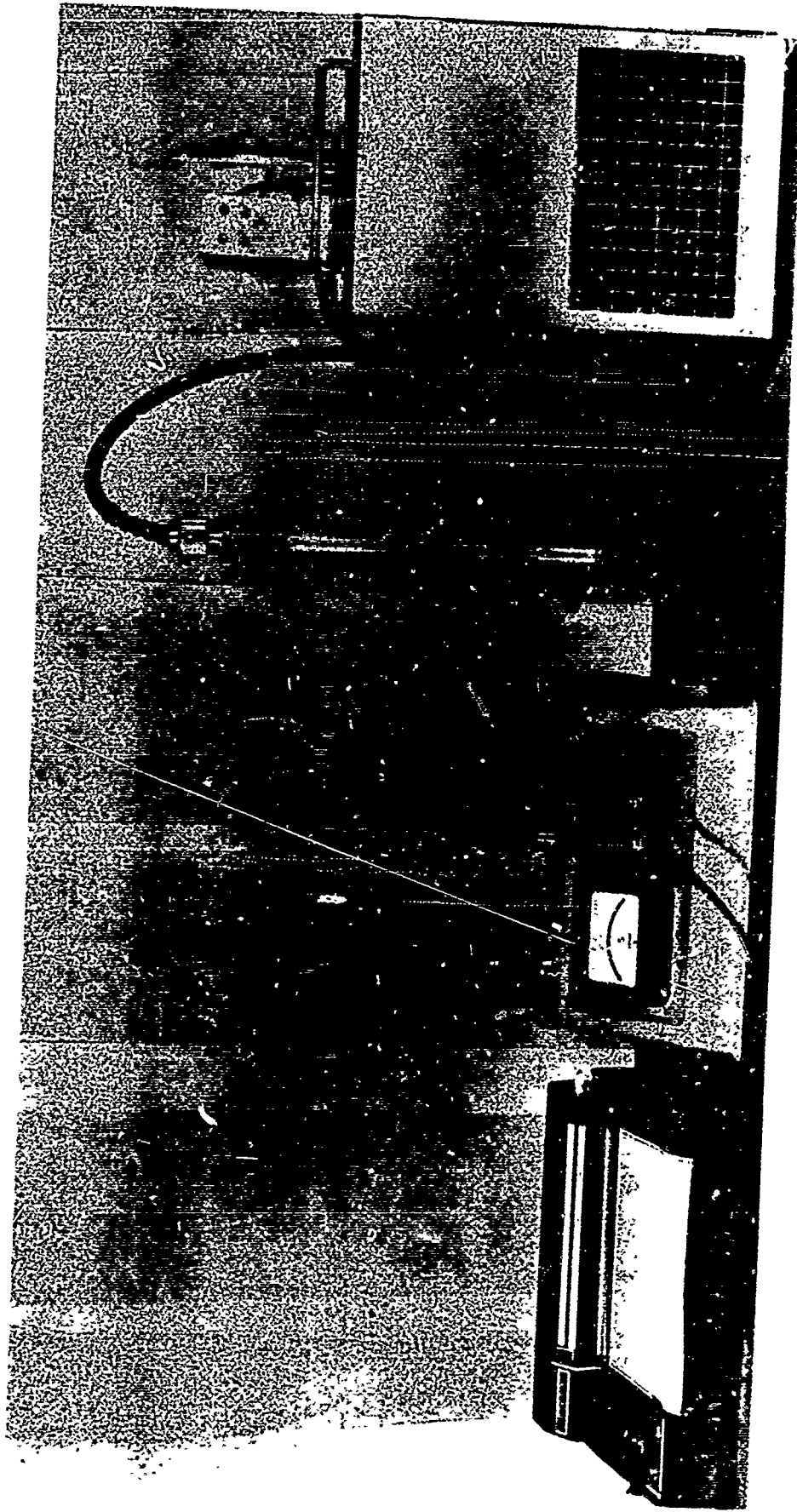


FIGURE 25. ROTOVISCO VISCOMETER WITH CONE AND PLATE ATTACHMENTS

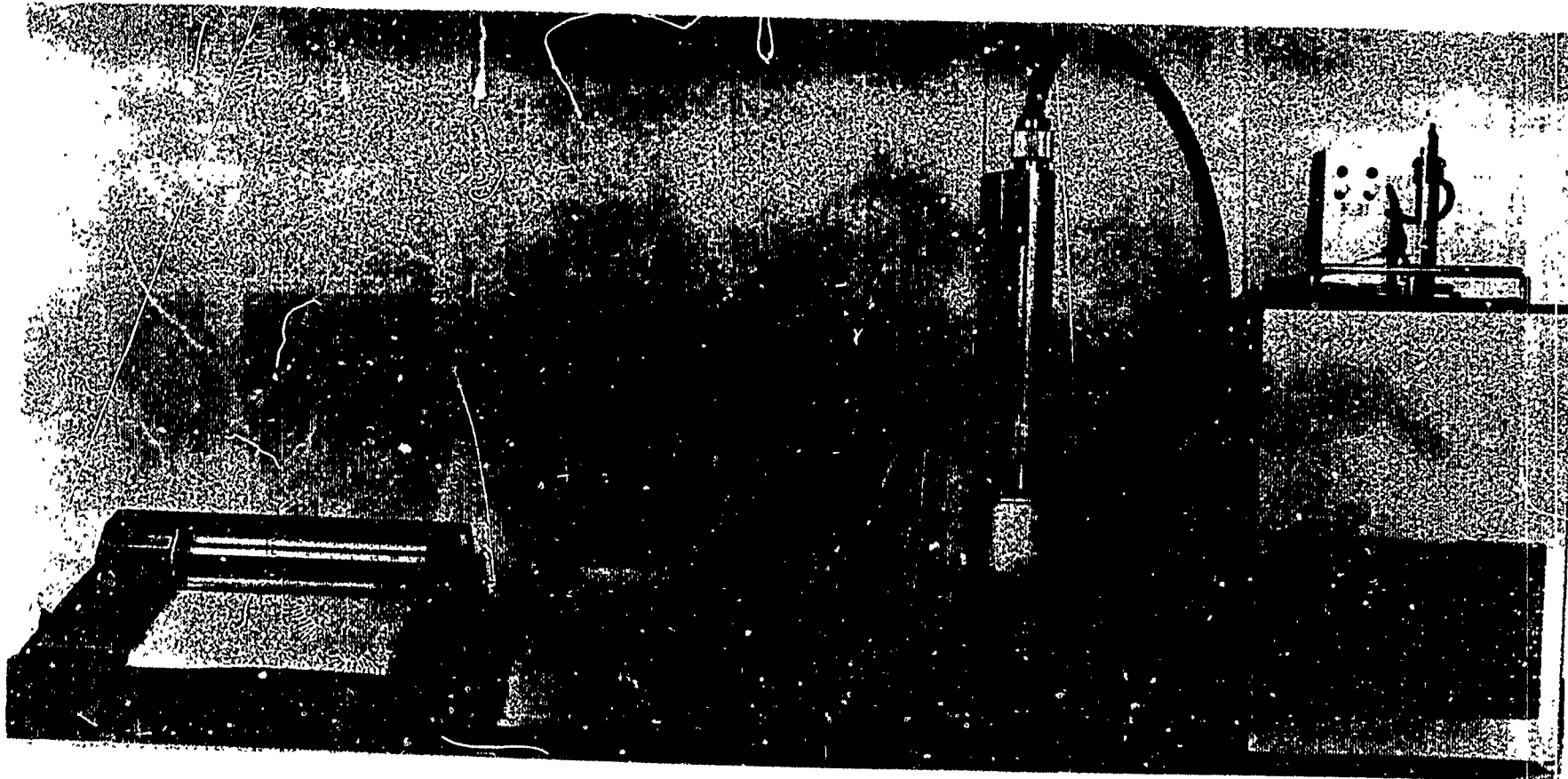


FIGURE 26. ROTOVISCO VISCOMETER WITH YIELD STRESS ATTACHMENT

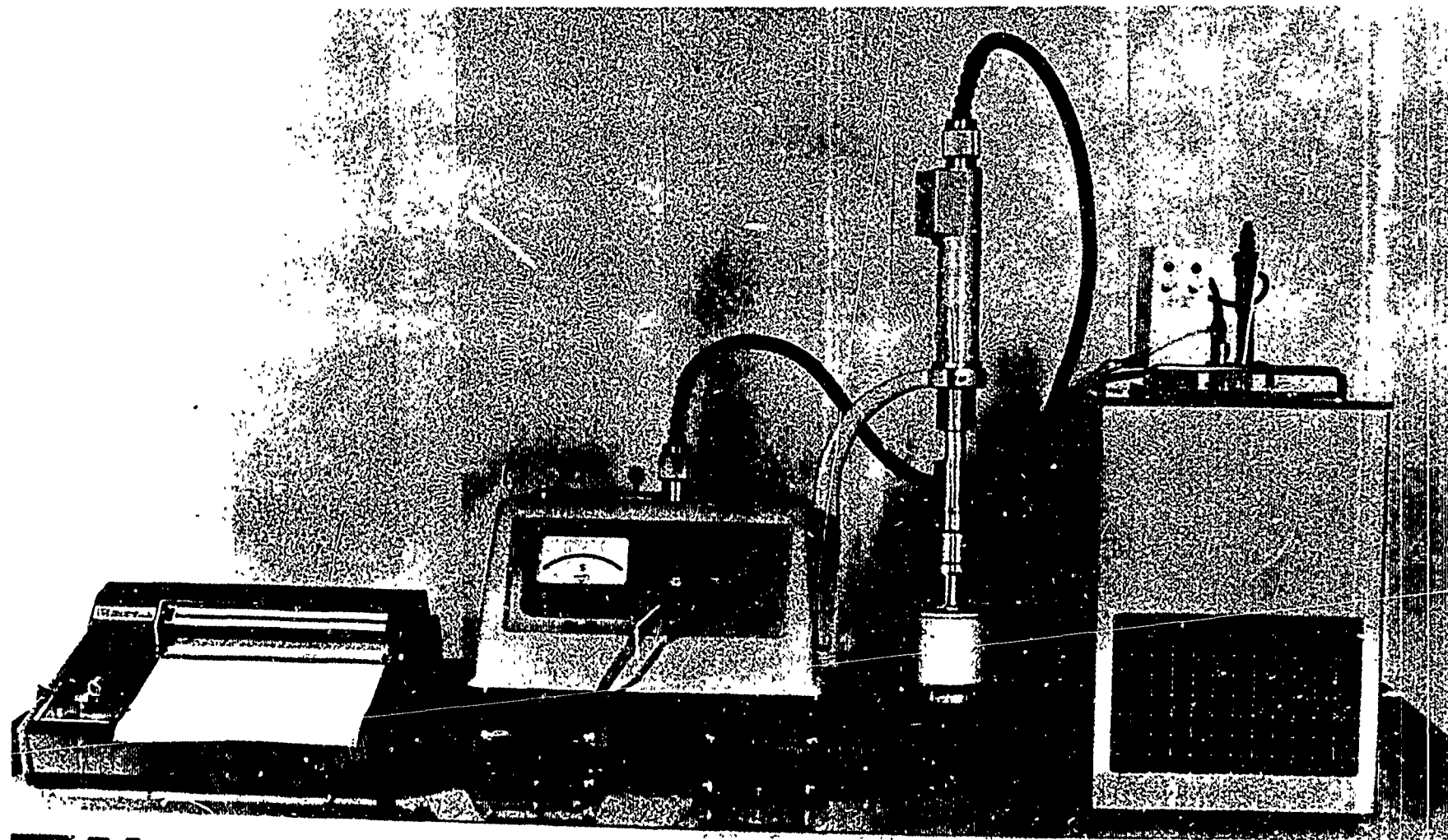


FIGURE 27. ROTOVISCO VISCOMETER WITH VISCOELASTIC ATTACHMENT

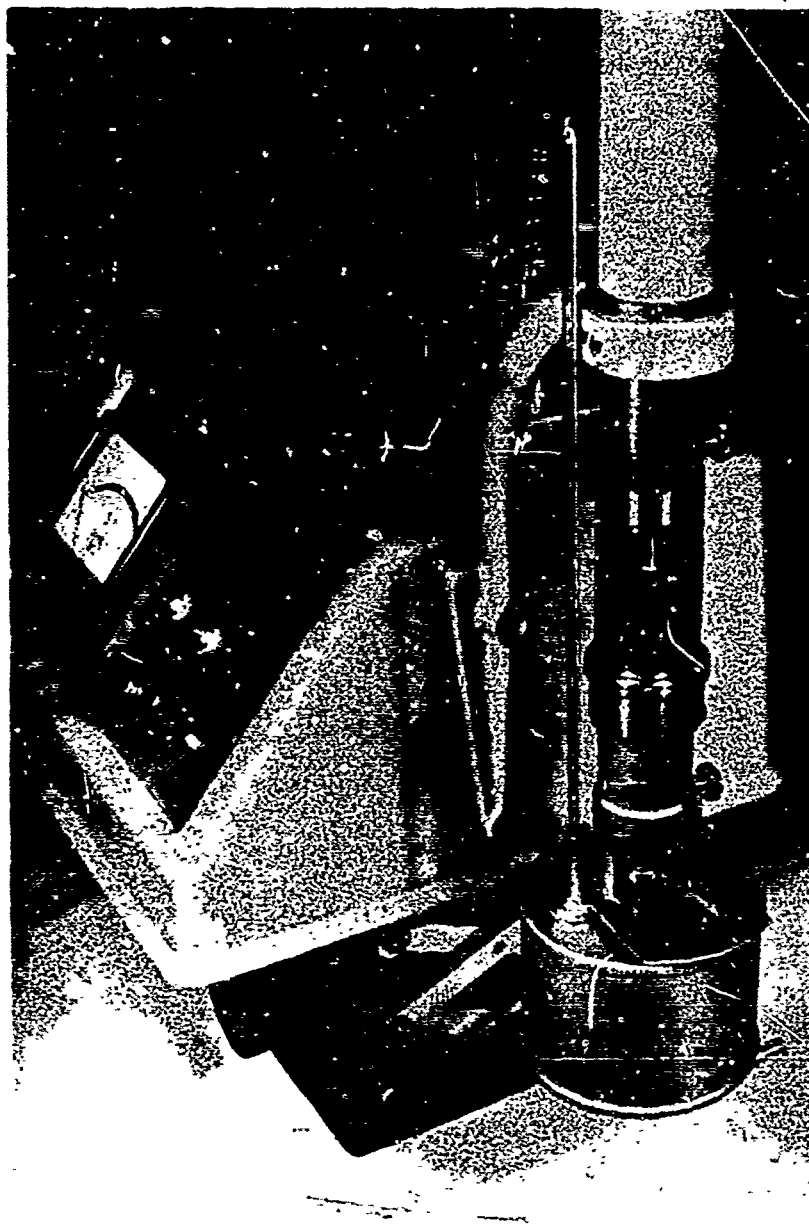


FIGURE 28. VISCOELASTIC MEASURING HEAD - ROTOVISCO VISCOMETER

The hysteresis loop was measured for each of the gels using the cone and plate attachment at  $25.0 \pm 0.1^\circ\text{C}$ . The shear rate was increased over a period of about 60 seconds in 10 steps from 75 to  $12,000 \text{ sec.}^{-1}$  (75, 150, 220, 440, 670, 1330, 2000, 4000, 6000 and  $12,000 \text{ sec.}^{-1}$ ). When the torque of the cone reached a maximum value, the speed of the cone was shifted to the next higher speed. The procedure was reversed using the same sample. The torque was measured at each consecutively lower speed. The shear stress was calculated from the value of the recorded torque. The complete hysteresis loop measurement was repeated three times using fresh samples for each loop measurement.

## RHEOLOGICAL CHARACTERIZATION - PART B

### Results and Discussion

Program - Part B of the rheological characterization deals with the gelled fuel made of the gelling agent FAA-CL-11. This gelling agent was developed at the end of this contract research program. It was designed specifically to meet the very low viscosity and smooth flowing requirements which were not completely satisfied by the gelled fuels made with gelling agent FAA-CL-10. The characterizations were performed on a sample (Gel E) having a gelling agent concentration of 2.52%. The same experimental procedures were employed in both Part A and Part B of the rheological characterization.

Plasticity and Yield Stress - Gel E flows like a Newtonian liquid at low shear rate (below 200 sec.<sup>-1</sup>) and at temperatures above 25°C. At high shear rate and low temperature, the gel still maintains plastic behavior. The yield stress of Gel E increases as the temperature decreases from 58°C. to -20°C. as shown in Table 6 and Figure 29.

TABLE 6

#### YIELD STRESSES AT VARIOUS TEMPERATURES

<u>Temperature, °C.</u>	<u>Yield Stress, dynes/cm<sup>2</sup></u>
58.0	70
25.0	120
1.0	190
-20.0	310

Shear Rate and Shear Stress Relationship - The shear rate and shear stress relationship was established in the shear rate range of 150 to 12,000 sec.<sup>-1</sup>. Figure 30 illustrates the relationship at several temperature levels. The shear rate and shear stress ratios are not constant. The ratio decreases as the shear rate increases.

The data may be presented conveniently and usefully as a family of curves. The differences between the shear stress and yield stress are plotted against shear rate in a logarithmic scale, Figure 31. The lines are represented by equation (1)

$$\log (\sigma - \psi) = \log k + n \log \dot{\gamma} \quad (1)$$

The data were analyzed by the method of least squares. The constant n in Equation 1 was 0.533 ± 0.035; it was independent of temperature. The values of k increased with temperature as shown in Table 7.

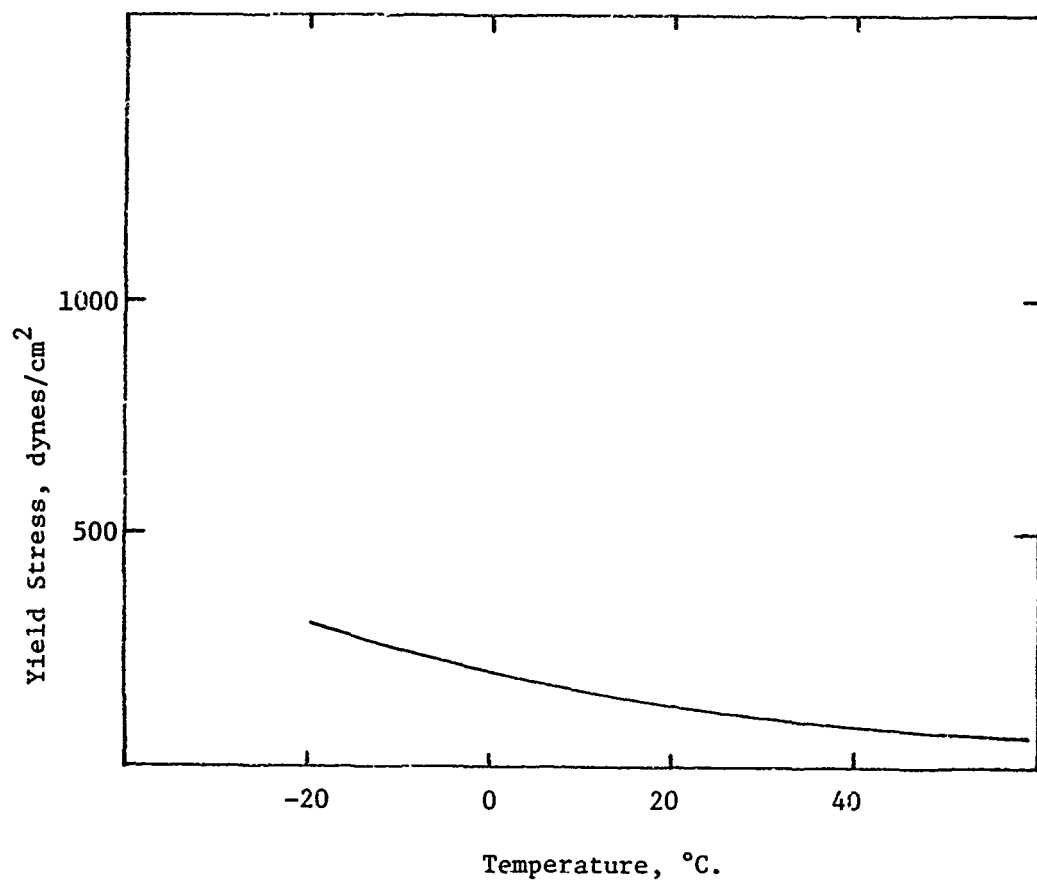


Fig. 29 - Yield Stress of Gel E at Various Temperatures

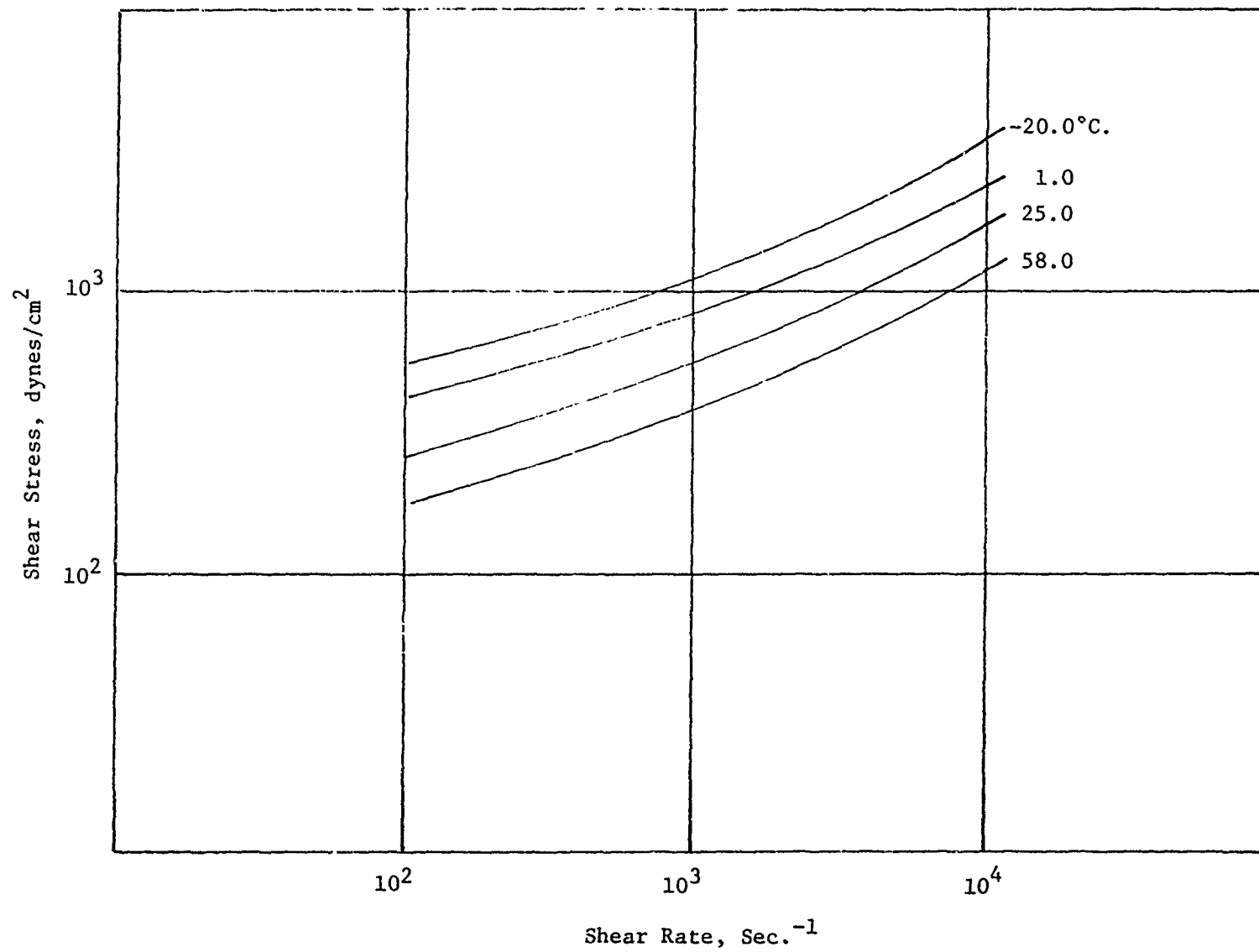


Fig. 30 - Shear Rate vs. Shear Stress at Various Temperatures - Gel E



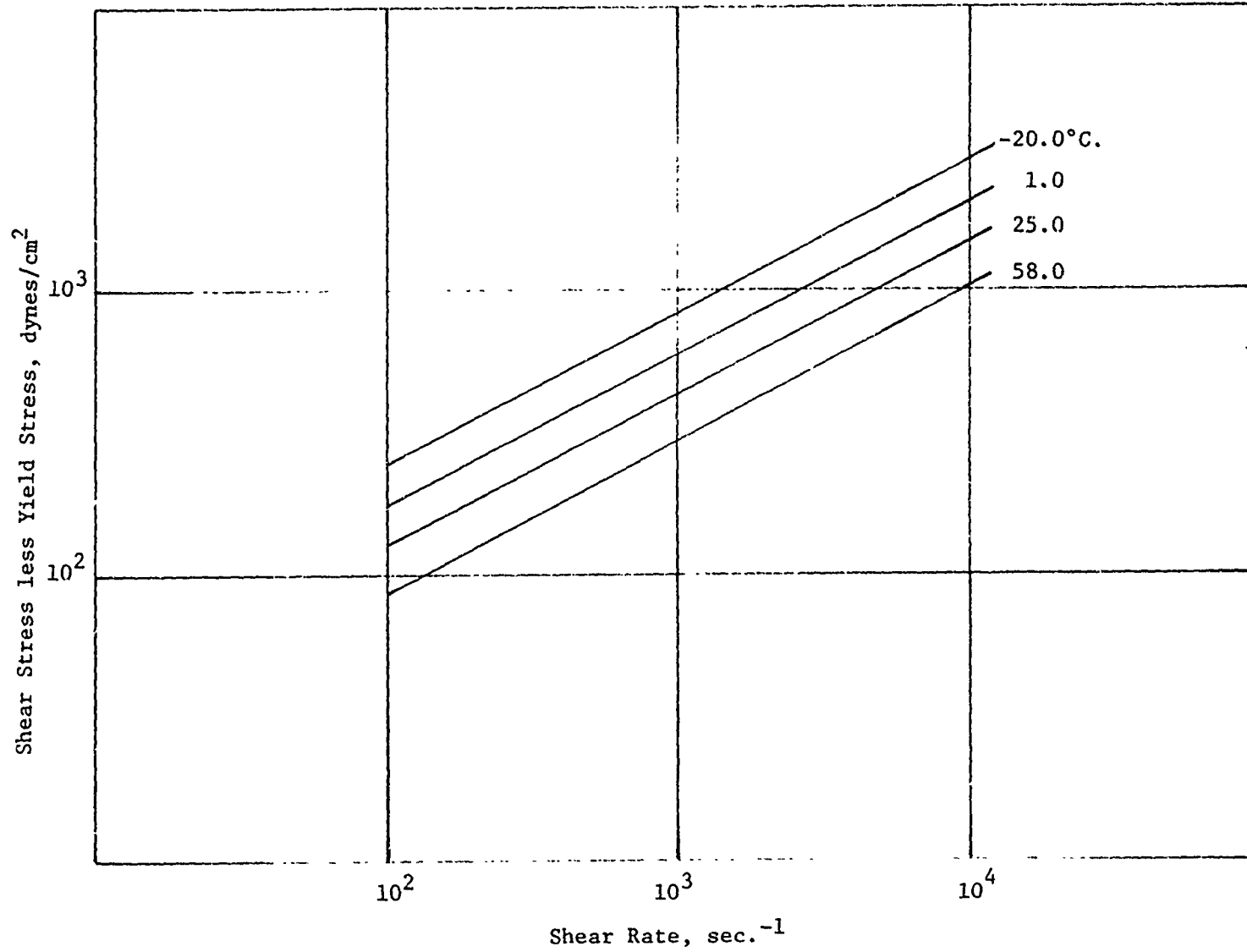


Fig. 31 - Shear Rate vs. (Shear Stress less Yield Stress) at Various Temperatures - Gel E

TABLE 7

EFFECT OF TEMPERATURE ON VALUES OF INTERCEPT (k)

Temperature, °C.	Intercept k, dynes x sec. cm <sup>2</sup>
58.0	9.63 ± 1.36
25.0	10.90 ± 1.13
1.0	15.99 ± 1.21
-20.0	20.70 ± 1.43

The shear stress-shear rate relationship of Gel E is much less sensitive to temperature change than the gelled fuels of FAA-CL-10.

Thixotropy - Gel E exhibited thixotropic properties at -20 and 1.0°C. Above that temperature, thixotropy diminishes. Figure 32 demonstrates the thixotropic property by means of a series of hysteresis loops. Figure 33 illustrates the same property at a constant shear rate. It was also observed by the use of Brookfield viscometer that the gel possesses some degree of dilatancy above 25°C. (Figure 34).

Viscoelasticity - The viscoelastic properties were measured by two parameters: equilibrium stress,  $\sigma_{ec}$ , and relaxation time,  $\tau_{rx}$ . The relaxation time of the gel between -20°C. and 58°C. was nearly constant at 2.0 + 0.2 for shear rates from 220 to 12,000 sec.<sup>-1</sup>. As the gel was sheared at a constant shear rate, the shear stress reached an equilibrium value after a few seconds. When the flow was abruptly stopped, the shear stress decreased with time. Typical rheograms are shown in Figure 35 for the gel at -20.0 and 58°C. and sheared at 4,000 sec.<sup>-1</sup>. The time for the shear stress to reach a constant value at a given shear rate follows the mathematical model of a maxwellian viscoelastic fluid which is described by the equation:

$$\frac{\sigma_t}{\dot{\gamma}} = \eta_0 e^{-t/\lambda} \quad (4)$$

where  $\sigma_t$  is the shear stress at time, t in seconds,  $\eta_0$  is the viscosity at zero shear rate and  $\lambda$  is the relaxation time constant. The value of  $\lambda$  is proportional to  $\tau_{rx}$  at all shear rates from 200 to 12,000 sec.<sup>-1</sup> and temperatures from -20 to 58°C.

The fuel passed, without causing ignition, the NAFEC Air Gun Safety Test. These results, in conjunction with the relaxation time, support the earlier recommendation that relaxation time could be a convenient criterion for screening safe fuel.

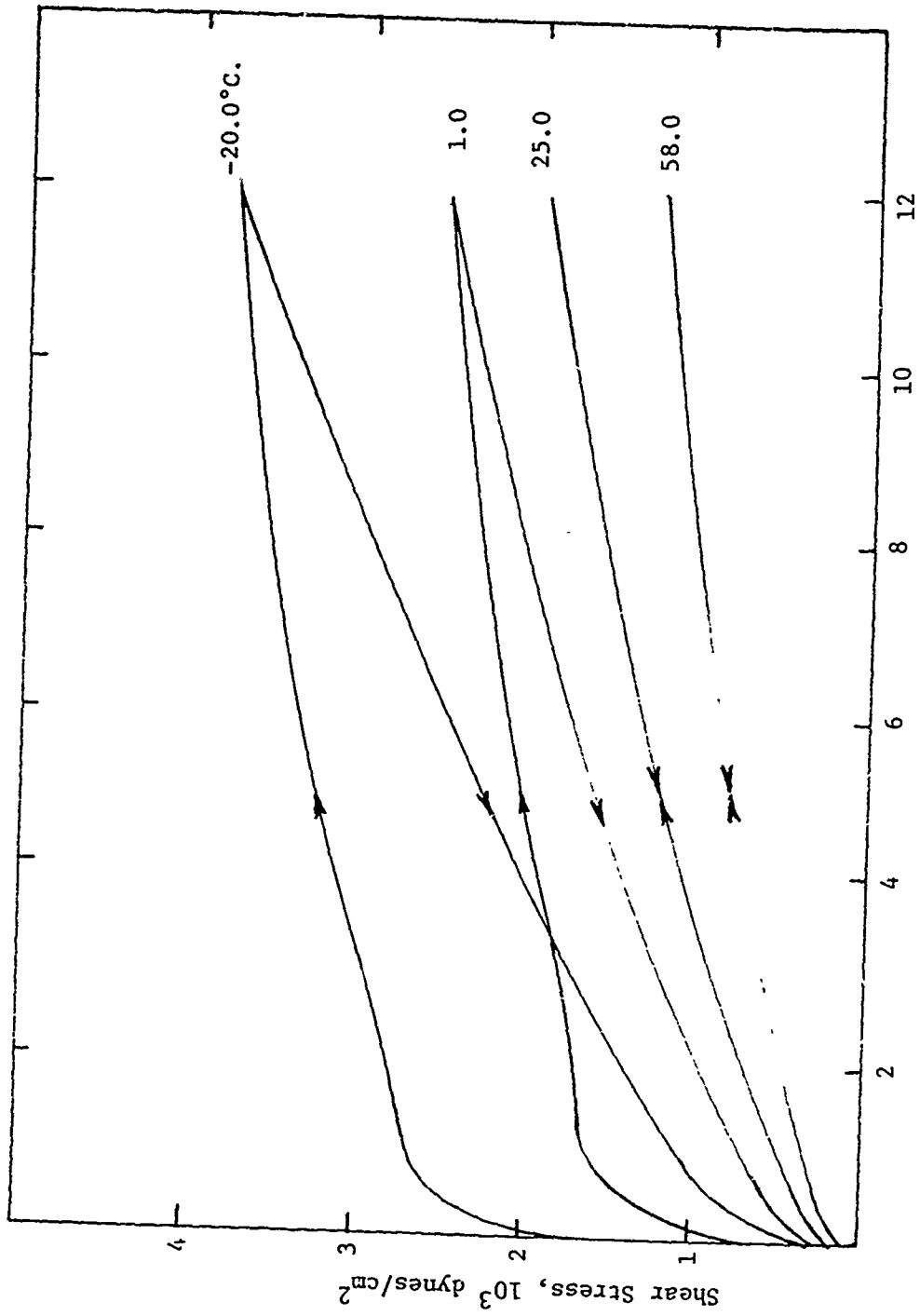


Fig. 32 -Hysteresis Loop of Gel E at Various Temperatures

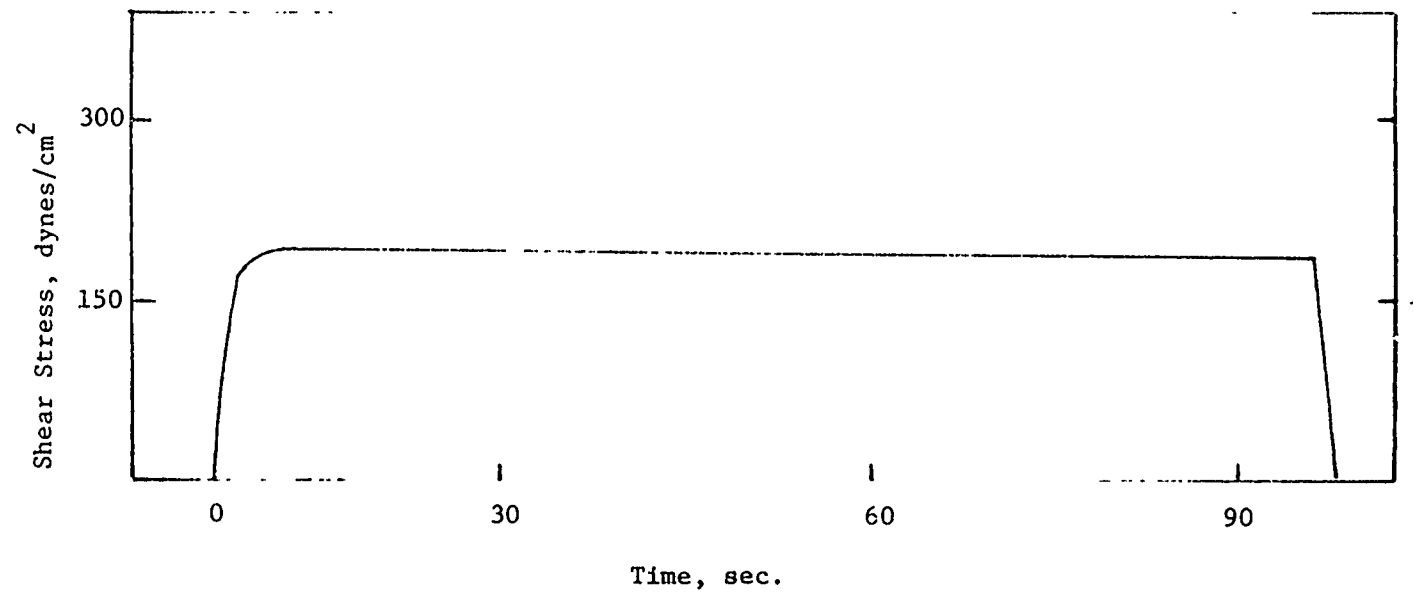


Fig. 33 - Thixotropy of Gel E at 25°C. Temperature

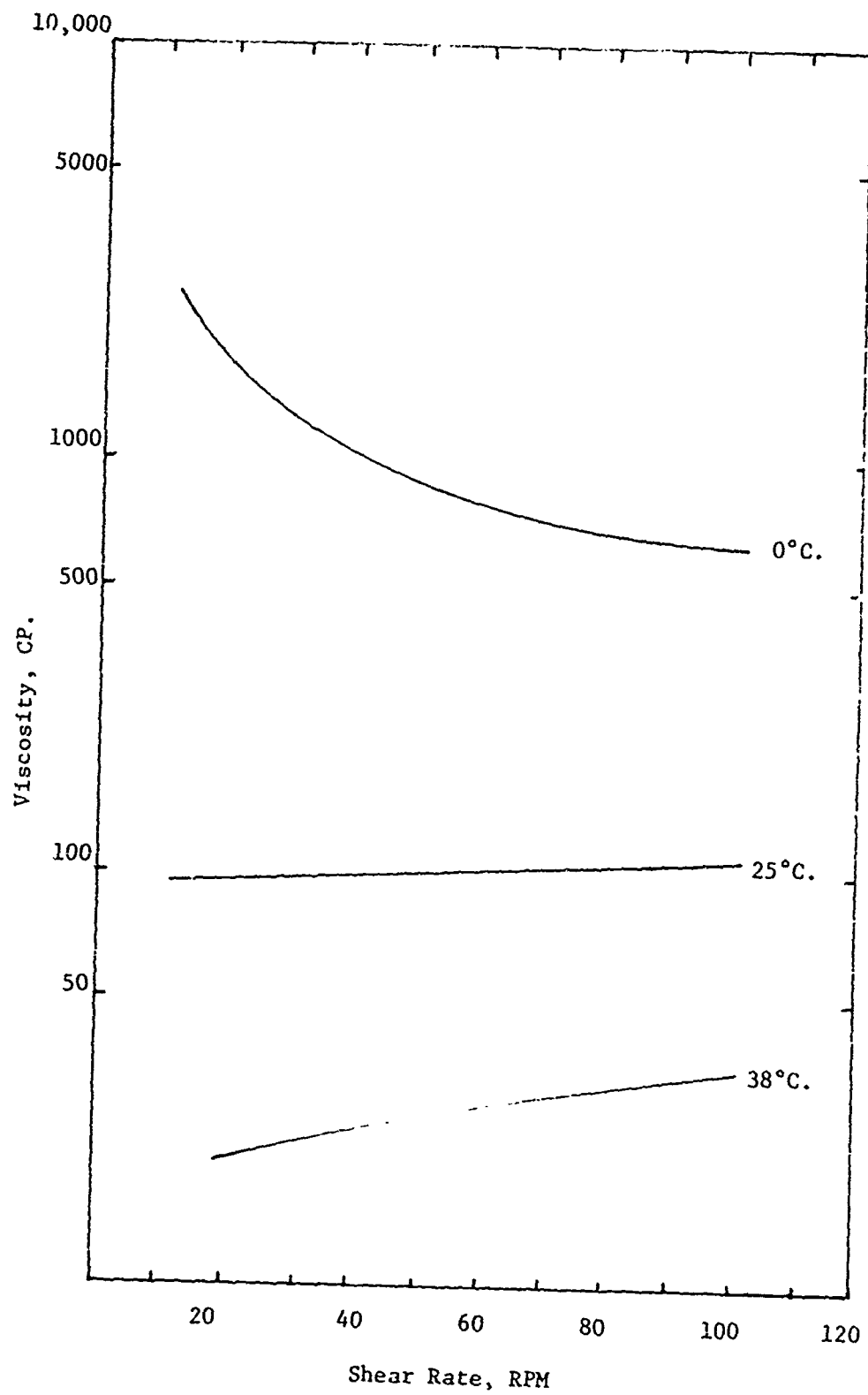


Fig. 34 - Viscosity Measurements of Gel E at Various Temperatures

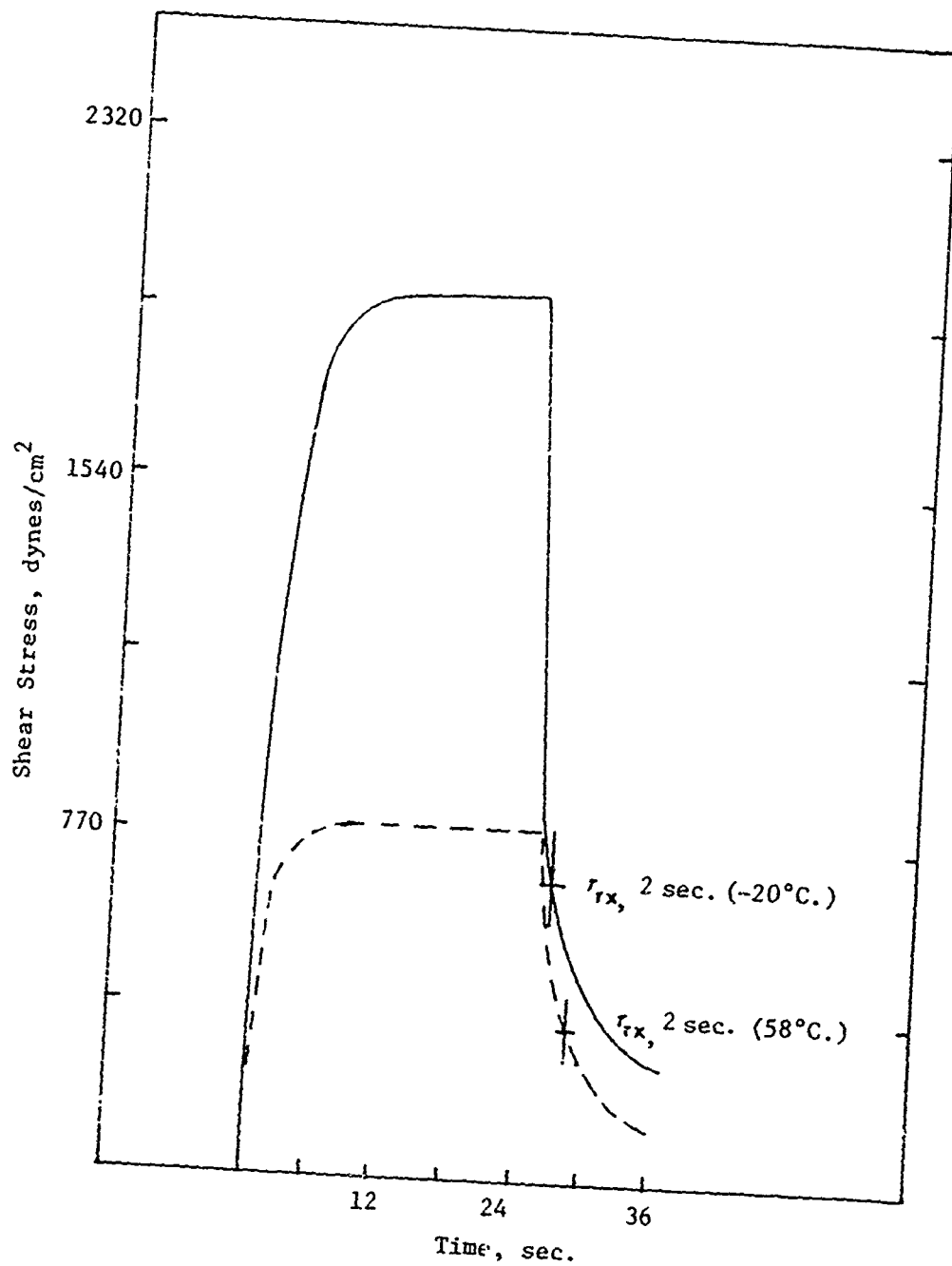


Fig. 35 - Viscoelastic Measurement of Gel E -  
 4000 sec.<sup>-1</sup> Shear Rate at -20°C. and  
 58°C. Temperatures

## SYSTEM COMPATIBILITY STUDY

### Results and Discussion

Vibrational Stability - The gel in an aircraft tank is subjected to many vibrational shocks. These shocks could conceivably cause the breakdown of gel structure resulting in syneresis and reduced viscosity. Samples of Gelled Fuels A, B, C and D were vibrated for 15 hours at 2900 cycles per minute and found to have the same shear stress and shear rate relationship. There was no sign of syneresis nor were there any other changes observed after the testing period.

Thermal Stability - Aircraft fuel experiences a wide range of temperatures due to climate and geographical conditions. The FAA requires fuel to perform acceptably throughout the temperature range from -65°F. to 130°F. Samples of the four selected gels underwent repeated freeze-thaw cycles (6), and the gels were shown to be thermally reversible, as indicated by the same shear rate and shear stress relationship before and after the repeated freezing and melting. Syneresis was not observed at any stage.

Filterability - The FAA contract requirement stipulates that gelled fuel be passable through 40 micron filters commonly used in aircraft fuel systems. Extraneous material in the AB gelling agent was removed during manufacturing by means of centrifugation. The fuel passed readily through a 400-mesh (nominal 38 micron) Type 304 stainless steel screen of 1.4 square inches. The flow rate was proportional to the pressure drop as exemplified in Figure 36. Flow rates were limited to lower pressures because of the ease with which the material flowed through the filtering apparatus. Approximately 2 gallons of each gel was filtered at a pressure of 10 pounds per square inch gauge (psig). A decrease in flow rate would have indicated that the filter was being clogged by nonfilterable particulate matter.

Residual Gel Measurement - There is serious concern about the excessive amount of unusable gelled fuel in aircraft tanks due to adhesion of the gel to the walls of the fuel cell. Estimates of the amount of unusable fuel ran to 4%<sup>8</sup> or higher, whereas unusable liquid fuel is generally about 0.2%. The amount of residual AB gelled fuel held on a container wall compared to that of ungelled modified fuel was estimated by empirical measurements. These consisted of submerging aluminum coupons in various fuel samples at several temperature levels and determining the weight of adhering fuel after a specified draining period.

The results are compiled in Table 8 and the same data are graphically displayed in Figures 37 and 38 to illustrate the comparative tendency to accumulate residual gel.

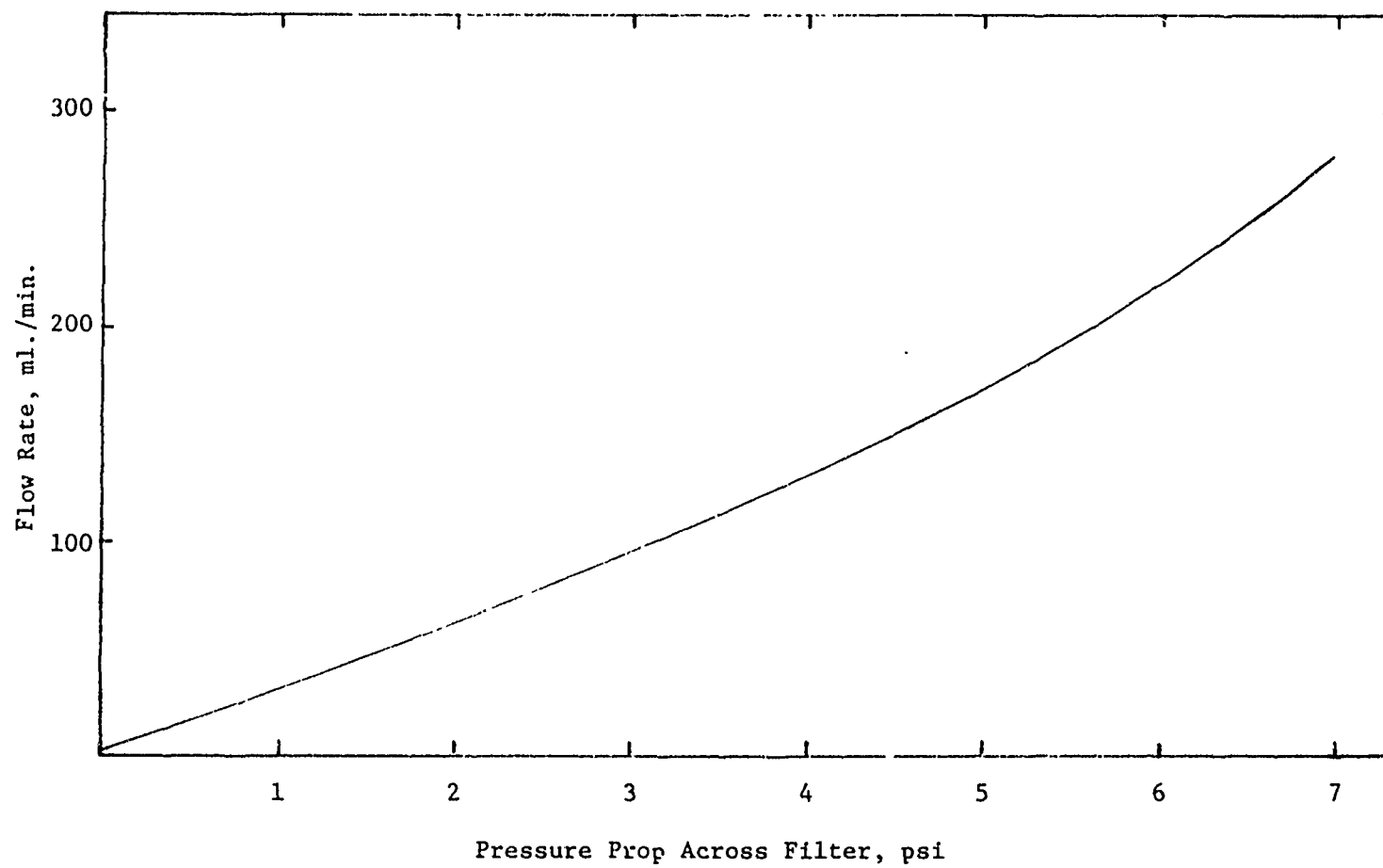


Fig. 36 - Flow Rate of Gel C in Relation to Pressure Drop



TABLE 8

RESIDUAL GEL ON ALUMINUM COUPONS

<u>Sample Identification</u>	<u>Residual Fuel Weight, Mg.</u>		
	<u>52°C.</u>	<u>0°C.</u>	<u>-52°C.</u>
Jet A	156	203	681
D	272	586	---
C	596	327	567
B	794	197	---
A	1732	163	---

Two reference fluids were used to establish the load correction for this ball. The load versus time curves for these fluids show a one-gram load correction requirement at  $25^\circ \pm 0.05^\circ\text{C}$ , Figure 22.

A number of compositions ranging in viscosity from Jet A-1 fuel to the viscous 2-10-0 composition was evaluated over a range of shear conditions. The temperature was maintained at  $25^\circ\text{C}$  and a fresh sample was used for each test.

The shear stress and shear rate constants were calculated as follows:

(a) Shear rate constant ( $K_2$ )

$$K_2 = \frac{5.08}{a^2} \left( 3r + a + \frac{2a^2}{2r + a} \right) = 61,700 \text{ cm/cm}$$

where "a" is the average annulus width (0.025 cm) and "r" is the ball radius (0.6415 cm).

$$\text{Shear Rate (S)} = \frac{K_2}{T}$$

where T = falling time of ball in seconds for a distance of 2 inches.

(b) Shear stress constant ( $K_3$ ).

Bail constant ( $K_1$ ) = 1.0 poise/kilogram/second

$$K_3 = K_1 \times K_2 = 61,700 \text{ dynes/cm}^2/\text{Kg}$$

$$K_1 = \frac{K_3}{K_2}$$

$$\text{Shear Stress} = K_3 \times \text{load (Kg)} = \text{dynes/cm}^2$$

The shear rate versus shear stress curves are shown in Figure 23. The viscosity versus shear rate is plotted in Figure 24.

In Figure 24 the significant differences in the curves of the fuel compositions are more vividly displayed than in Figure 23. In both graphs the dilatant character at relatively low shear rates is noted for compositions containing the flow modifier. Both compositions, 1.5-1.5-50 and 1.7-1.5-100, that showed excellent resistance to fire explosion have very similar rheological profiles with the viscosity

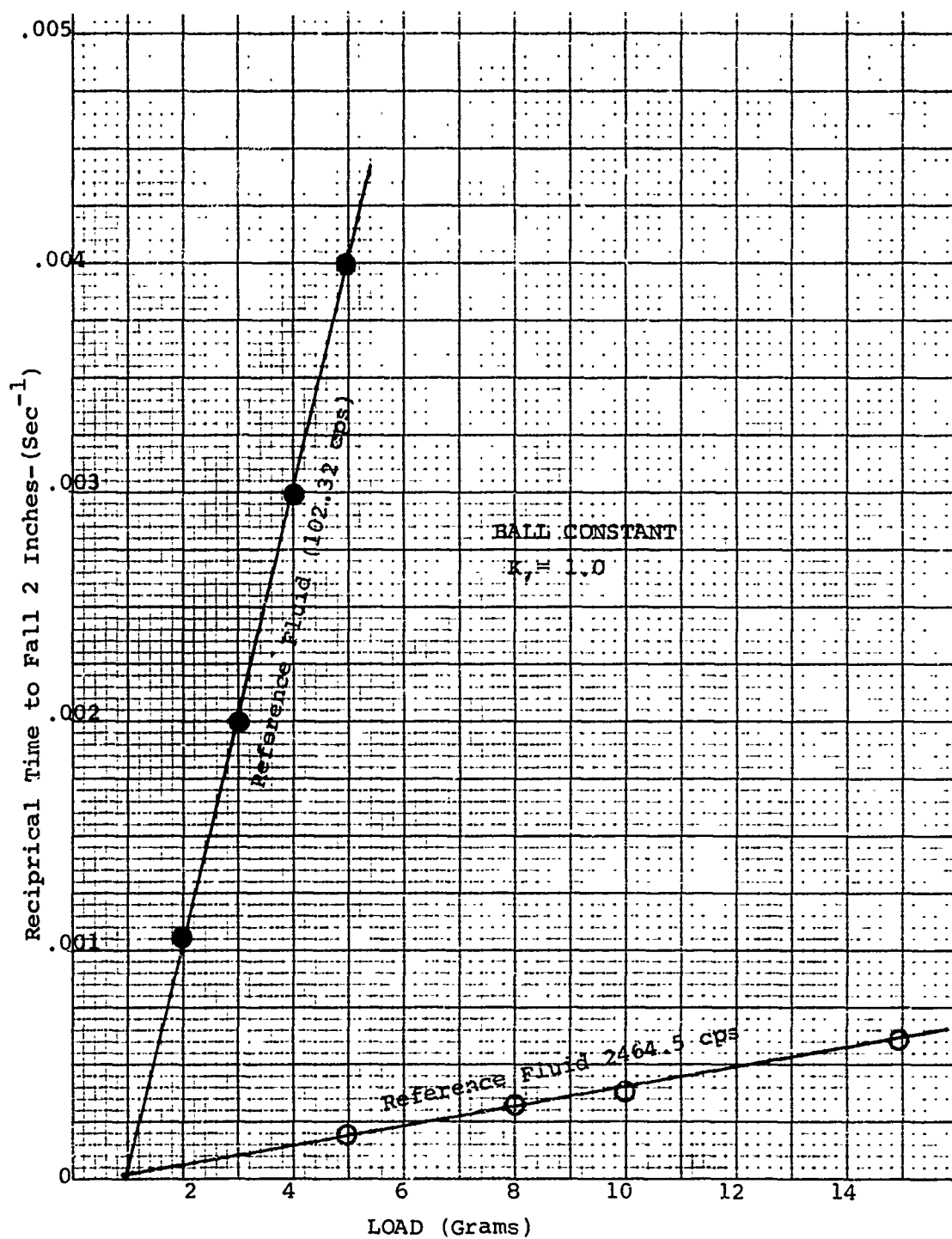


FIGURE 22 - TIME VERSUS LOAD FOR REFERENCE FLUIDS  
(FORCED-BALL VISCOMETER)

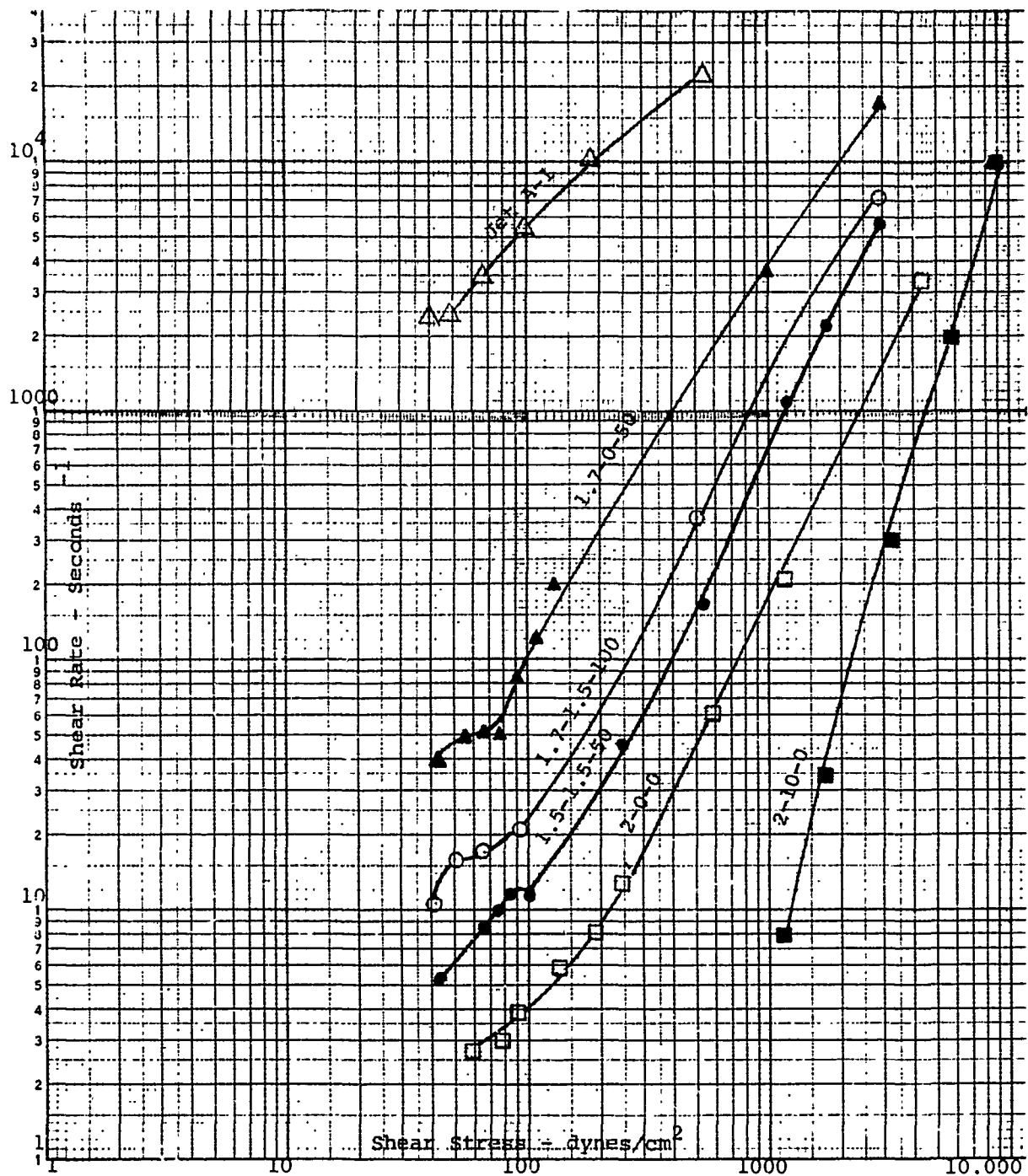


FIGURE 23. SHEAR RATE VERSUS SHEAR STRESS (FORCED BALL VISCOMETER). VARIOUS MODIFIED THICKENED FUEL COMPOSITIONS

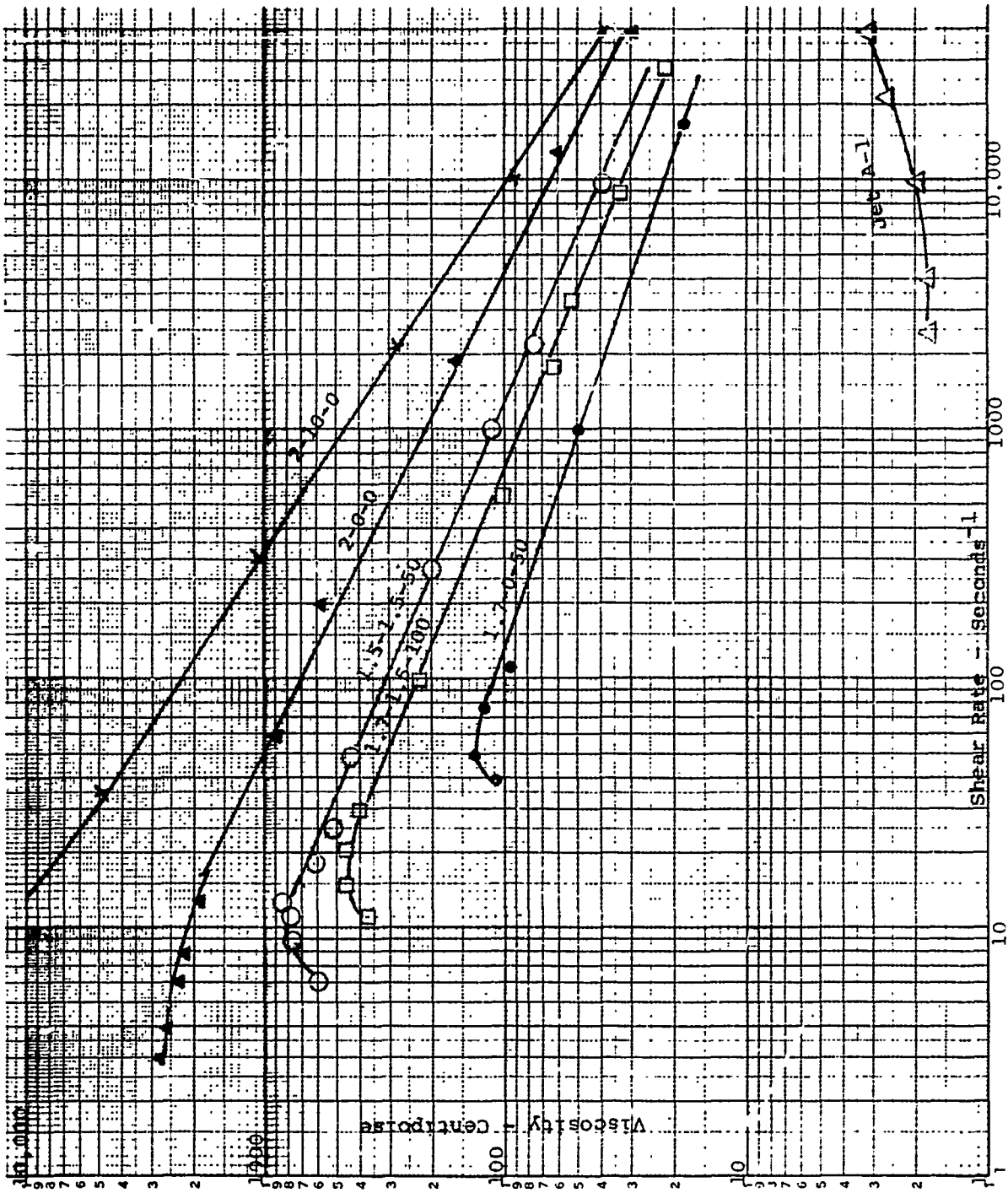


FIGURE 24. VISCOSITY VERSUS SHEAR RATE (FORCED BALL VISCOMETER) VARIOUS MODIFIED THICKENED FUEL COMPOSITIONS

peak occurring at about the same shear rate. As the shear rate increases the viscosity decreases, which indicates adaptability to existing aircraft engine fuel control systems, including atomization in the burner cans.

The rheological behavior of the thickened fuels at very low shear rates ( $<10 \text{ seconds}^{-1}$ ) could not be reliably tested with the Forced-Ball Viscometer, although this instrument is very effective at high shear rates.

## 2. Rotovisco Viscometer

The Rotovisco is a rotational viscometer having a broad shear rate range capability, and a recorder to measure the time dependency of shear stress at a given rate of shear. This easily operated instrument is shown in Figure 25.

The apparent viscosity of a liquid is calculated in poises according to the equation

$$N = U \times S \times K$$

where U represents the gear position number recorded on the top of the control unit, S equals the scale reading and K is the constant obtained from the geometry of the rotor and cup and the spring constant for the measuring head. For these tests  $K = 0.0023$  for the standard head, and  $K = 0.23$  for the geared head. Additional factors are used to calculate shear stress and rate of shear. Complete reference information is available in the handbook "Viscosity and Flow Measurement" by Van Wager, et al, published by Interscience Publishers.

Viscosity versus shear rate curves are shown in Figure 26. Note that the apparent viscosity is shown at very low shear rates and indicates that the new thickened-fuel compositions are very fluid or demonstrate very low apparent viscosity at near static conditions. The contrast between the former base-thickened fuel (2-10-0) and the new composition (1.7-2.0-100) is very significant in this respect.

The shear rate shear stress curves in Figure 27 indicate a more significant difference among the various thickened-fuel compositions. The curve for

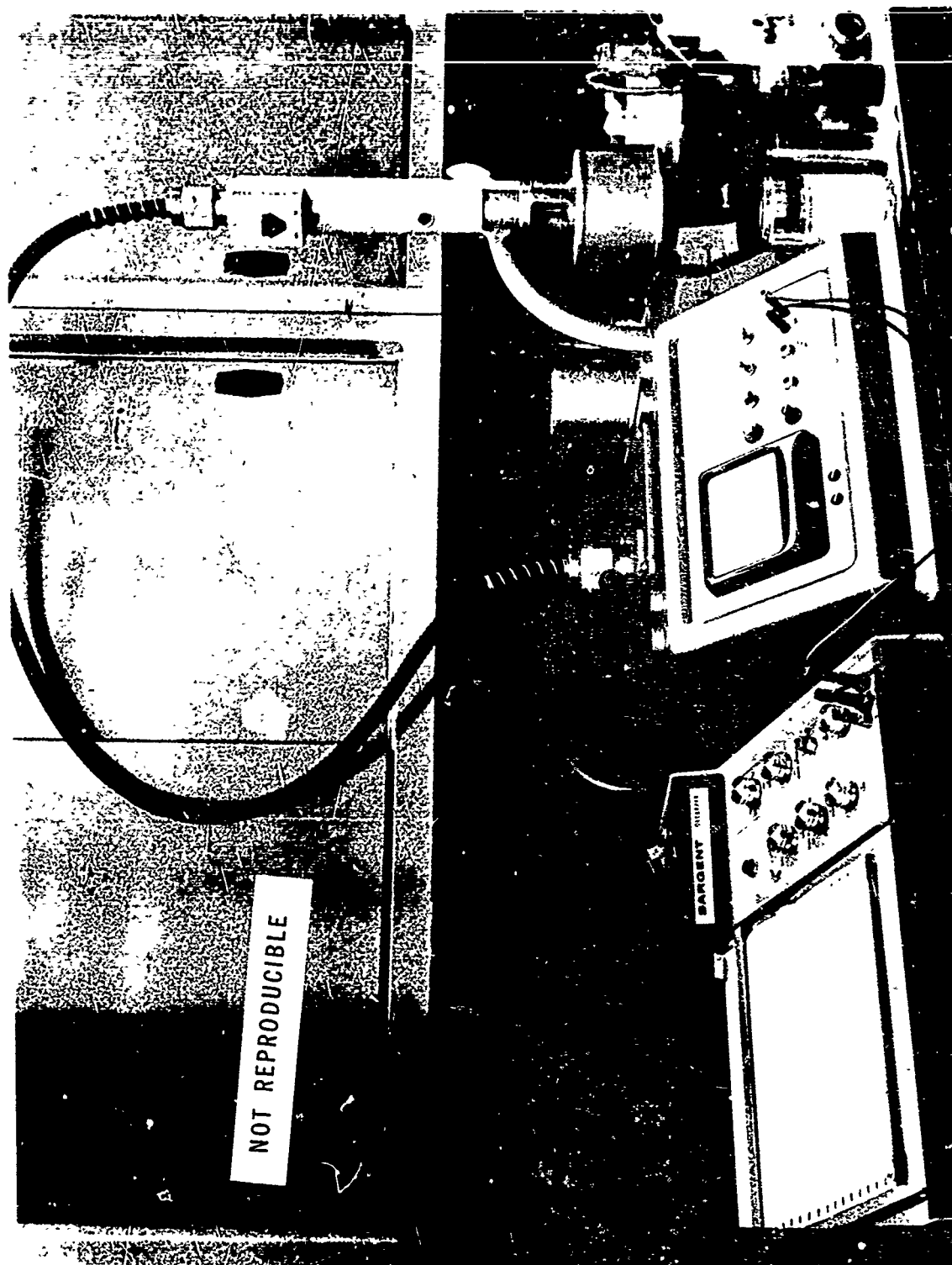


FIGURE 25. ROTOVISCO VISCOMETER

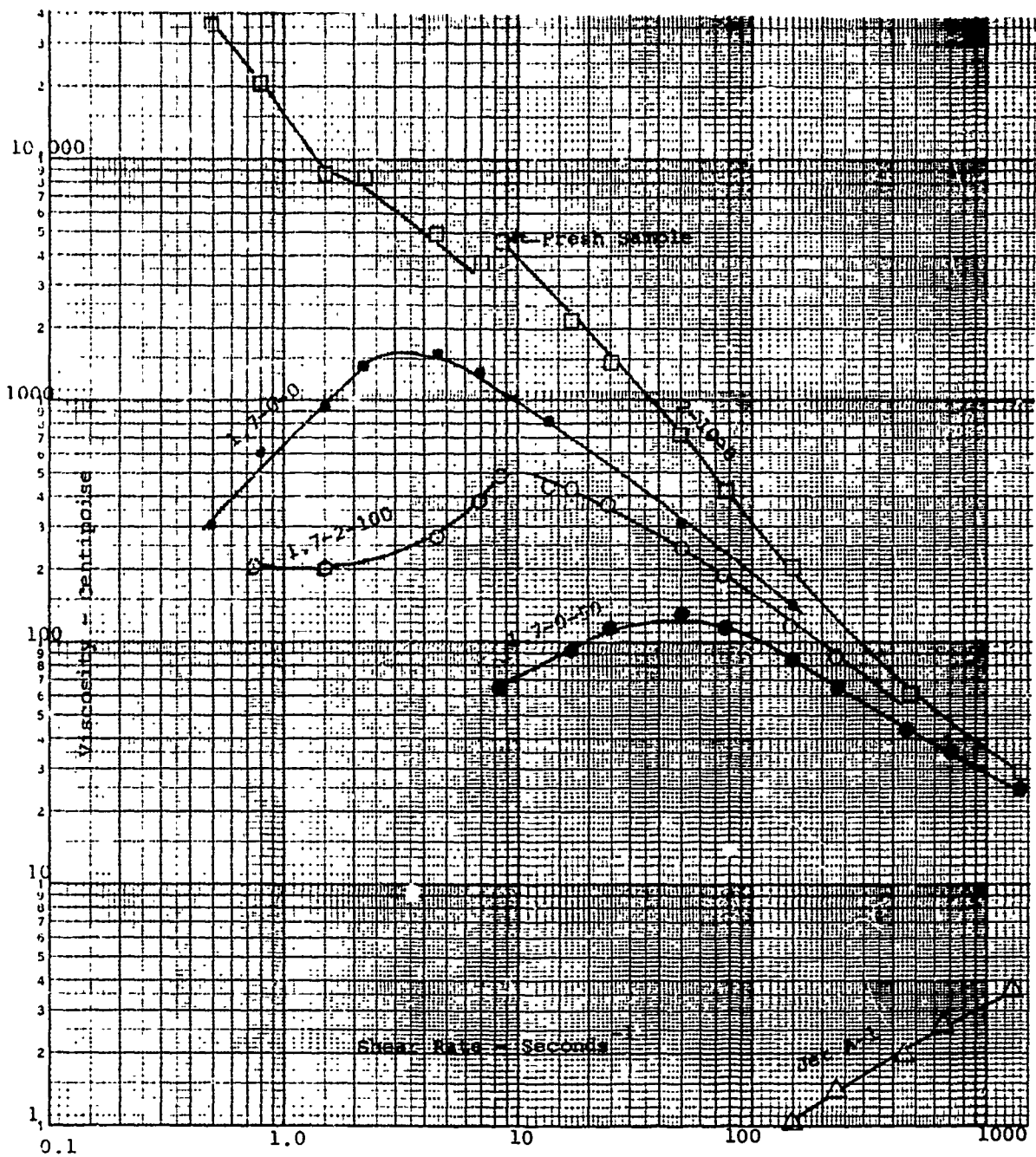


FIGURE 26. VISCOSITY VERSUS SHEAR RATE (ROTOVISCO VISCOMETER) VARIOUS MODIFIED THICKENED FUEL COMPOSITIONS



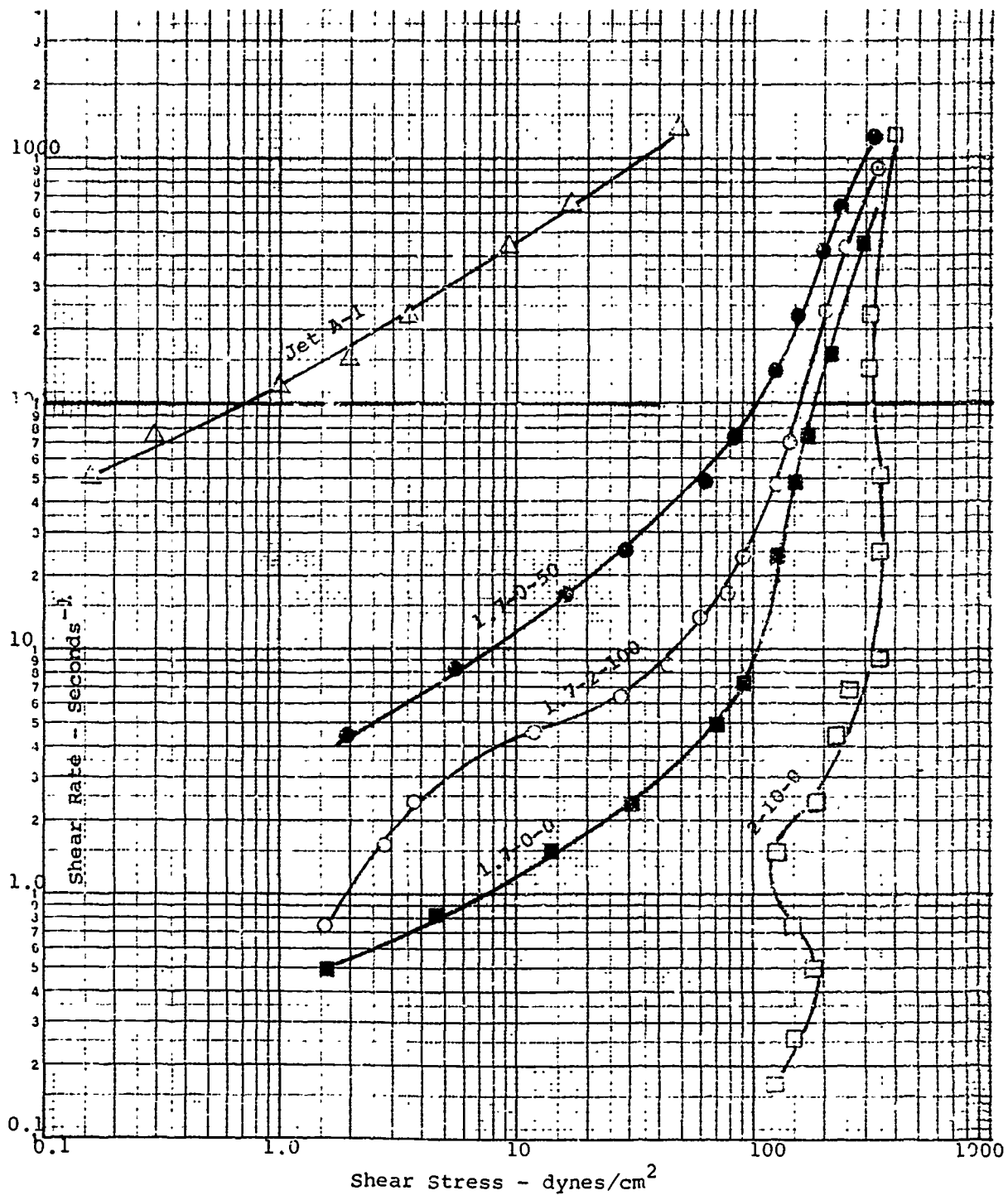


FIGURE 27. SHEAR RATE VERSUS SHEAR STRESS (ROTOVISCO VISCOMETER) VARIOUS MODIFIED THICKENED FUEL COMPOSITIONS

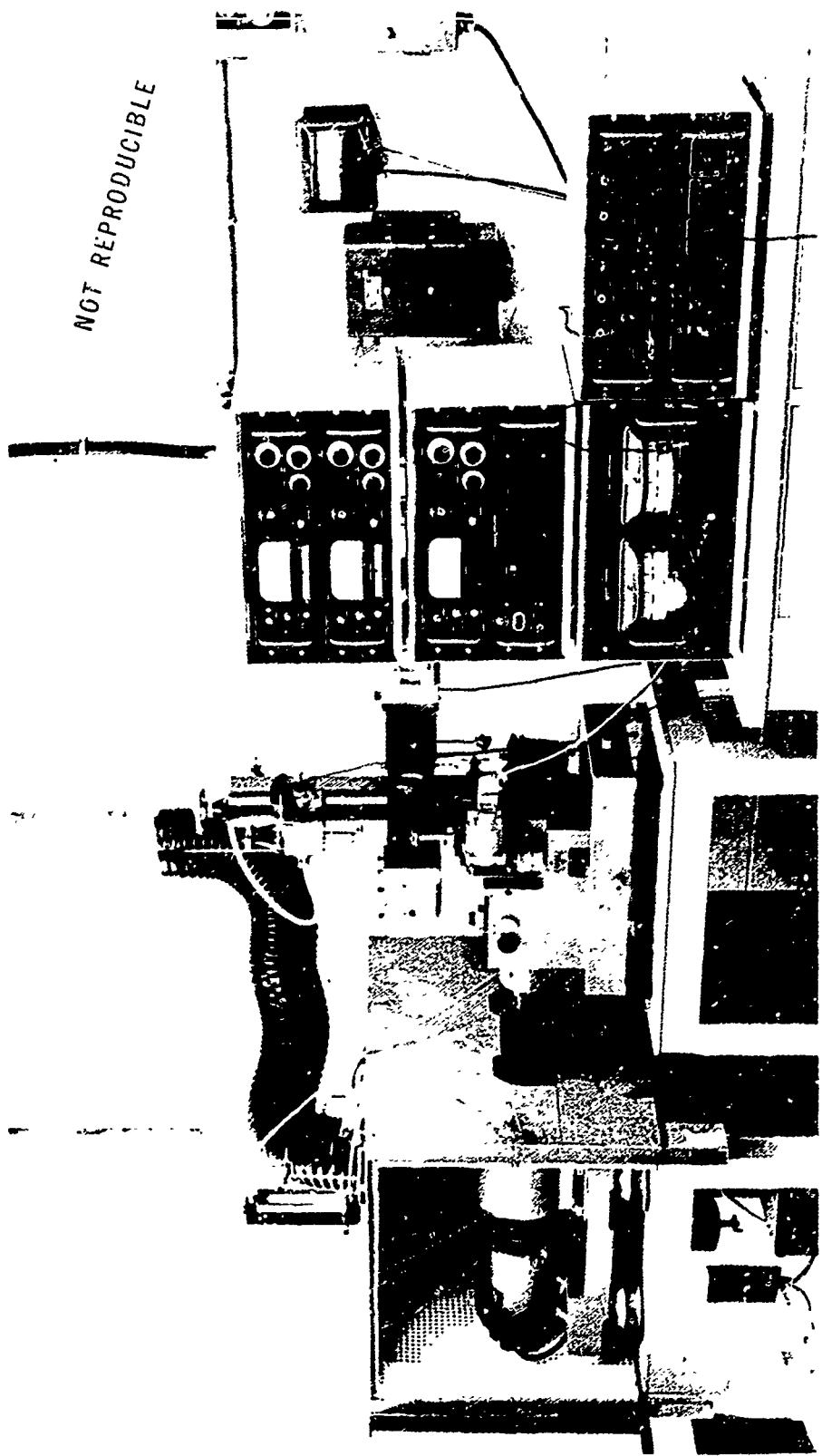


FIGURE 28. WEISENBERG RHEOGONIOMETER

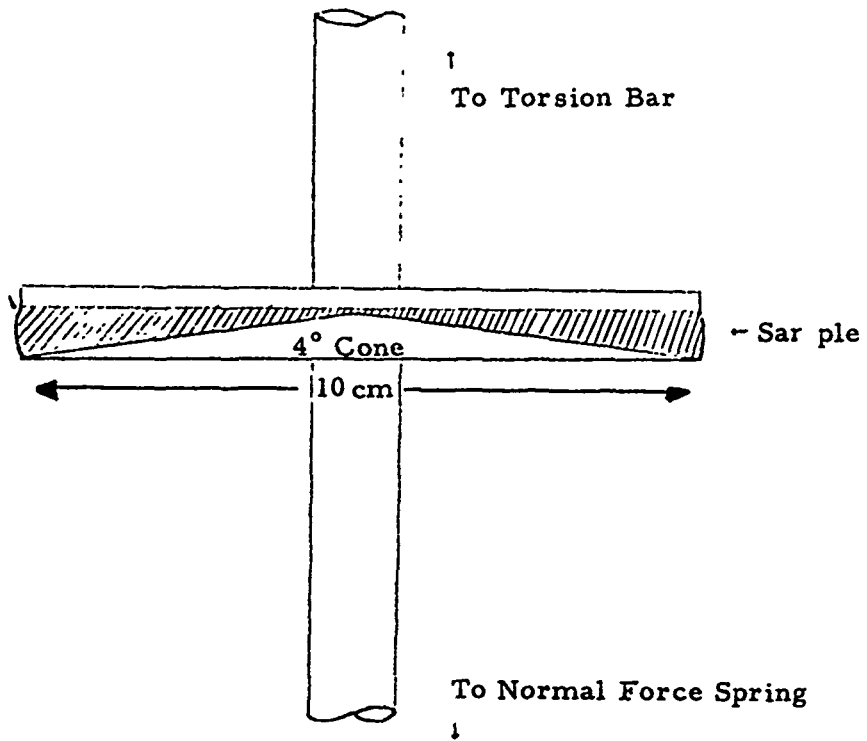


FIGURE 29 - DIAGRAM OF RHEOGONIOMETER  
CONE AND PLATE

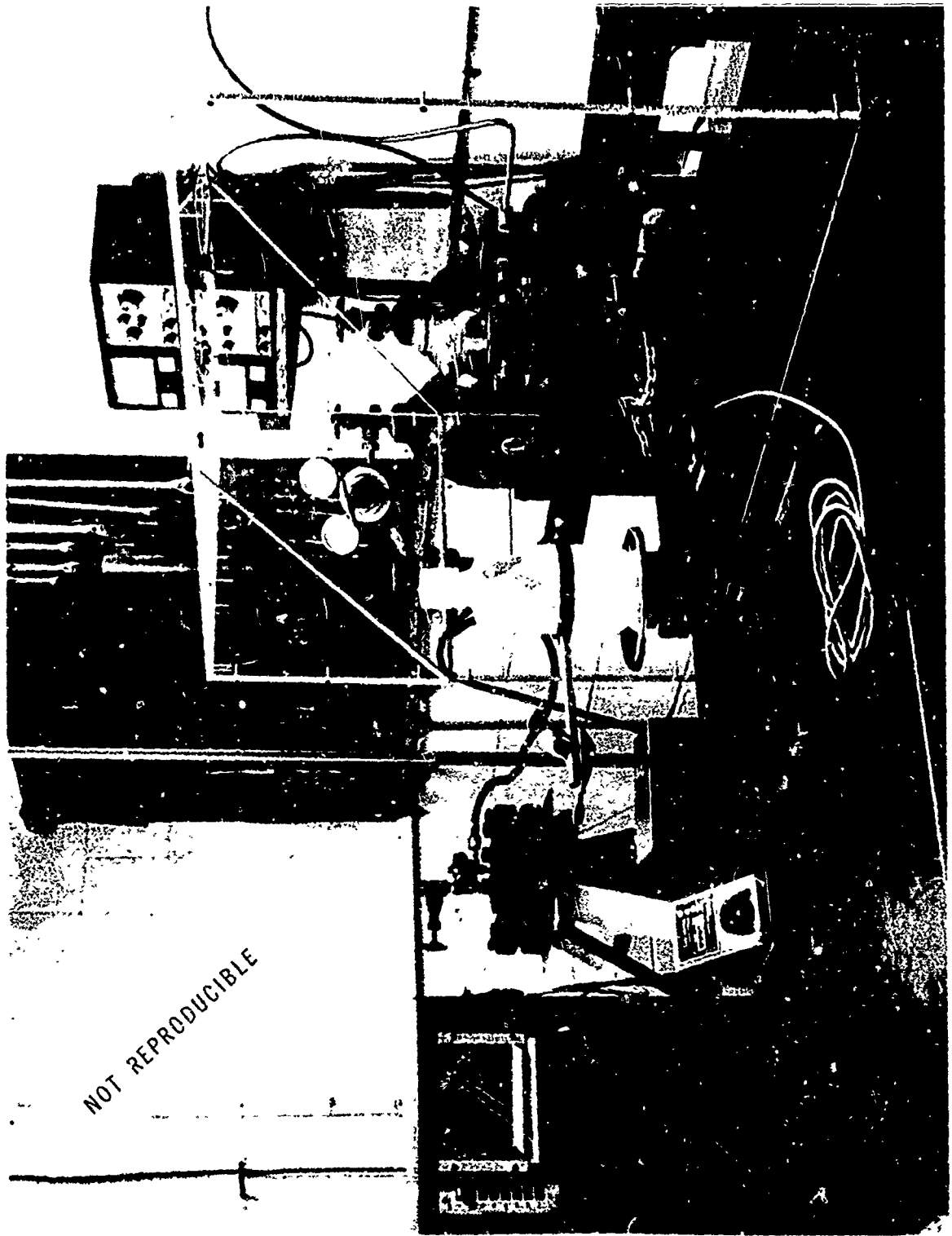


FIGURE 30. THRUST JET INSTRUMENT

The viscosity can be calculated from the pressure drop. The flow rate is measured by collecting the fluid on a timed balance. The shear rate can then be calculated and corrected for the velocity profile in the tube. The capillary tube is mounted on a leaf spring so that the thrust of the jet of fluid leaving the tube can be measured by displacement of the calibrated leaf spring, as shown in the diagram, Figure 31. The decrease in thrust from that which a Newtonian fluid of the same density exerts is a direct measure of the primary normal stress difference. The shear rate range covered by this instrument is from  $100 \text{ sec}^{-1}$  to  $100,000 \text{ sec}^{-1}$ . Data from the rheogoniometer and thrust jet can be combined to yield viscosity data over the shear rate range from  $.005 \text{ sec}^{-1}$  to  $100,000 \text{ sec}^{-1}$  which includes all shear rates of practical interest. For high viscosity materials, there is a range of shear rates that cannot be measured by either instrument.

The viscosity shear rate curves for the modified jet fuels are shown in Figure 32. The effect of polymer concentration is demonstrated by the four fuels (1.25-0-0 to 2-0-0) where the first number is the weight percent XD-7038.00 in the fuel. The viscosity at all shear rates is increased by increasing the concentration of XD-7038.00. The viscosity at very low shear rates ( $.01 \text{ sec}^{-1}$ ) is most strongly affected by XD-7038.00 concentration increasing from 350 centipoise for the 1.25 weight percent, 1,500 centipoise for the 1.5 weight percent, 9,000 centipoise for the 1.7 weight percent to 30,000 centipoise for the 2.0 weight percent. At a shear rate of  $10,000 \text{ sec}^{-1}$ , the range is considerably reduced to 7-10 centipoise for the four compositions. All four compositions show the same general shape of viscosity curve, increasing viscosity in increasing shear rate (dilatant) at low shear rates to a maximum viscosity at a shear rate of  $.10$  to  $1.0 \text{ sec}^{-1}$  and then a sharply decreasing viscosity with further increase in shear rate (pseudoplastic) up to an approximate limiting infinite shear viscosity of 4 centipoise at a shear rate of  $100,000 \text{ sec}^{-1}$ . From a rheological point of view, the maximum in the viscosity shear rate curve indicates two types of interactions occurring in the composition, a bonding mechanism and a molecular entanglement mechanism. Shearing of the fuel causes more contacts between molecules and increases the rate of formation of bonds. This mechanism controls at low shear rates, increasing the viscosity. When the shear rate exceeds the reciprocal of the maximum relaxation times in the fuel, the molecular entanglements are pulled apart and the relaxation times

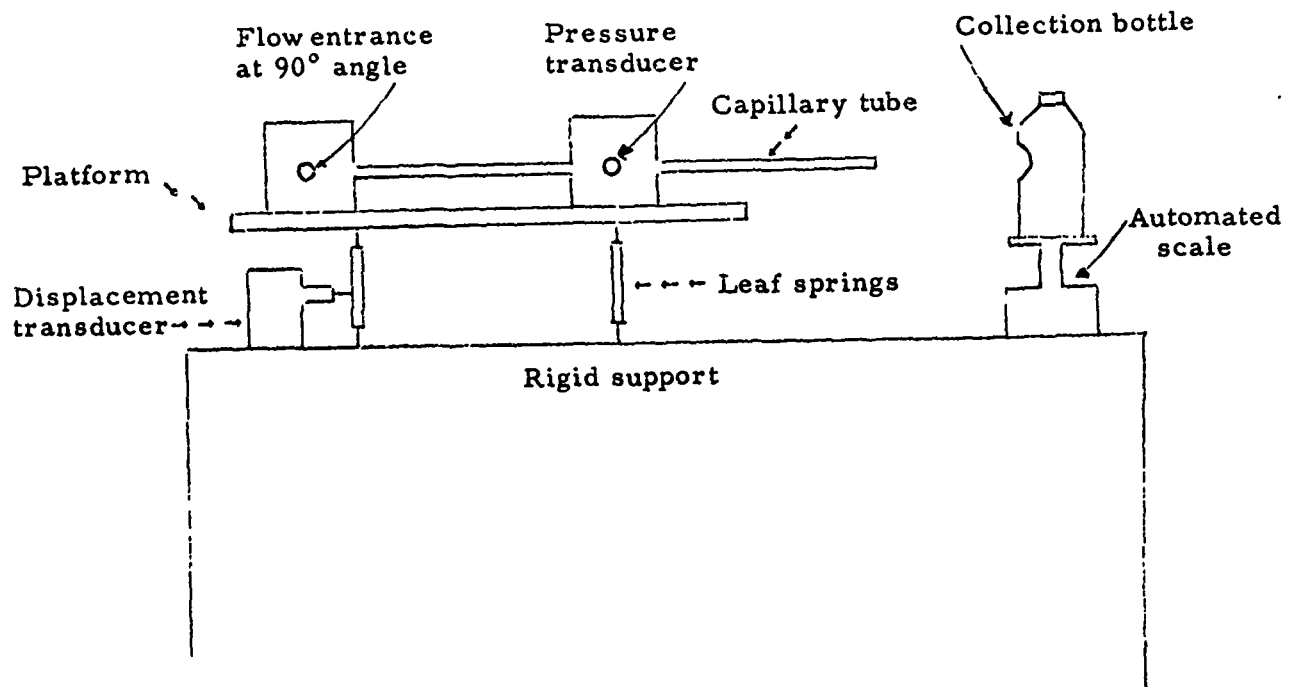


FIGURE 31 - DIAGRAM OF THRUST JET INSTRUMENT

thickened-fuel composition (1.7-2.0-100) in Figure 27 shows a dilatant characteristic between 1 and 30 dynes/cm<sup>2</sup> which the two curves on either side do not possess. Composition (1.7-2.0-100) exhibited good resistance to fire explosion while the other two compositions were unsatisfactory.

### 3. Rheogoniometer and Thrust Jet

Although a considerable amount of rheology data was obtained to this point, a more thorough investigation was considered appropriate. This effort was made primarily in an attempt to determine if a significant rheological characteristic was present in thickened fuels that effectively resisted fire explosion versus those thickened fuels that had only moderate fire explosion resistance.

Two instruments were used to obtain a complete rheological characterization of the modified jet fuels. The Weissenberg rheogoniometer (Figure 28) is a cone-and-plate viscometer in which the cone is rotated by a variable speed gearbox. The shear rate which is constant across the diameter of the cone-and-plate instrument is determined by the rate of rotation and the cone angle. (See Figure 29.) Viscosity is measured by measuring the torque exerted by the rotating cone on the plate. In this study, a 10-cm-diameter cone with a 4° cone angle was used. The primary normal stress difference (a measure of elasticity) is measured by the force normal to the direction of flow exerted on a bar spring mounted below the cone. Both measurements can be performed over a wide range of shear rate from .005 sec<sup>-1</sup> to 1,000 sec<sup>-1</sup>. The upper shear rate limit was much lower for many of the jet fuels due to a secondary flow pattern that develops in viscoelastic materials at high rates of rotation. The rheogoniometer has proven accuracy over most of the above shear rate range of ± 5% for viscosity readings and ± 10% for normal stress readings. In addition to steady shear measurements, transient measurements such as stress relaxation and stress formation can be performed.

To obtain high shear rate viscosity and normal stress data, a second instrument called a thrust jet (Figure 30) was employed. In this instrument, the fluid is forced through a capillary tube of known dimensions by means of nitrogen pressure. A pressure transducer at a fixed distance from the end of the tube is used to measure the pressure drop through the capillary.

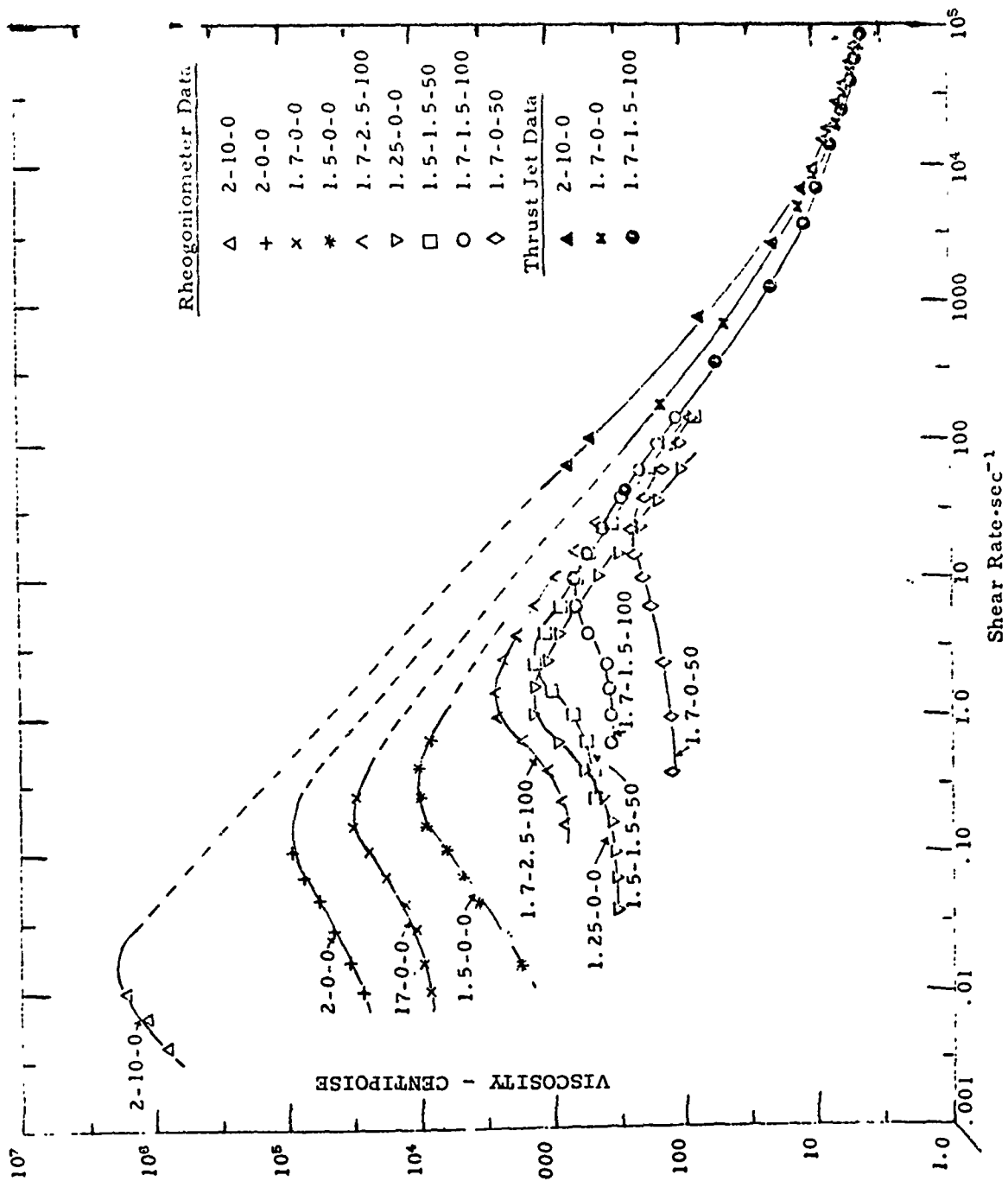


FIGURE 32. VISCOSITY VERSUS SHEAR RATE (RHEOGONIOMETER AND THRUST JET) VARIOUS MODIFIED THICKENED FUEL COMPOSITIONS



decreased. This mechanism shows up as a decrease in viscosity. The shear rate at which the maximum in the curve occurs is approximately the reciprocal of the mean relaxation time of the fuel.

The viscosity curve in Figure 32, labeled 2-10-0, illustrates the effect of adding ammonia to the thickened jet fuel composition. A significant increase in the low shear rate viscosity is obvious by comparing to the 2.0 weight percent XD-7038.00 composition without ammonia. At  $.01 \text{ sec}^{-1}$ , the viscosity is increased from 30,000 centipoise to 1,800,000 centipoise, or a factor of 60 by adding 10 microliters of ammonia to 150 grams of thickened fuel. At shear rates greater than  $1 \text{ sec}^{-1}$  the increase is only a factor of 2.0. For the XD-7038.00 composition, both with and without ammonia, there is a general correlation between high viscosity and reduction of flammability in the NAFEC fire explosion test.

The curve labeled 1.7-0-50 in Figure 32 illustrates the effect of adding 50 microliters of DOWANOL DE to 150 grams of the 1.7 weight percent thickened jet fuel. A large reduction in the low shear viscosity is observed on addition of the DOWANOL DE. At a shear rate of  $10 \text{ sec}^{-1}$  the reduction is from 20,000 centipoise to 130 centipoise. This tremendous reduction in viscosity is not accompanied by any major change in reduction of flammability in the NAFEC fire explosion test, although neither the 1.7-0-0 nor 1.7-0-50 were considered satisfactory.

The three curves in Figure 32 labeled 1.7-2.5-100, 1.5-1.5-50, and 1.7-1.5-100 are examples of fuels that contain all three components, XD-7038.00, ammonia, and DOWANOL DE. All three of these materials have extrapolated zero shear viscosities in the 400 centipoise to 800 centipoise range and all three are considered satisfactory for fire explosion resistance. Considering that the 1.7 weight percent composition, with a zero shear viscosity of 9,000 centipoise does not pass the test, these viscosity curves yield definite proof that high viscosity alone is not the controlling factor in fire explosion resistance.

An interesting feature of the viscosity curves in Figure 32 is the observation that above shear rates of  $10,000 \text{ sec}^{-1}$ , the effects of both ammonia and DOWANOL addition are negligible. The viscosity at these high shear rates reflects principally the amount of XD-7038.00 in the fuel.

A principal reason for using sophisticated instruments like the Weissenberg rheogoniometer and the thrust jet for the characterization of thickened jet fuels is that additional rheological parameters can be measured. Among these is the primary normal stress difference, a ramification of viscoelasticity in steady shear flow. The material property involved is the normal stress coefficient which is the primary normal stress difference divided by two times the square of the shear rate. It was hoped that this property might better correlate with the results of the NAFEC fire explosion tests, as elasticity is known to stabilize flow fields and make major rearrangements of fluid geometry such as atomization more difficult. The results of the measurements are shown in Figure 33. The range of measurements of normal stresses is smaller than for viscosity but the trends are apparent. Also, only limited normal stress data were obtained from the thrust jet which did not yield accurate normal stress measurements on these fuels. The curves are almost identical in shape to the viscosity curves, although different in numerical value. The low shear ranking of the magnitude of the normal stress coefficient is identical to the ranking according to viscosity. The curves also show maxima at approximately the same shear rates as the viscosity curves and tend to approach one another at high shear rates. The normal stress data at shear rates of  $30,000 \text{ sec}^{-1}$  to  $100,000 \text{ sec}^{-1}$  from the thrust jet on the 1.7-0-0 and 1.7-1.5-100 compositions were identical within experimental error.

The data were analyzed further using the generalized Maxwell model for viscoelasticity. (Reference: "Viscoelastic Properties of Polymers," page 42, J. D. Ferry, Wiley Publishers, 1961.) Using this model, the data for the viscosity and normal stress coefficient can be separated into a mean relaxation time and a mean shear modulus. The mean relaxation time is the average disentanglement time of the molecular interactions and the modulus is proportional to the total number of interactions per unit volume of fuel.

Figure 34 shows the mean relaxation time versus shear rate for the eight compositions. All of the curves approach a base line that is inversely proportional to shear rate. At low shear rates, the curves approach a constant value of relaxation time which is the natural time of motion of the thickened fuel. If we rank the fuels according to their natural relaxation time, we obtain the same ranking as was obtained for viscosity and normal stress coefficient.

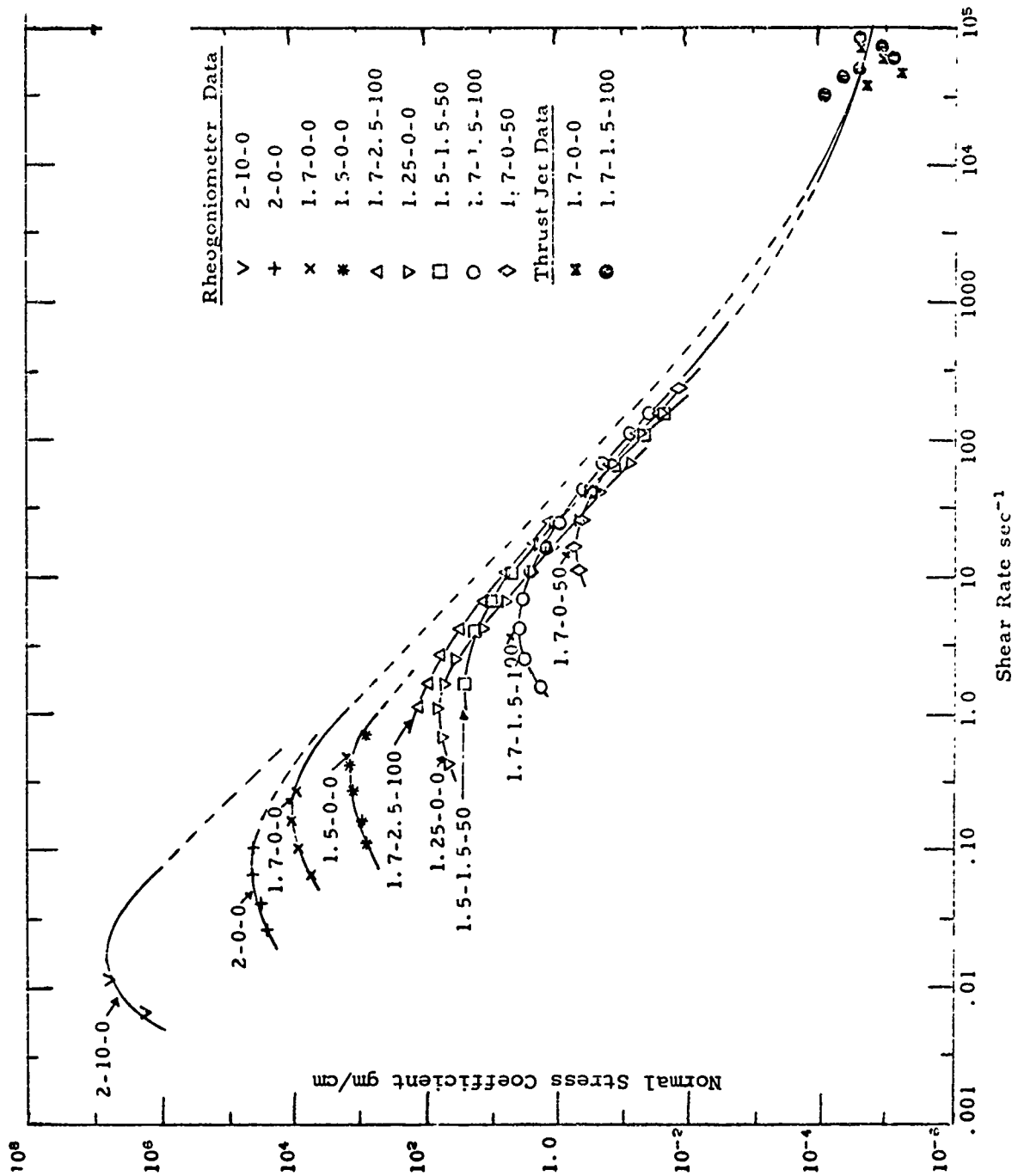


FIGURE 33. NORMAL STRESS COEFFICIENT VERSUS SHEAR RATE (RHEOGONIOMETER AND THRUST JET) VARIOUS MODIFIED THICKENED FUEL COMPOSITIONS

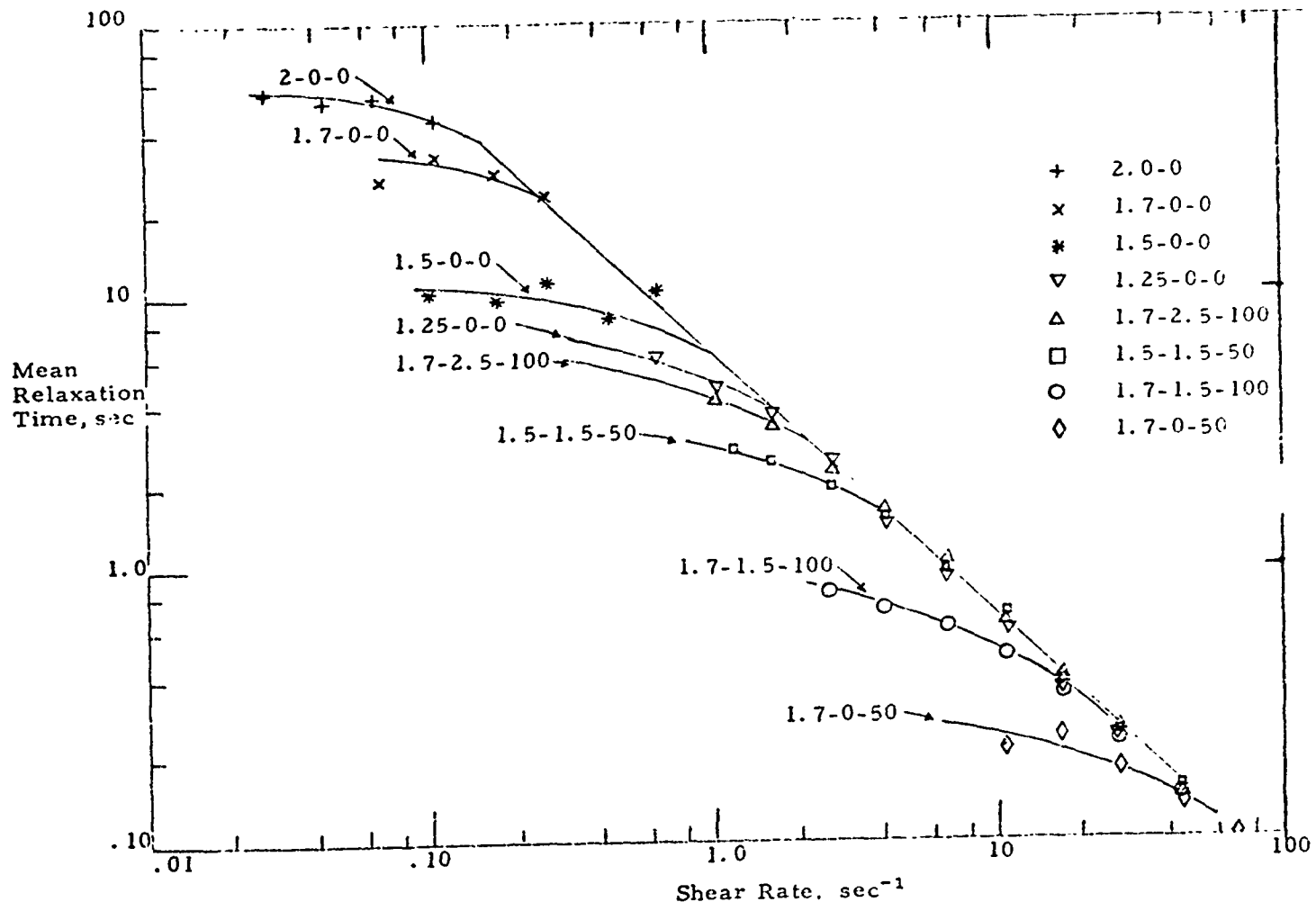


FIGURE 34. MEAN RELAXATION TIME VERSUS SHEAR RATE (RHEOGONIOMETER AND THRUST JET) VARIOUS MODIFIED THICKENED FUEL COMPOSITIONS

Figure 35 shows the mean shear modulus or entanglement density of the fuel as a function of shear rate. The data for all of the fuel compositions show a gradually increasing modulus with increasing shear rate. The curves are closer together, indicating that changes in concentration of XD-7038.00 and other additives affect the times of disentanglement much more than the entanglement density. However, the information could not explain the differences in the fire explosion test for the various compositions.

Two additional rheological tests were performed on the thickened fuels to investigate transient behavior which is directly related to the viscoelastic response in impact tests. Both of these tests were performed on the Weissenberg rheogoniometer. In the stress relaxation test, the cone was rotated in steady shear, the instantaneous brake was applied and the stress decay measured with time. The relaxation curve was then differentiated to obtain the shear modulus density function as a function of relaxation time. Three representative curves are shown in Figure 36, illustrating the effect of XD-7038.00 concentration and the effect of DOWANOL addition on the relaxation spectra. In general, an increase in XD-7038.00 concentration increases both the shear modulus and the relaxation time as exemplified by the 1.25-0-0 and 1.7-0-0 curves. Addition of ammonia hydroxide increases the relaxation time and addition of DOWANOL decreases the relaxation time. The net effect is shown for the composition labeled 1.7-1.5-100. Much of what has commonly been described as the entanglement plateau has been removed from this composition.

Stress formation tests were also performed on the thickened fuels to determine if the modulus of the fuel in response to a sudden force was significantly different from the modulus calculated from steady shear measurements. However, the shear moduli calculated from the initial slopes of the stress formation curves agreed reasonably well and demonstrated the same trends as the steady-state measurements.

It is apparent from the rheological characterization studies that something other than macroscopic rheological behavior is having a significant effect on the atomization behavior in the fire explosion test. Although the macroscopic rheological properties are significant in determining product usefulness, they are difficult to use as a product specification.

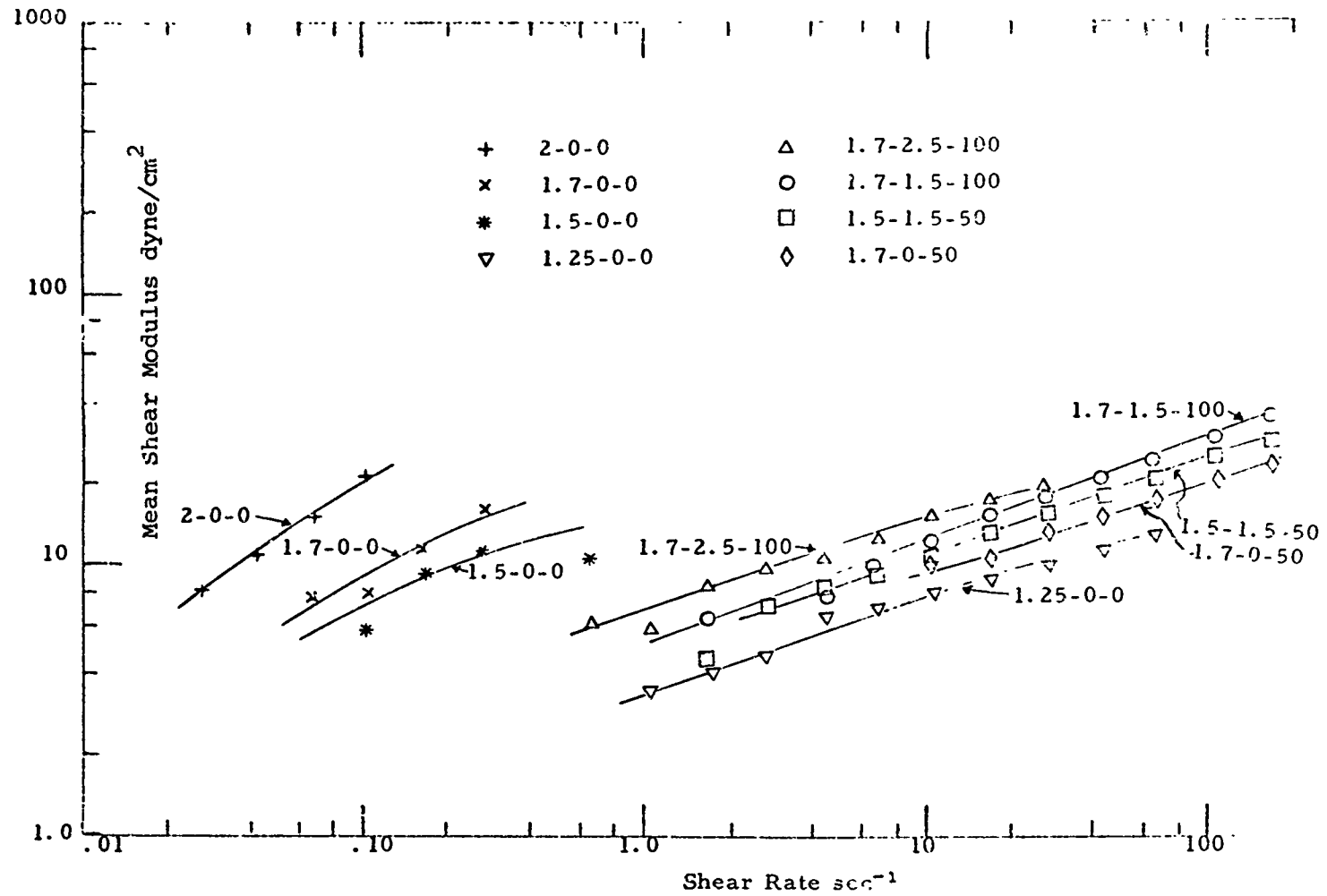


FIGURE 35. MEAN SHEAR MODULUS VERSUS SHEAR RATE (RHEOGONIOMETER) VARIOUS MODIFIED THICKENED FUEL COMPOSITIONS

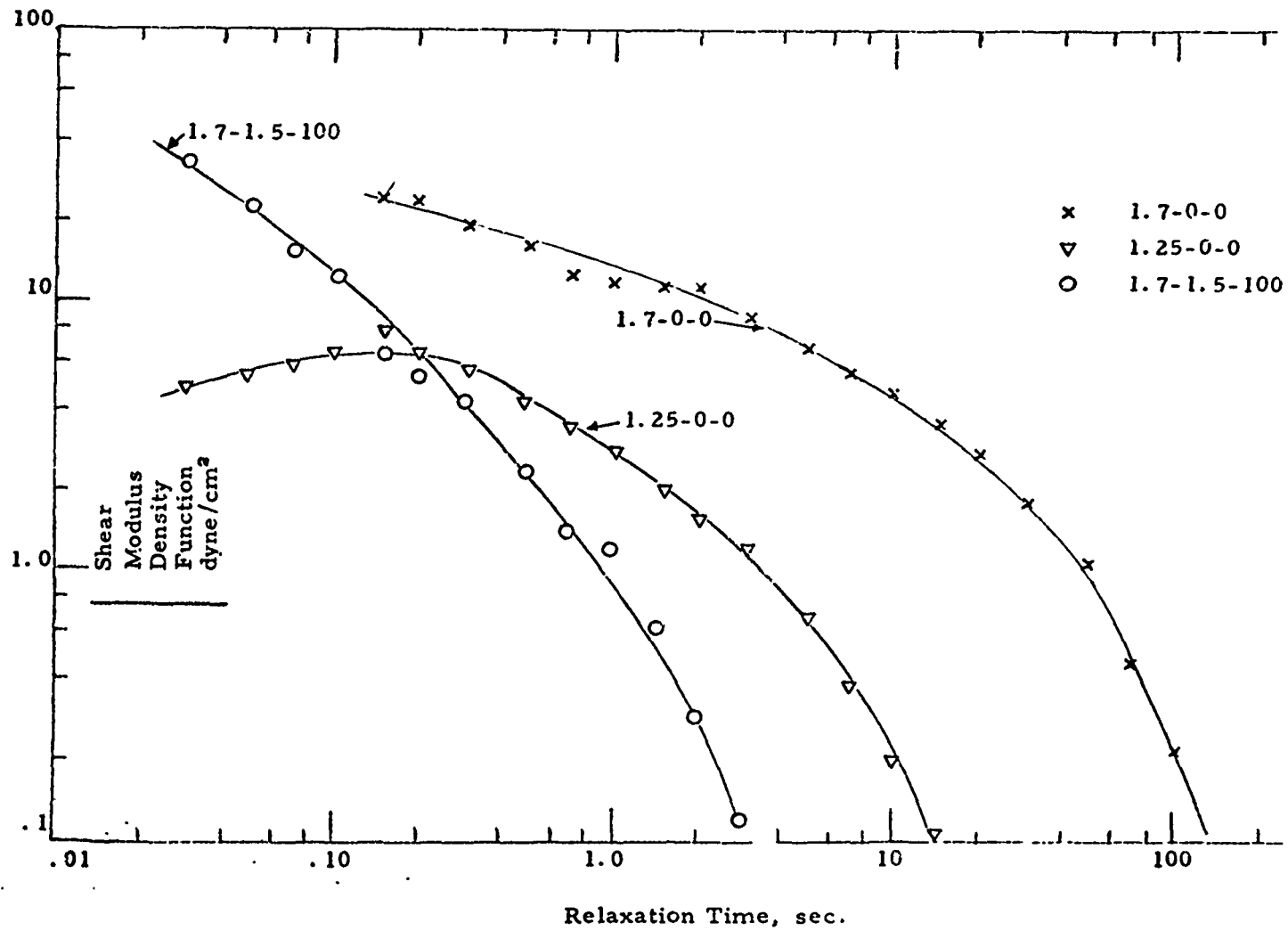


FIGURE 36: SHEAR MODULUS DENSITY FUNCTION VERSUS RELAXATION TIME (RHEOGONIOMETER). VARIOUS MODIFIED THICKENED FUEL COMPOSITIONS

V. FUEL FLOW TESTS

1. Pump-Out Rates

To determine an indication of flowability of thickened fuels in a simulated use condition, a pump-out test was designed. The equipment for this test is shown in Figure 37. A Jabsco pump rated at 10,000 pounds per hour was used to pump the fuel from a small rectangular tank with dimensions of 48.5 inches long, 14.5 inches wide and 4.75 inches high. The tank was tilted 4° over the width and 6° over the length. The inlet pipe from the pump (the bottom end of the pipe having four, one-quarter-inch half-moon cutouts) was placed 2.5 inches from each side in the lowest level of the tank with one edge touching the bottom.

Approximately 10,000 to 15,000 grams of test fuel were used for each test with the pump operating at maximum capacity. The test was terminated as soon as the pump began cavitation, evidenced by suction of air. A record of the test data is shown in Table 9.

Although the pump out rate for the low viscosity thickened fuels was equivalent to the rate for Jet A-1, the residual fuel was approximately doubled.

2. Gravity Flow (NAFEC Facilities)

A flow test unit was constructed at the FAA, NAFEC, Atlantic City, New Jersey, to measure the gravity flow of fuels through various size orifices and pipes. A photograph of this apparatus is shown in Figure 38. The various size orifices and pipes are listed below:

Orifices:

A. Oval

(a) 0.75 Inch x 0.156 inch (See sketch, Figure 39)

B. Triangular

(a) 1.875 Inch x 2.5 inch (See sketch, Figure 40)



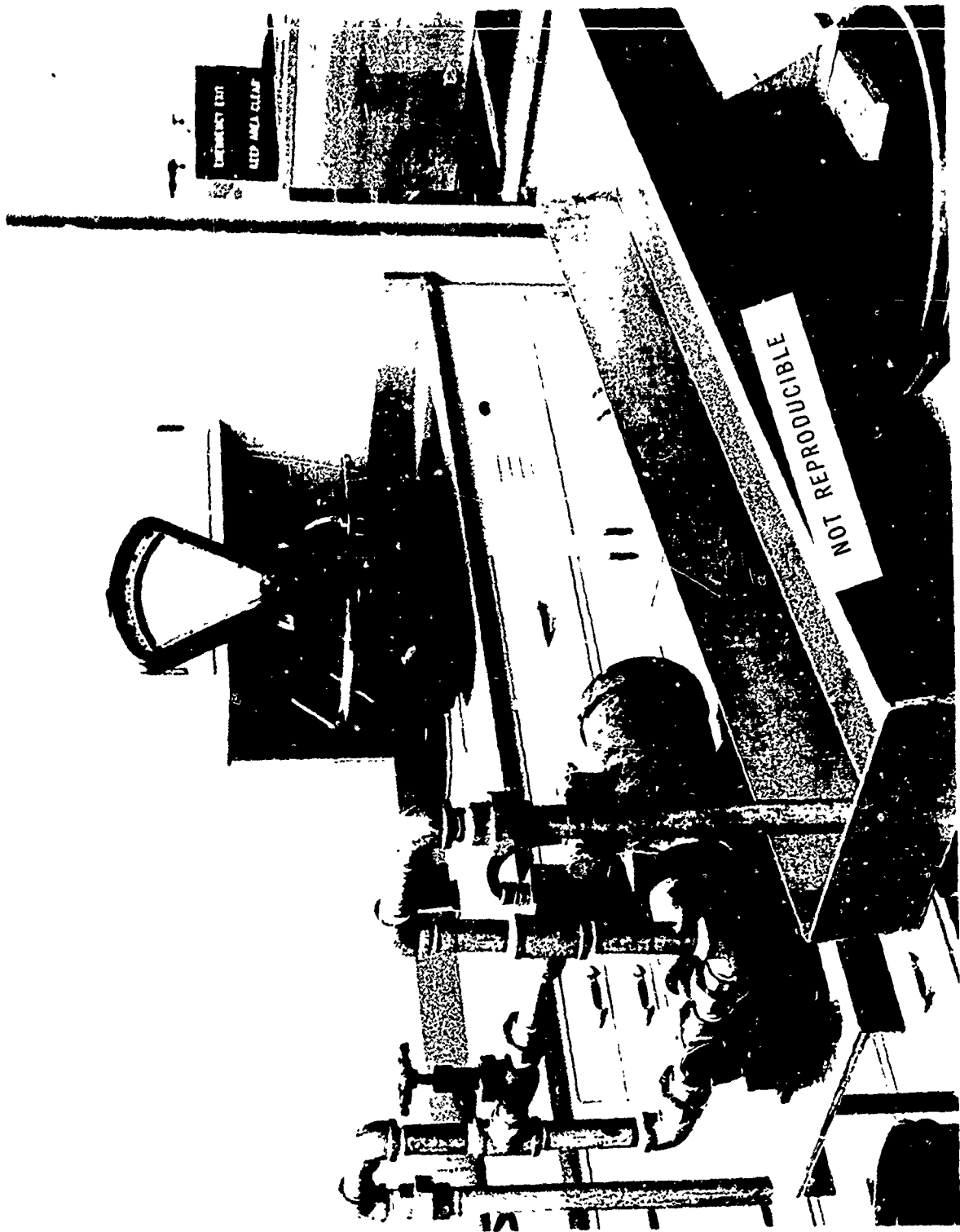


FIGURE 37. PUMP-OUT TEST EQUIPMENT

TABLE 9. - PUMP-OUT RATES FOR VARIOUS THICKENED FUEL COMPOSITIONS

<u>Formulation No.</u>	<u>Composition</u>	<u>Fuel Wgt. Pumped (Grams)</u>	<u>Pumping Time (Sec.)</u>	<u>Pumping Rate (lb./hr.)</u>	<u>Residual Fuel (%)</u>	<u>Fuel Viscosity (Brookfield 10 RPM)</u>
-	Jet A-1	10,595	8.5	10,250	8	4
199-8-16	1.7-0-50	9,000	6.8	10,260	14	180
199-37-6	1.7-2-100	6,500	5.0	10,250	15	350
199-8-3	2-0-50	8,575	6.8	10,100	18	750
199-6-2	2-0-0	7,770	6.25	9,900	30	3000
199-6-1	2-10-0	6,200	5.2	9,300	43	15,000



FIGURE 38. GRAVITY FLOW TEST EQUIPMENT (FAA, NAFEC, ATLANTIC CITY, NEW JERSEY)

Pipes

- (a) 3/16 Inch ID x 5 inch length
- (b) 0.028 Inch x 1/2 inch x 48 inch length
- (c) 0.049 Inch x 1-1/2 inch x 72 inch length
- (d) 0.062 Inch x 2-1/2 inch x 72 inch length

The test fuel is poured into the vertical test chamber to the desired height. The desired orifice or pipe is mounted at the base of the vertical chamber and the gate opened for a selected time and/or head height. The fuel released is collected in a container and weighed.

The thickened fuel selected for testing was composition 1.7-2-100 (Dow Reference No. 199-45), hereafter designated Experimental Jet Fuel XD-7129.02 (FAA). Base Jet A was tested as a control fuel. The thickened fuel was supplied to NAFEC and NAFEC personnel conducted the flow tests. The NAFEC data is shown in Figures 39, 40, 41, and 42, 42A, 42B.

VI. PROPERTY PROFILE OF FINAL COMPROMISE THICKENED FUEL

The final compromise thickened fuel selected by Dow and FAA (NAFEC) as a result of these studies was given the designation Experimental Jet Fuel XD-7129.02 (FAA). Within the scope of time and funds allotted, some of the properties of this thickened fuel were obtained.

1. Composition

The composition of the selected fuel, Experimental Jet Fuel XD-7129.02 (FAA) is listed:

Jet A-1	344 Pounds
Experimental Resin XD-7038.00	6 Pounds
DOWANOL DE	0.23 Pound
28% Ammonium Hydroxide 0.36 g./gallon	0.005 Pounds

2. Rheological Characteristics

(a) Viscosity (Brookfield RVT, #3 Spindle)

The viscosity profile is shown in Figure 43 covering the shear range (rpm) of the viscometer and spindle. It should be noted that the viscosity increases with shear over this particular shear range. A significant secondary shear thickening is repeatedly shown beyond a shear rate of 10 rpm.

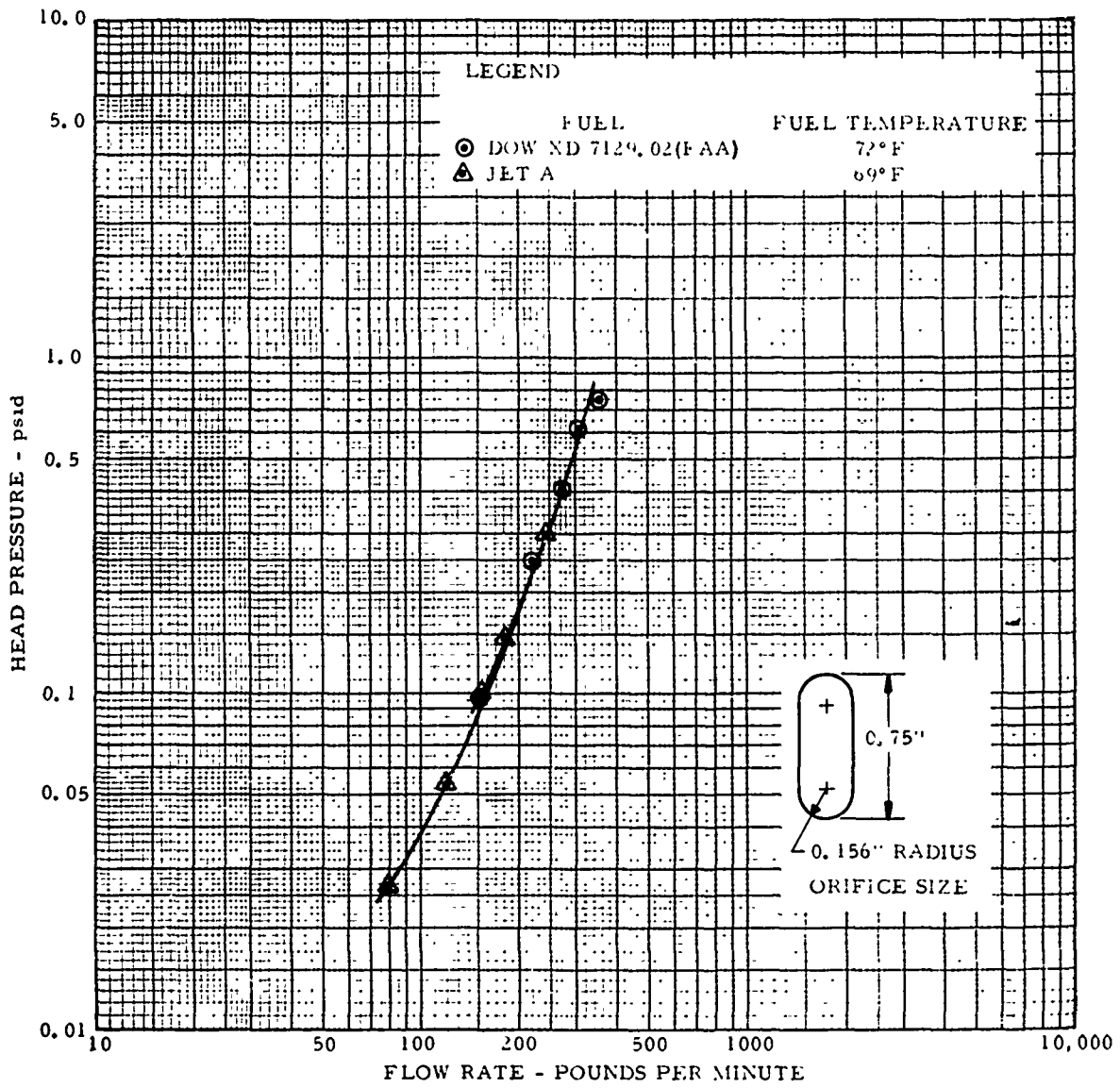


FIGURE 39. ORIFICE FLOW - OVAL (SEE SKETCH ON GRAPH)

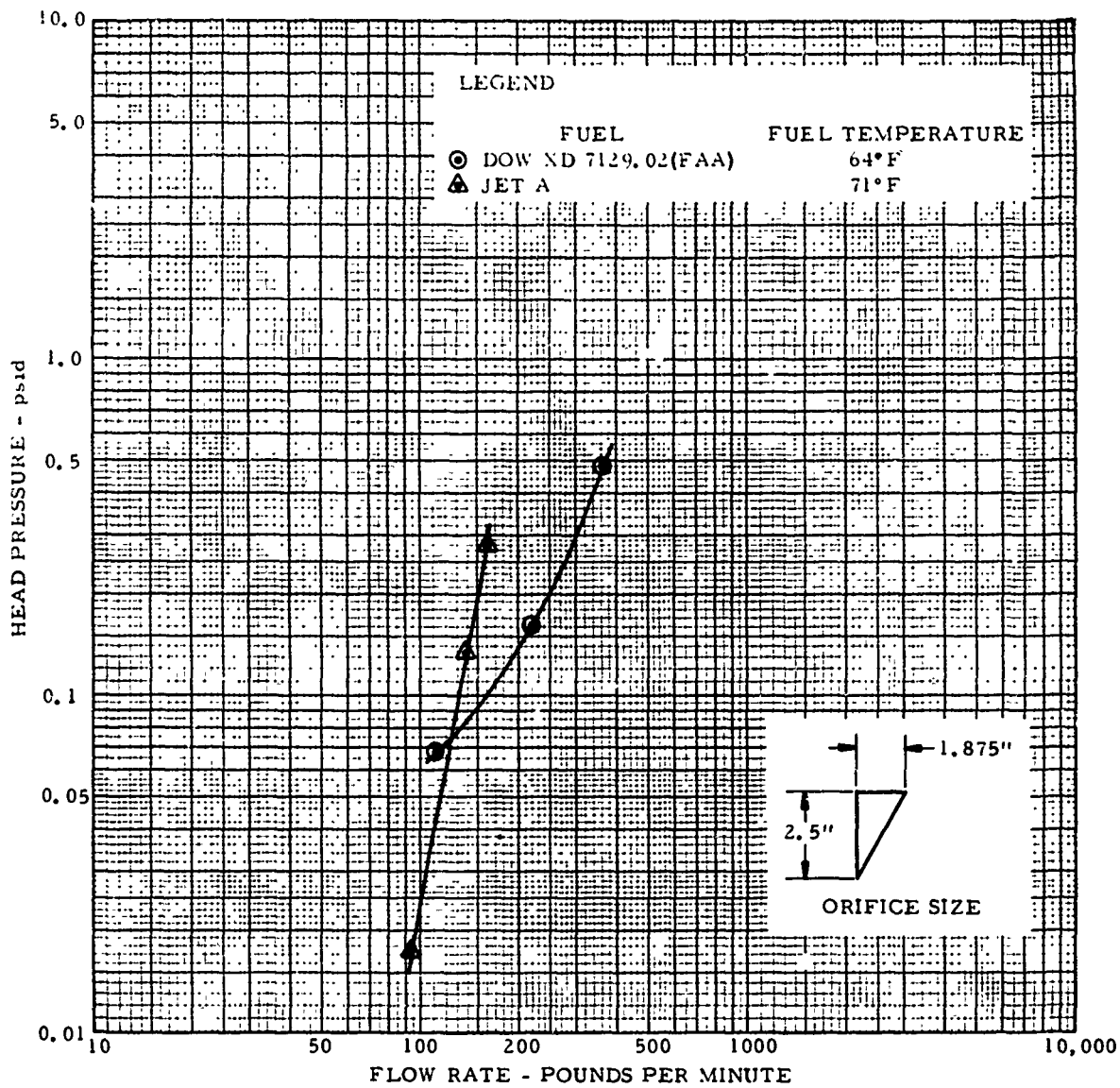


FIGURE 40. ORIFICE FLOW - TRIANGLE (SEE SKETCH ON GRAPH)

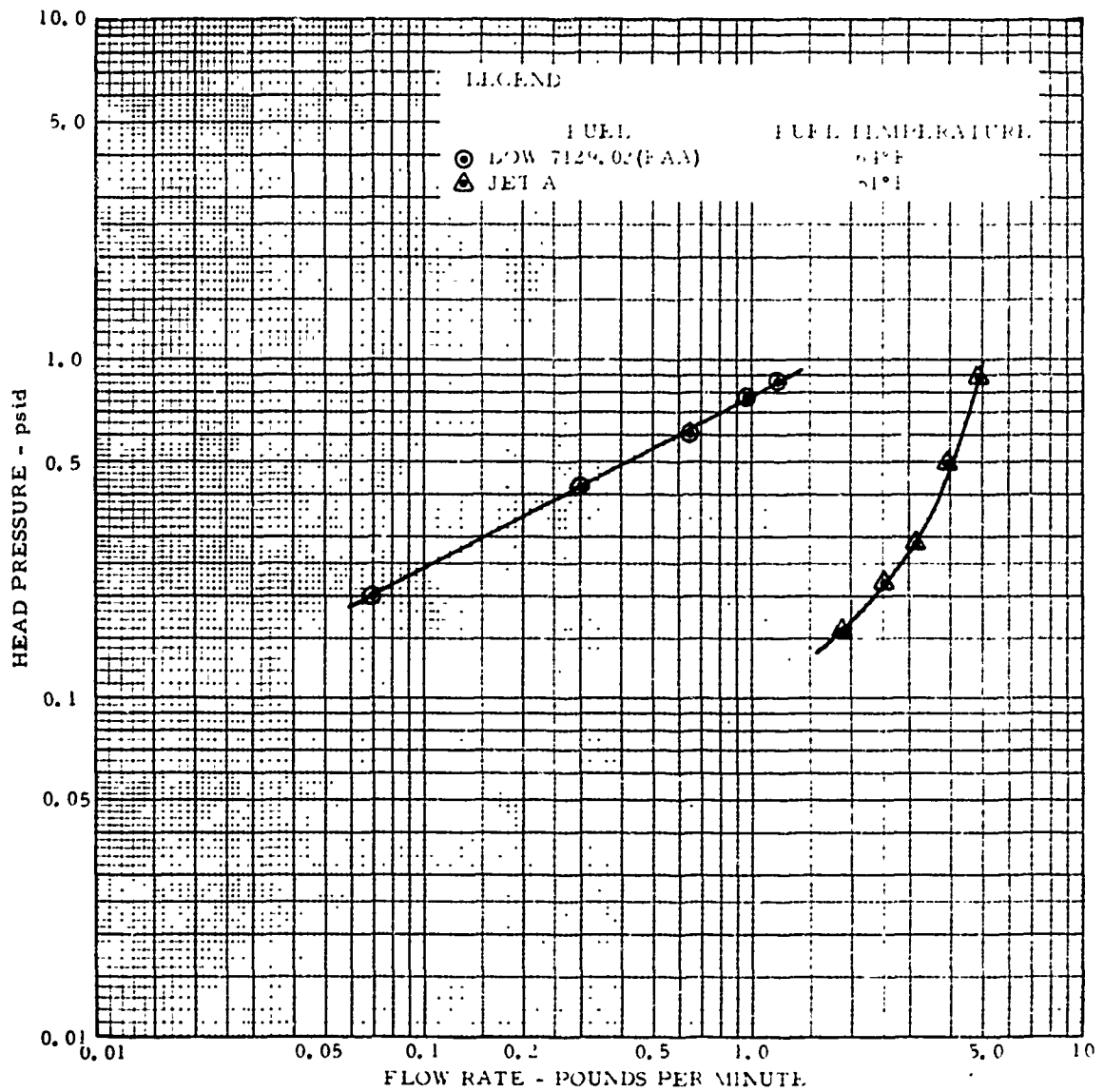


FIGURE 41. DRAIN PASSAGE FLOW - 3/16" ID x 5" LGT. (3° SLOPE)

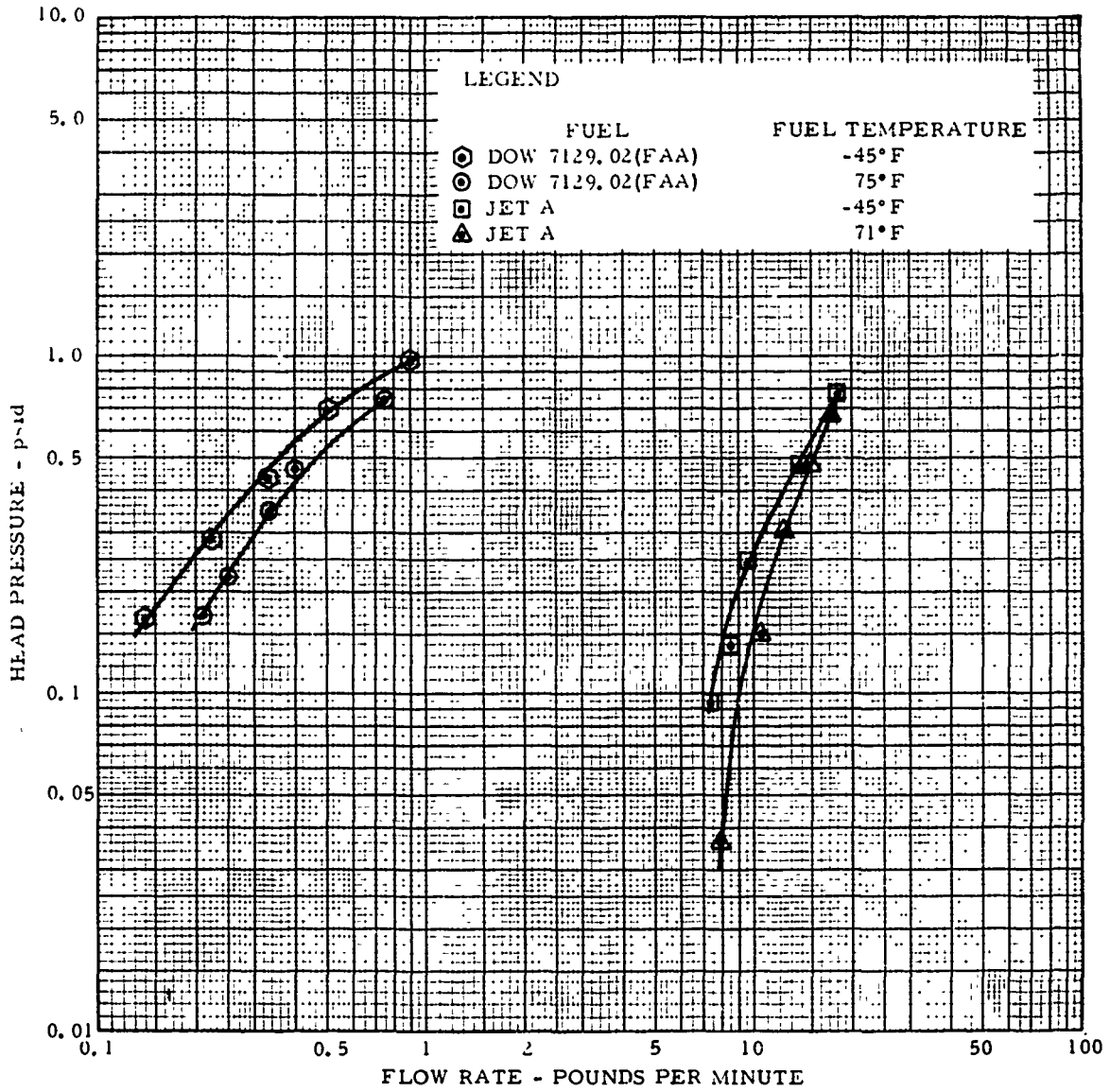


FIGURE 42. PIPE FLOW - .028" x 1/2" x 48" LGT. (6° SLOPE)



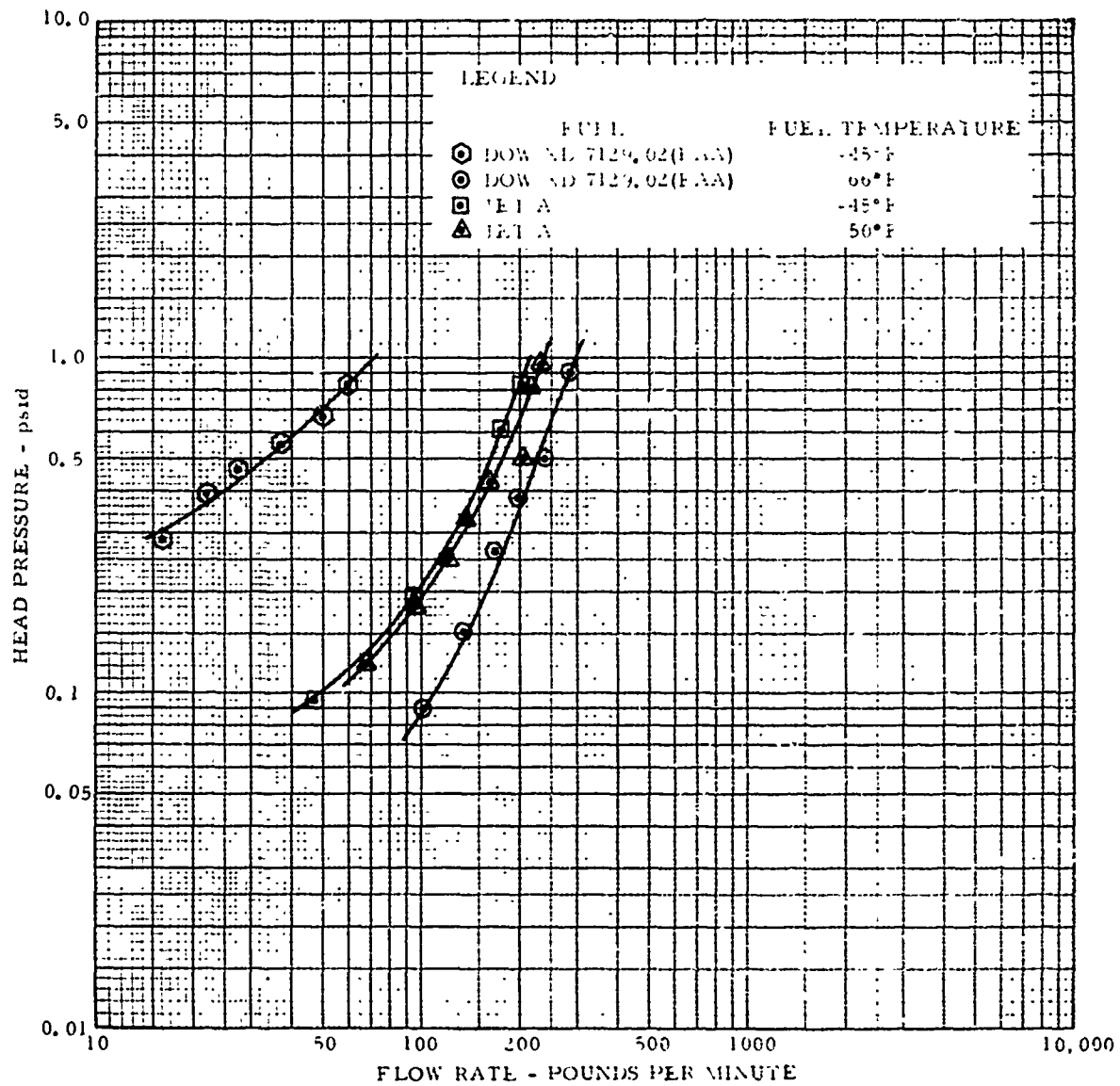
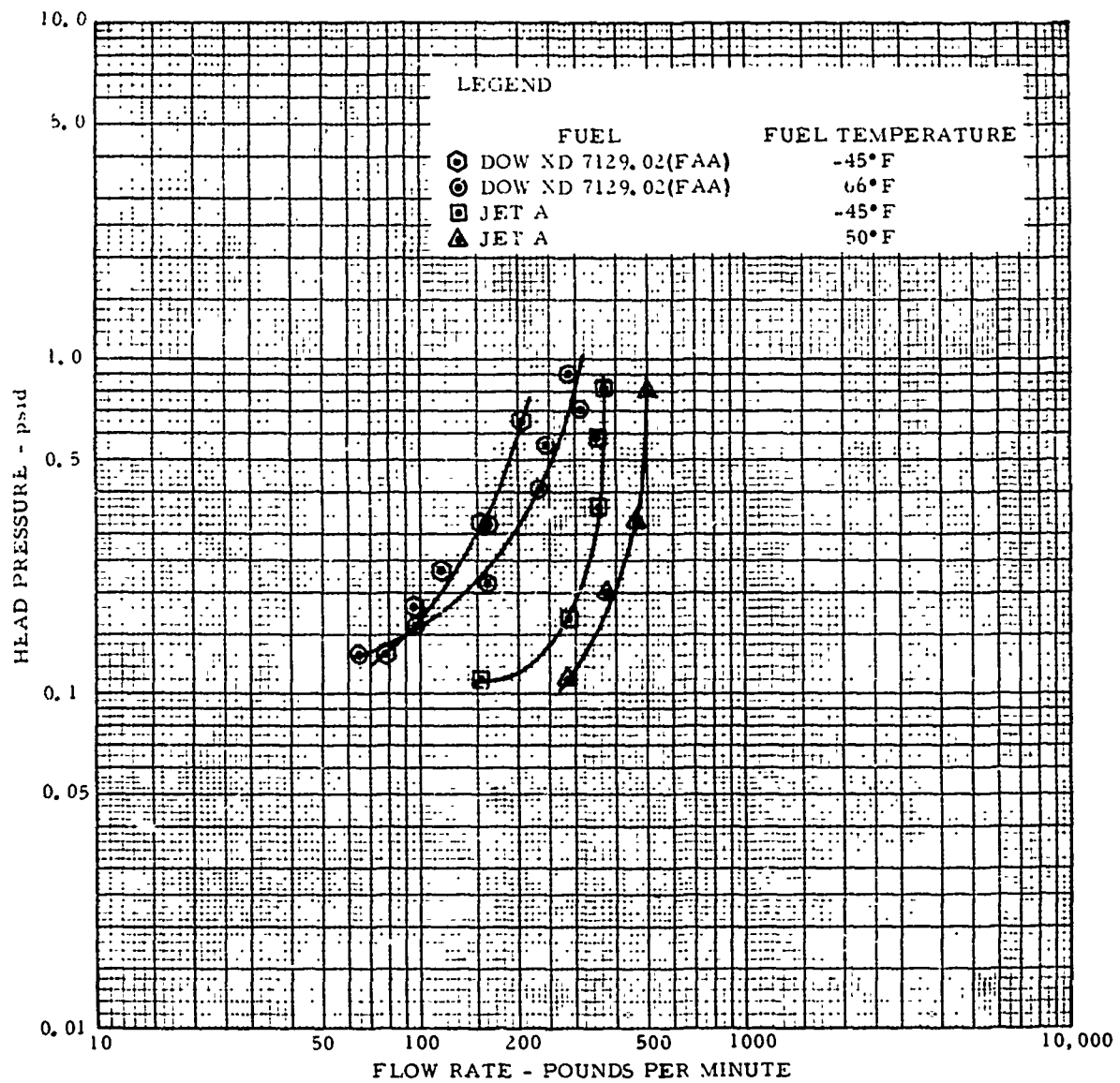


FIGURE 42A. PIPE FLOW - .049" x 1 1/2" x 72" LGT. (6° SLOPE)



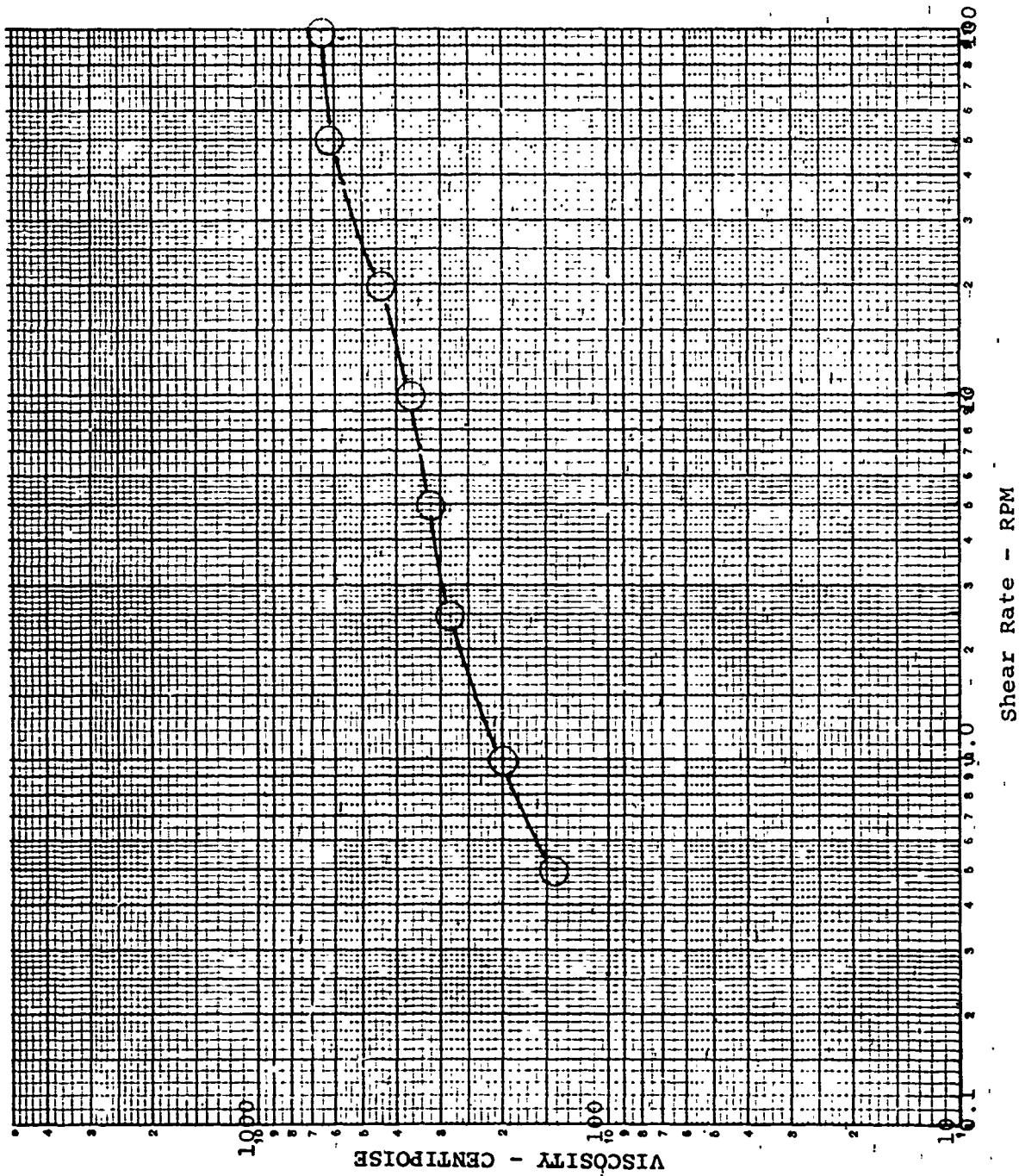


FIGURE 43. VISCOSITY VERSUS SHEAR RATE (BROCKFIELD VISCOMETER, #3 SPINDLE) EXPERIMENTAL JET FUEL XD-7129.02 (FAA)

(b) Rheogram (Forced-Ball Viscometer)

Figure 44 shows the type of flow when viscosity is plotted versus shear rate and emphasizes the high shear rate effect. Note that at high shear rates the viscosity decreases dramatically and approaches the viscosity of the base Jet A-1.

(c) Rheogram (Rotovisco Viscometer)

In Figure 45 the viscosity versus shear rate curve covers a broader rate of shear range and emphasizes the sharp peak viscosity at about 10 reciprocal seconds ( $\text{seconds}^{-1}$ ). The data to date indicates that this characteristic is present in the fuel regardless of the initial static viscosity.

3. Flowability

(a) Pump Out (Ref. Figure 37)

<u>Type Fuel</u>	<u>Rate</u>	<u>Time</u>	<u>Residual</u>
Exp. Jet Fuel XD-7129.02 (FAA)	10,250 Lbs/Hr	5.0 Sec	15 Percent
Jet A-1	10,250 Lbs/Hr	8.5 Sec	8 Percent

(b) Gravity Flow (NAFEC, Ref. Figure 38) at Ambient Temperature

	<u>0.156" x 0.75" Oval</u>		<u>2.5" x 1.875" Triangle</u>		<u>3/16" ID x 5" lgt (3° slope)</u>	
	<u>Head</u>	<u>Flow Rate</u>	<u>Head</u>	<u>Flow Rate</u>	<u>Head</u>	<u>Flow Rate</u>
	<u>Pressure</u>	<u>(Lbs/Min)</u>	<u>Pressure</u>	<u>(Lbs/Min)</u>	<u>Pressure</u>	<u>(Lbs/Min)</u>
	<u>psid</u>		<u>psid</u>		<u>psid</u>	
XD-7129.02 (FAA)	0.1	160	0.1	160	0.5	0.42
XD-8129.02 (FAA)	0.5	300	0.5	375	1.0	2.2
Jet A-1	0.1	160	0.1	130	0.5	4.0
Jet A-1	0.5	300	0.5	170	1.0	5.0

4. Gel Structure

The nature of the gel structure in the thickened fuel is partially portrayed in the rheological curves shown in Section VI-2-a, b and c. The thickened fuel evidences a

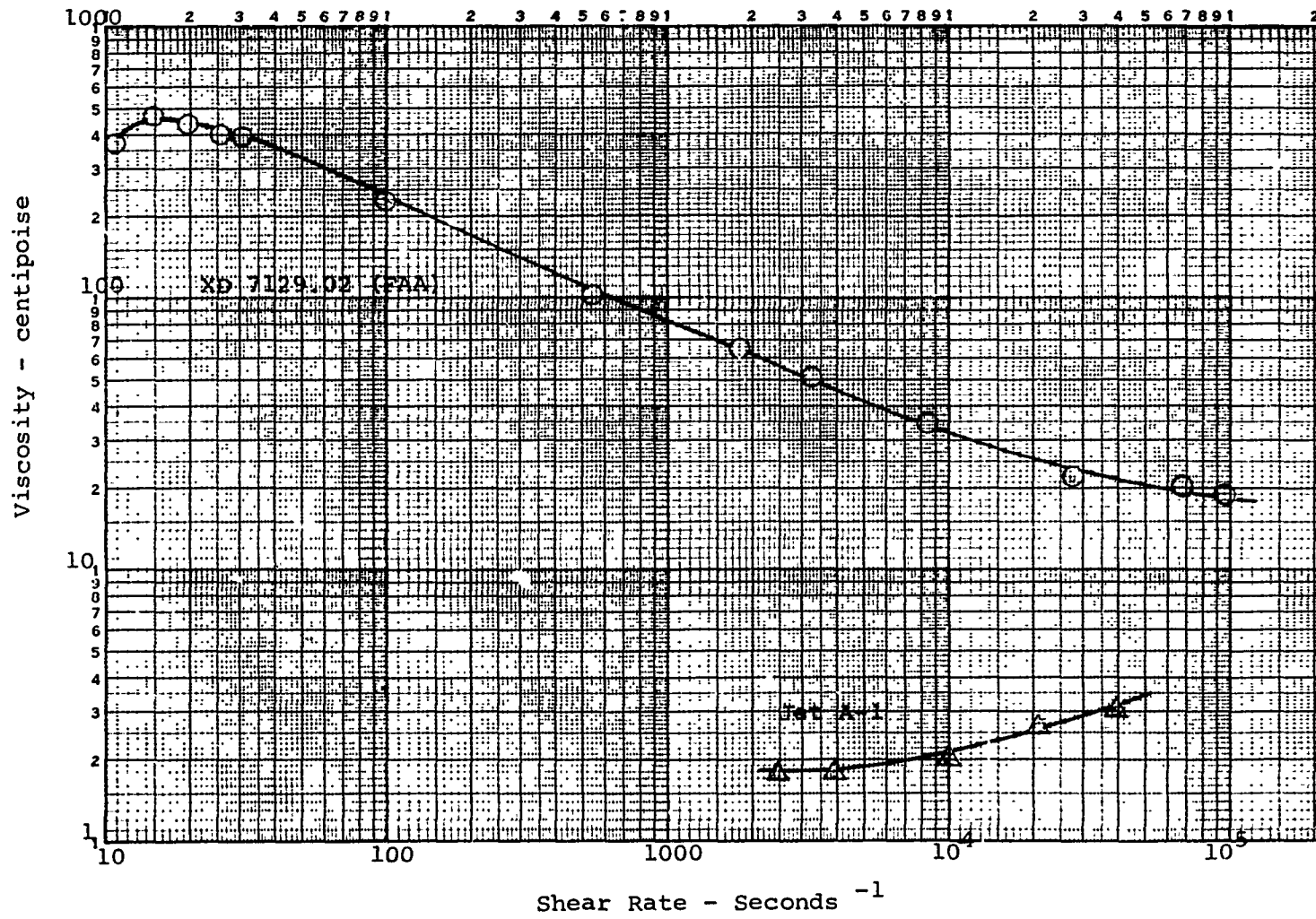


FIGURE 44. VISCOSITY VERSUS SHEAR RATE (FORCED BALL VISCOMETER)  
EXPERIMENTAL JET FUEL XD-7129.02 (FAA)

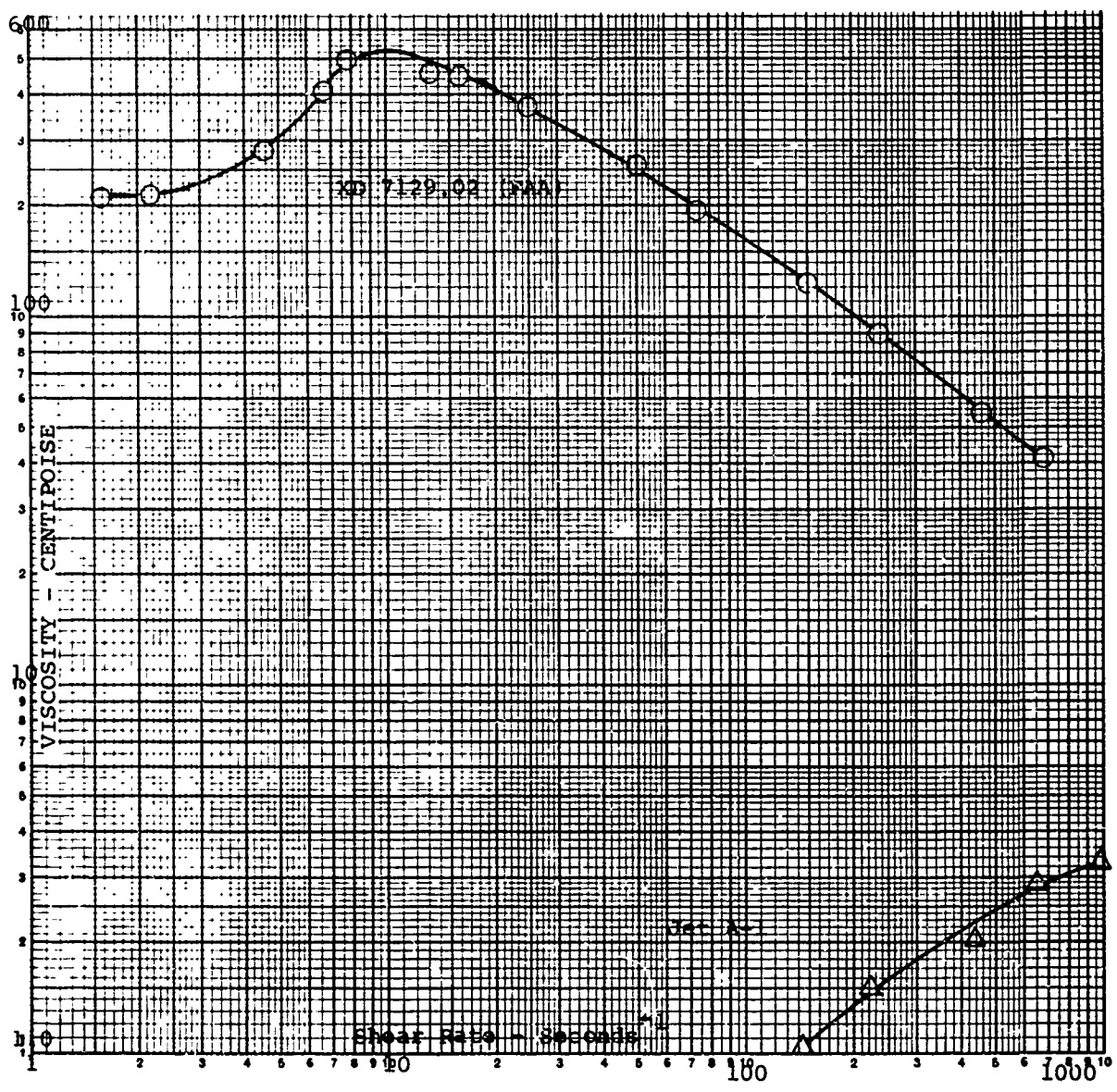


FIGURE 45. VISCOSITY VERSUS SHEAR RATE (ROTOVISCO VISCOMETER) EXPERIMENTAL JET FUEL XD-7129.02 (FAA)

number of rheological characteristics dependent on the rate of shear. Initial dilatancy occurs in the low shear range of 0 to 2 seconds<sup>-1</sup>, with a secondary shear thickening in the 6-10 seconds<sup>-1</sup> range, building viscosity to a peak at about 10 seconds<sup>-1</sup>. This is followed by pseudoplasticity in the higher shear ranges. Figure 46 shows a shear-rate/shear-stress curve obtained with the Rotovisco where the shear rate cycle is complete. This curve gives definite evidence of thixotropy also being a characteristic.

Rheopecticity, shear thickening with time at a constant shear rate, is shown in Figure 47 at 8.5 seconds<sup>-1</sup>.

## 5. Thermal Properties

### (a) Heat Transfer Values

These data were obtained by the Dow Thermal Laboratory using the thin film concentric shear sphere method (Reference, W. N. Vanerkooi, D. L. Hildebrand and D. R. Stull, Journal of Chemical and Engineering Data, Volume 12 (No. 3), 377 (1967)), Figure 48.

The data are plotted in Figure 49, thermal conductivity versus temperature. These data show that the thermal conductivity of the Jet A-1 and XD-7129.02 (FAA) are essentially the same at temperatures between 55° and 120°C, but quite different between temperatures of -40° and 55°C. The thermal conductivity of Jet A-1 increases at the lower temperatures and XD-7129.02 (FAA) decreases. However, it is predicted that if the XD-7129.02 was subjected to shear at the lower temperatures, it would be less viscous and thus its thermal conductivity should not decrease at the lower temperatures.

### (b) Heat of Combustion

The apparatus used to obtain these data by the Dow Thermal Laboratory is shown in Figure 50. The weighed jet fuel sample is sealed in a polypropylene bag and burned in a platinum-lined calorimeter bomb charged with 30 atm of pure oxygen and one ml of distilled water. The calorimeter temperature is measured by a quartz

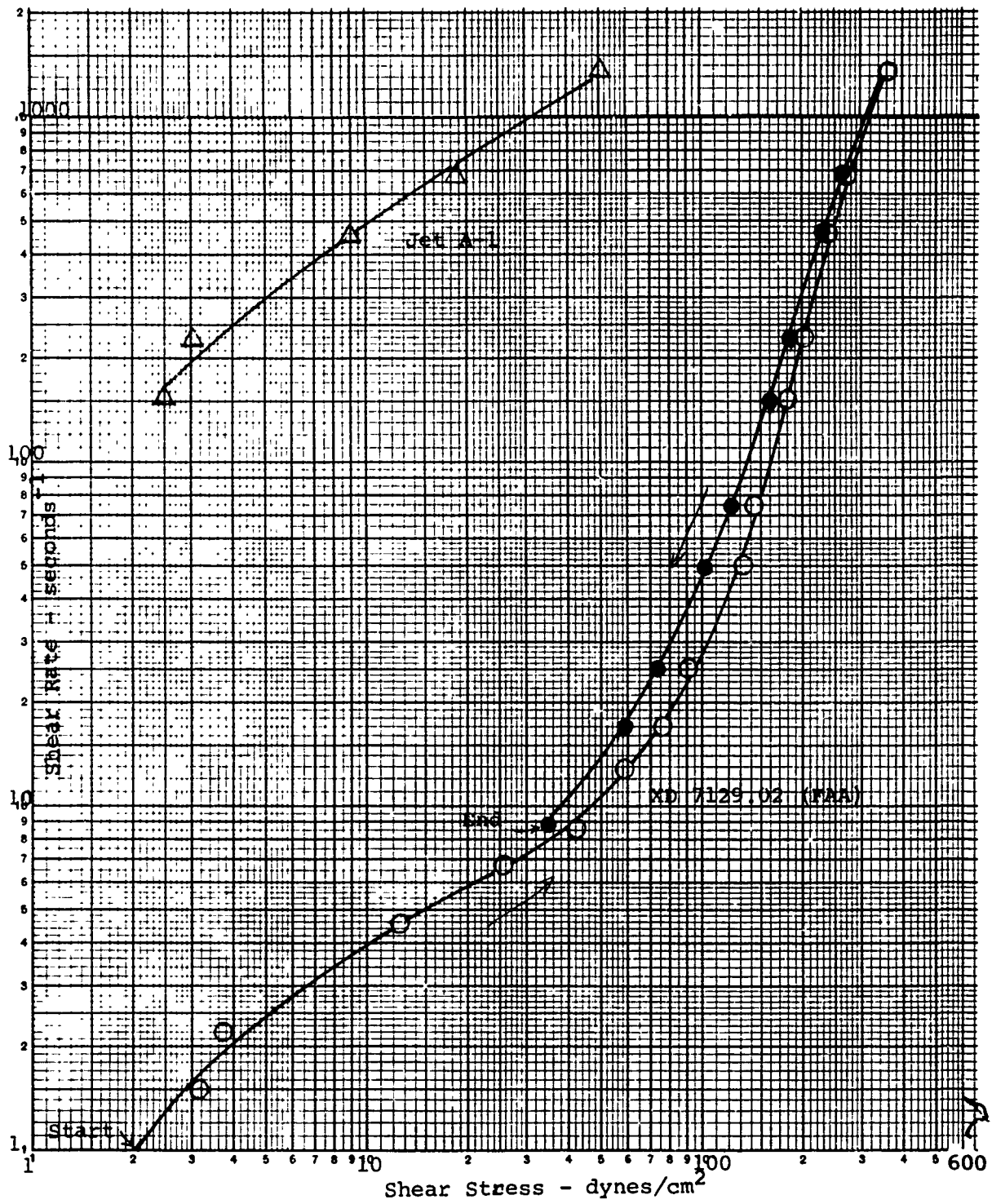


FIGURE 46. SHEAR RATE VERSUS SHEAR STRESS (ROTOVISCO VISCOMETER) EXPERIMENTAL JET FUEL XD-7129.02 (FAA)



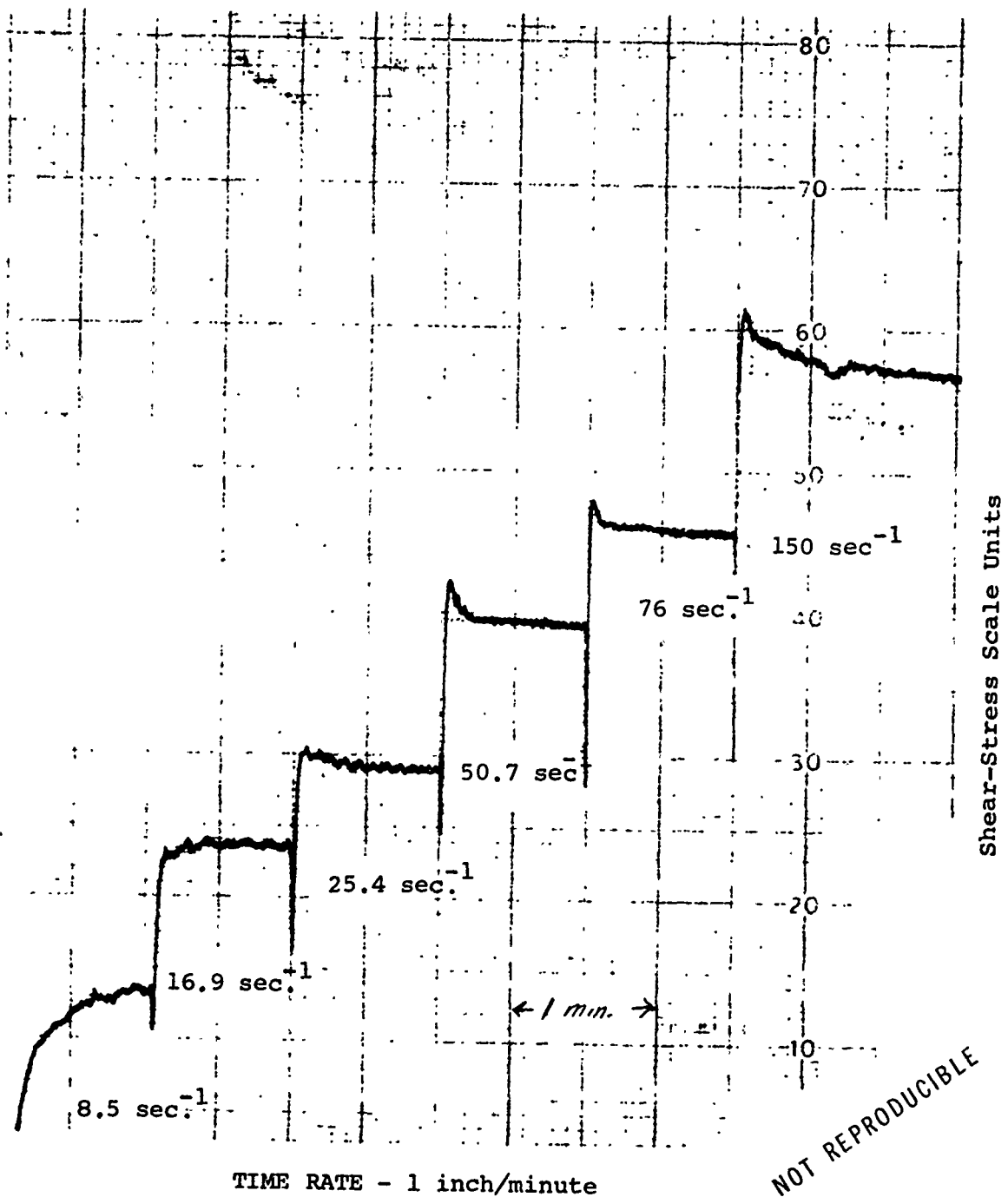


FIGURE 47. SHEAR THICKENING AT CONSTANT SHEAR RATE (ROTOVISCO VISCOMETER) EXPERIMENTAL JET FUEL XD-7129.02 (FAA)

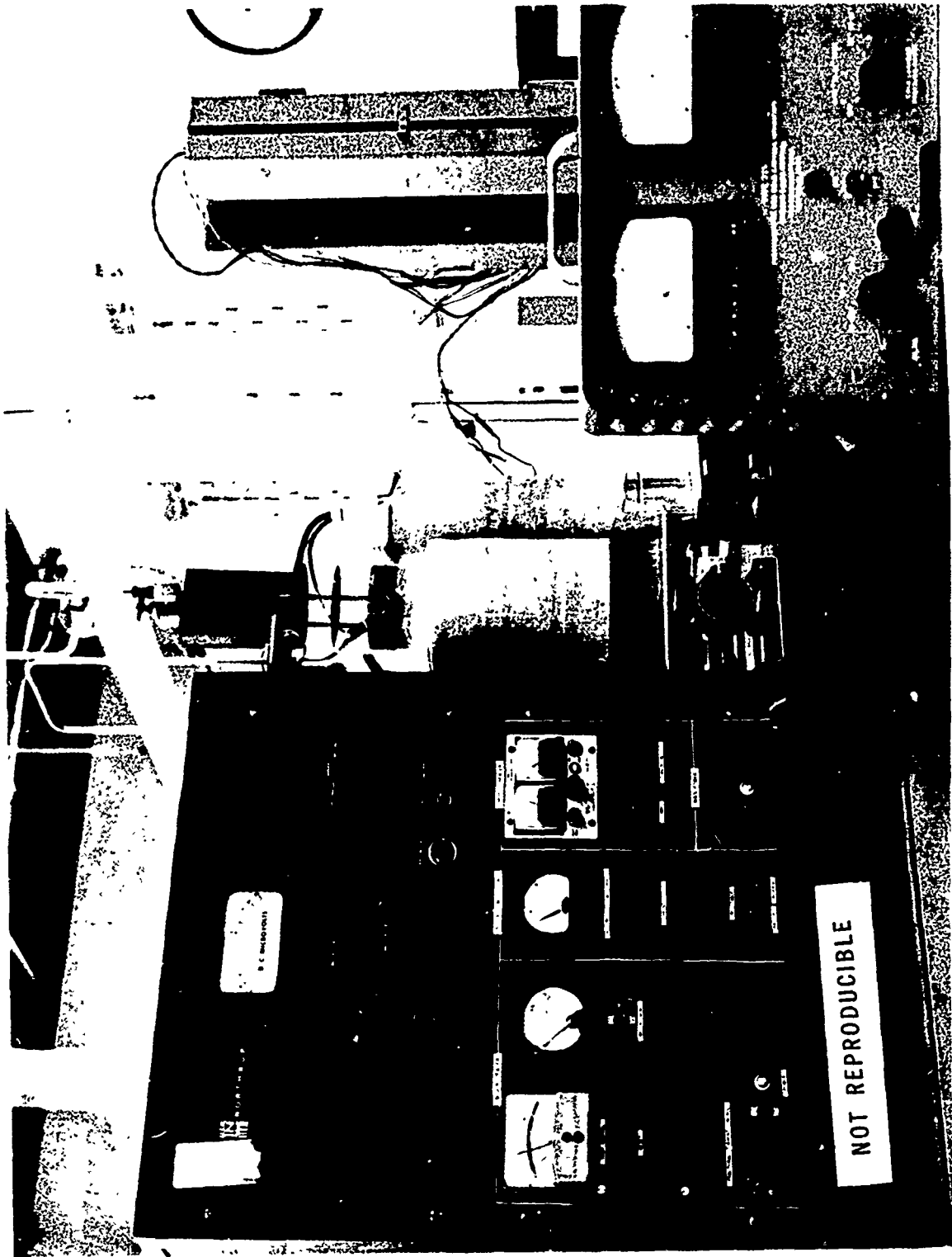


FIGURE 48.1 THERMAL CONDUCTIVITY EQUIPMENT

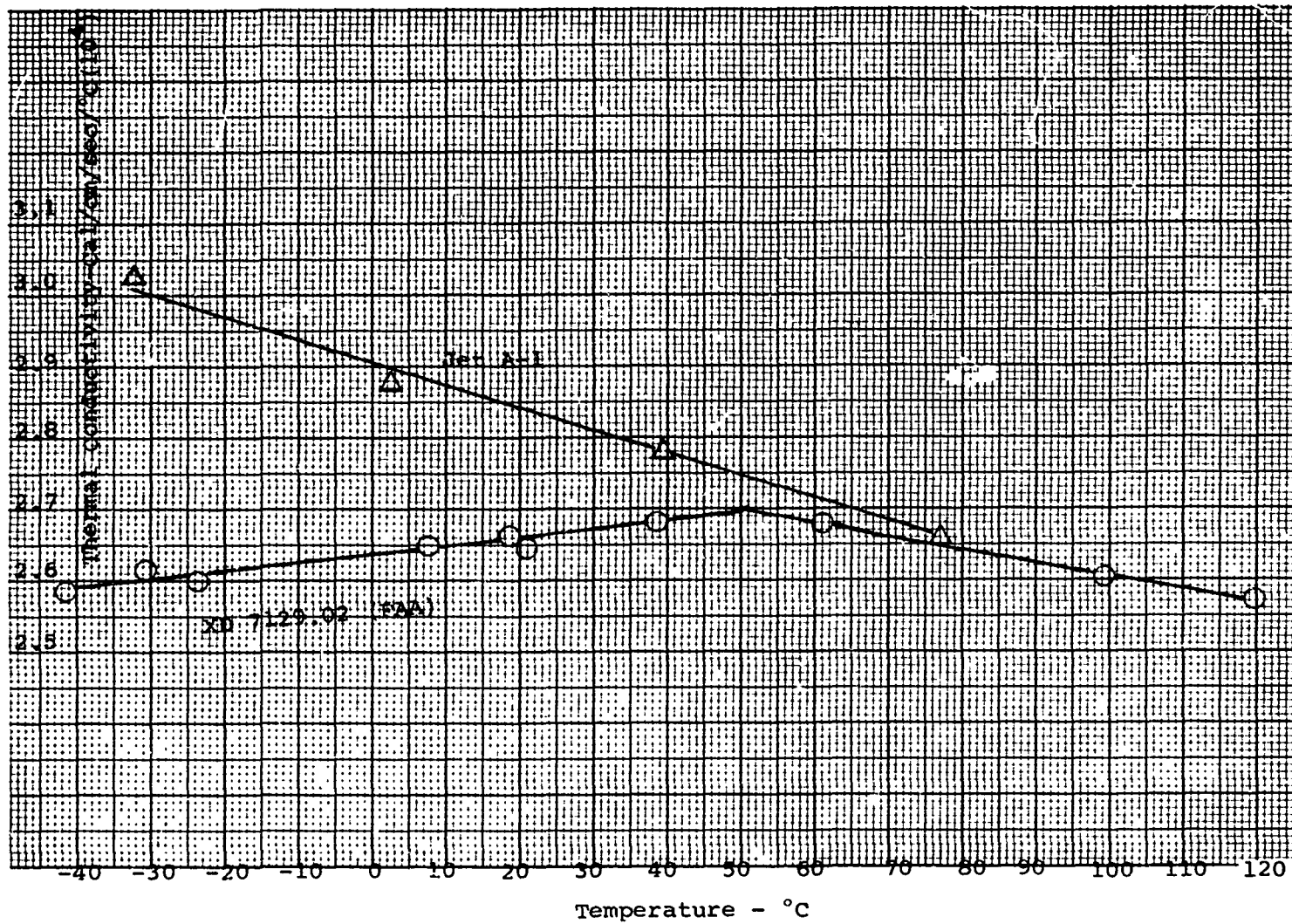


FIGURE 49. THERMAL CONDUCTIVITY VERSUS TEMPERATURE  
EXPERIMENTAL JET FUEL XD-7129.02 FAA

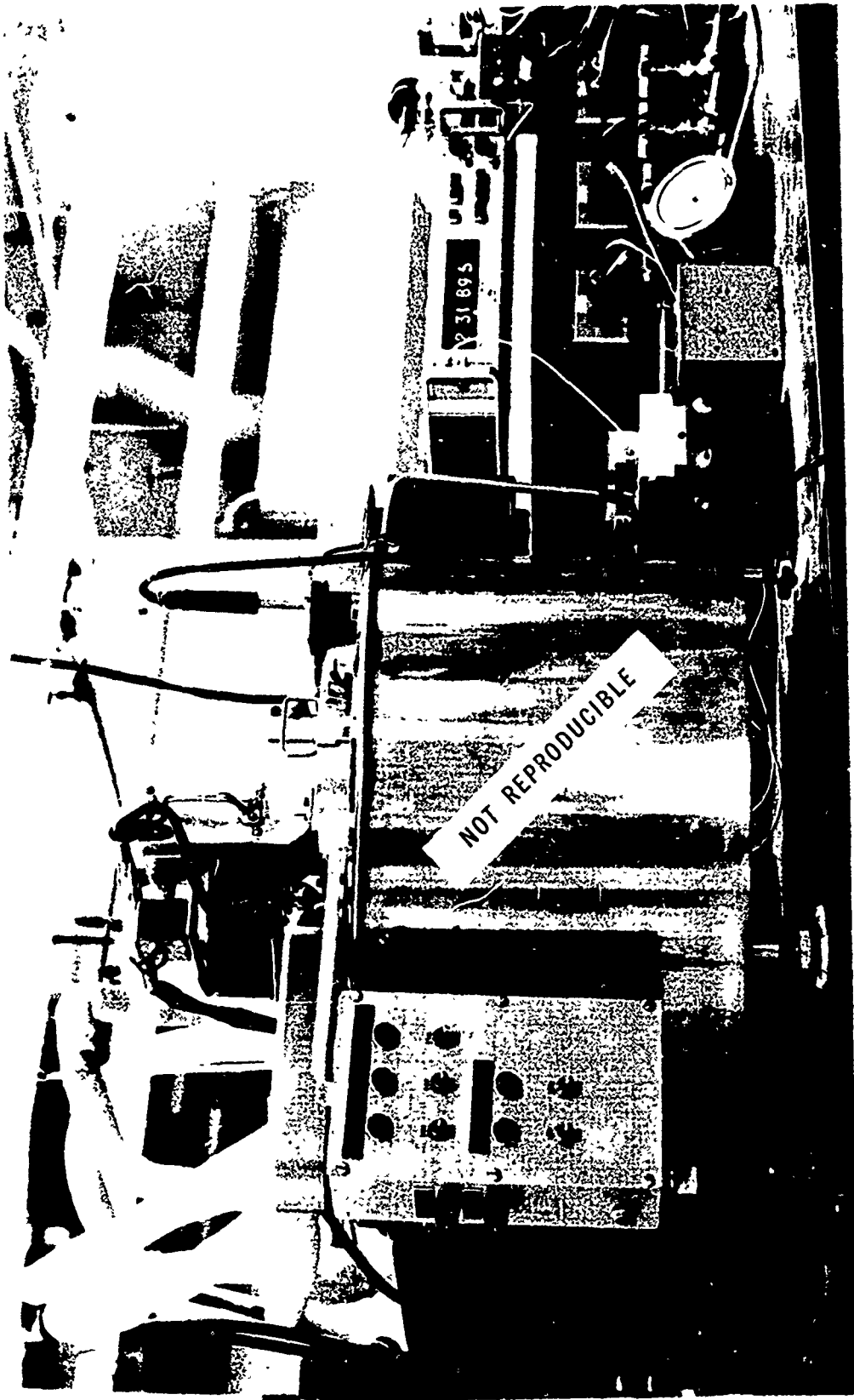


FIGURE 50. HEAT OF COMBUSTION EQUIPMENT

thermometer. The corrected temperature rise ( $\Delta T_{\text{corr}}$ ) is calculated by means of a computer program, based on Dickinson's method. The energy equivalent of the calorimetric system ( $E_{\text{calor}}$ ) is established by calibration with NBS benzoic acid to 3419.2 cal/deg.

The American Society for Testing Materials Method D2382-65 is adopted to determine the gross heat of combustion of the test fuel. The gross heat of combustion is calculated from the equation:

$$\Delta H_{\text{c}}^{\circ} \text{ (gross)} = \frac{E \text{ (calor} \times \Delta T_{\text{corr}} - \Delta E_{\text{corr}}}{\text{weight of sample}}$$

where  $\Delta E_{\text{corr}}$  is the sum of the thermochemical corrections for ignition energy, the heat of combustion of the polypropylene bag and cotton thread.

The data shows no difference in gross heat of combustion between Jet A-1 and Experimental Jet Fuel XD-7129.02 (FAA)

	<u>Gross Heat of Combustion</u>	
	<u>Cal/g</u>	<u>BTU/Lb</u>
Jet A-1	11,020	19,840
Experimental Jet Fuel XD-7129.02 (FAA)	11,000	19,800

#### 6. Stability to Temperature Change

Duplicate samples of XD-7129.02 (FAA) were exposed to temperatures of -65°F, 0°F, 75°F and 135°F for 24 hours. The samples were allowed to return to room temperature (75°F) before testing (approximately 8 hours). The viscosity of all samples was tested with the Brookfield Viscometer and the Rotovisco Viscometer was used to measure the rheological profile.

<u>Aging Temperature</u>	<u>Average Brookfield Viscosity at 75°F 10 RPM, #3 Spindle</u>
-65°F	400 cps
0°F	300 cps
75°F	300 cps
135°F	120 cps

The data from the Rotovisco is plotted in Figure 51, shear rate versus apparent viscosity. Note the shape of the curves are the same but the position has shifted due to the slight change in viscosity. A significant change was observed only for the high temperature aged sample.

#### 7. Viscosity Stability

Previous data in this report (Reference II-3b) indicated evidence of viscosity drift with aging. This characteristic is still apparent with XD-7129.02 (FAA) as indicated below:

<u>Aging Time at Room Temperature</u>	<u>Brookfield RVT Viscosity #3 Spindle, 10 RPM</u>	
	<u>Sample 1</u>	<u>Sample 2</u>
1 Day	370 cps	320 cps
21 Days	210 cps	200 cps
28 Days	200 cps	--
42 Days	--	190 cps

Whether or not this drift in viscosity presents a practical problem is still questionable.

#### 8. Fire Explosion Resistance

Three different tests have been performed on XD-7129.02 (FAA) in an effort to predict its fire explosion safety features in an aircraft crash environment. Extensive testing at the FAA, NAFEC, has consistently shown excellent fire explosion resistance using the air gun explosion test equipment. A number of test results are shown below:

<u>XD-7129.02 (FAA) Ref. No.</u>	<u>Visual Rating</u>	<u>Radiometer Reading BTU/Ft<sup>2</sup>/Sec</u>		
		<u>A</u>	<u>B</u>	<u>C</u>
199-18-4	--	0.4	0.1	0.3
199-18-5	--	0.6	0.4	0.4
199-18-6	--	0.1	0	0
199-37-3	2	0.05	0.14	0.12
199-41-7	2	0	0.09	0.12
199-45-9	2+	0.27	0.27	0.06
199-47-9	2+	0.27	0.27	0.12
199-41-9	2++	0.37	0.59	0.30
199-41-8	2	0.05	0.18	0.12

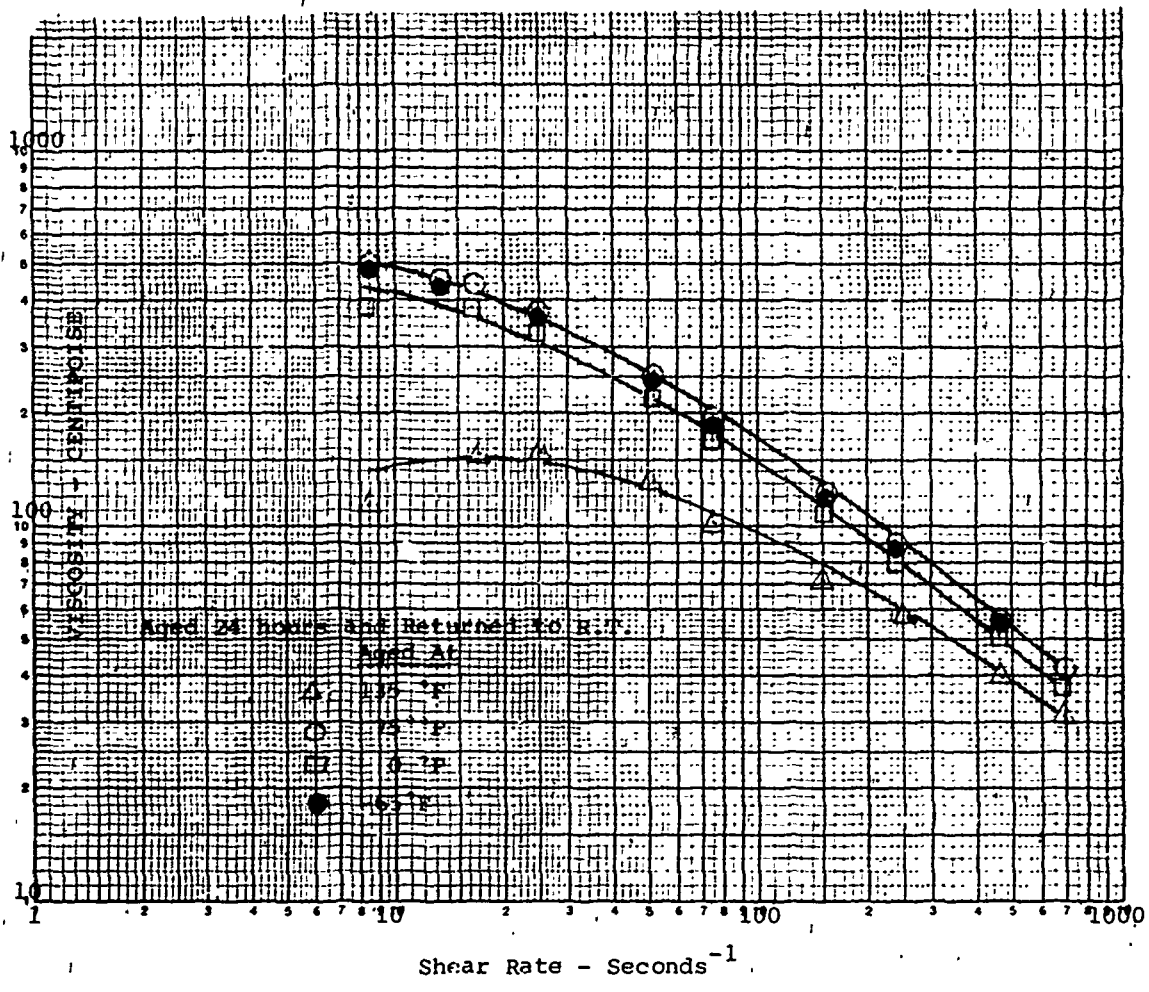


FIGURE 51. VISCOSITY VERSUS SHEAR RATE (ROTOVISCO VISCOMETER) EXPERIMENTAL JET FUEL XD-7129.02 (FAA) AGED AT VARIOUS TEMPERATURES

Tests conducted by the Bureau of Mines using XD-7129.02 (FAA) showed this fuel to have definite resistance to fire and fire explosion compared to base Jet A. These tests were 5 gallon drop tests where the can of fuel was impacted near ignition sources. Both vertical and 60° angle drop tests were conducted.

The fire and fire explosion resistance of XD-7129.02 (FAA) gave excellent results in a simulated crash test conducted by Dynamic Sciences, Inc., for the U.S. army. In this test 13 gallons of XD-7129.02 (FAA) (at 100°F) were impacted at 44 miles per hour against a 45° angle solid block, the tank ruptured and the fuel was sprayed over different type ignition sources. No fire or fire explosion occurred in any of these tests.



## SUMMARY OF RESULTS

Proprietary work at Dow Chemical Company resulted in a thickened jet fuel with excellent fire explosion resistance, but it was viscous with a gel-like consistency at static conditions. Feedback from various authoritative sources stated that thickened fuels with high viscosity at low shear (very thick at static conditions) were impractical for utility in modern aircraft. However, this gel-type thickened fuel possessed enough unique characteristics to consider a study to find a suitable compromise between fluidity and simulated crash misting hazard.

The base gel-type thickened jet fuel is a Jet A-1 type fuel thickened with a unique hydrocarbon additive (designated Experimental Resin XD-7038.00) developed by Dow. By minor modifications of this basic system, a suitable compromise thickened fuel should be possible.

In this project many modifications of the XD-7038.00 thickened fuel were evaluated using a variety of modifiers and test equipment. As soon as a trend was identified for making a low viscosity (at low shear), thickened fuel, such fuels were submitted to the FAA, NAFEC, to determine their simulated crash fire misting characteristics. Complete details of this study is discussed in the report section "Test Results and Discussion."

Gradually the number of test fuels was reduced to a single composition and a number of properties of the thickened fuel were determined, Reference Section VI.

The final compromise thickened fuel is designated Experimental Jet Fuel XD-7129.02 (FAA). It has very low viscosity at low shear, being in the 100 to 500 centipoise (cps) viscosity range at 75°F when tested with a Brookfield Viscometer at 10 RPM with a #3 spindle. The viscosity/shear rate curves, demonstrated by a number of viscometers, show evidence that the fuel possesses a number of typical rheological characteristics; i.e., dilatancy, pseudoplasticity and thixotropy, dependent on the shear rate. It appears to possess several ideal characteristics assumed to be desirable in designing a crash fire explosion resistant fuel.

### (a) Low Viscosity at Static Conditions

Although more viscous than base Jet A-1, the gravity flow is fast enough to minimize the former pump-out problems shown with the very viscous thickened fuels.

(b) Dilatancy or Shear Thickening, and Rheopecticity

The fuel resists misting or atomization at the test shear conditions assumed to exist in a survivable crash environment.

(c) Pseudoplasticity

The fuel viscosity decreases with shear, in the shear range associated with pumping, filtering and atomization for burning, so that its use performance should be similar to base jet fuels.

(d) Heat of combustion equal to base Jet A-1

(e) Simple Mixing Procedure

The XD-7038.00 is a fine powder that can be mixed into the base jet fuel with a high shear pump. The other two modifiers are liquids and are easily distributed in the fuel.

Obviously, at this early development stage there are many unknown features yet to be tested.

Further testing under actual use conditions will be required to determine if there are deficiencies in this fuel and the magnitude of such problems.

## CONCLUSIONS

Based on the data presented in this report it is concluded that:

1. Jet A-1 or Jet A can be modified to give fire explosion resistance while maintaining relatively low viscosity at low shear rates.
2. Fuel flow rates at gravity conditions of the modified fuels are significantly increased compared to former high viscosity thickened fuels, and approach the rates for unmodified jet fuel.
3. The rheological profile of the modified thickened fuel shows it to be dilatant at low shear, pseudoplastic at high shear, with thixotropy existing across the entire shear range.
4. The rheological profile of the modified thickened jet fuel is most completely characterized by the Rotovisco Viscometer since this instrument has broad shear rate range capability.
5. The Brookfield viscometer continues to be a useful instrument to monitor the rheology of these modified fuels at low shear ranges.
6. A reduction in viscosity at low shear is apparent at elevated temperatures; however, no adverse effect on fire explosion resistance has been observed.

The contents of this report reflect the views of the contractor, who is responsible for the facts and the accuracy of the data presented herein, and do not necessarily reflect the official views or policy of the FAA. This report does not, in itself, constitute a standard specification or regulation.

The Federal Aviation Administration is responsible for the promotion, regulation and safety of civil aviation and for the development and operation of a common system of air navigation and air traffic control facilities which provides for the safe and efficient use of airspace by both civil and military aircraft.